

Review

Unique Diagnostic and Therapeutic Roles of Porphyrins and Phthalocyanines in Photodynamic Therapy, Imaging and Theranostics

Leanne B. Josefsen and Ross W. Boyle 

Department of Chemistry, The University Of Hull, Kingston-Upon-Hull, HU6 7RX, U.K.

 Corresponding author: Dr. Ross W. Boyle. Tel: +44 (0)1482 466353; E-mail: R.W.Boyle@hull.ac.uk

© Ivyspring International Publisher. This is an open-access article distributed under the terms of the Creative Commons License (<http://creativecommons.org/licenses/by-nc-nd/3.0/>). Reproduction is permitted for personal, noncommercial use, provided that the article is in whole, unmodified, and properly cited.

Received: 2012.05.09; Accepted: 2012.08.10; Published: 2012.10.04

Abstract

Porphyrinic molecules have a unique theranostic role in disease therapy; they have been used to image, detect and treat different forms of diseased tissue including age-related macular degeneration and a number of different cancer types. Current focus is on the clinical imaging of tumour tissue; targeted delivery of photosensitisers and the potential of photosensitisers in multimodal biomedical theranostic nanoplatforms. The roles of porphyrinic molecules in imaging and pdt, along with research into improving their selective uptake in diseased tissue and their utility in theranostic applications are highlighted in this Review.

Key words: tetrapyrrolic photosensitisers, phototherapy, imaging, nanoagents, theranostics

Introduction

Porphyryns

Porphyryns are a group of naturally occurring intensely coloured compounds, whose name is drawn from the Greek word *porphura* (purple) [1, 2]. These molecules are involved in a number of biologically important roles, including oxygen transport and photosynthesis, and have applications in a number of fields, ranging from fluorescence imaging to medicine [3-15]. Porphyrins are classified as tetrapyrrolic molecules with the heart of the skeleton a heterocyclic macrocycle, known as porphine. The fundamental porphine framework consists of four pyrrolic sub-units linked on opposing sides (α -positions, numbered 1, 4, 6, 9, 11, 14, 16 and 19, figure 1) through four methine (CH) bridges (5, 10, 15 and 20) known as the *meso*- carbon atoms/positions (figure 1). The resulting conjugated planar macrocycle may be substituted at the *meso*- and/or β -positions (2, 3, 7, 8, 12, 13, 17 and 18); if a single hydrogen atom is attached to each of the *meso*- and β -carbons and two of the inner

nitrogen atoms (pyrrolenines) are protonated, the compound becomes known as a free-base porphine. If the *meso*- and/or β -hydrogens are substituted with non-hydrogen atoms or groups, the resulting compounds are known as porphyrins.

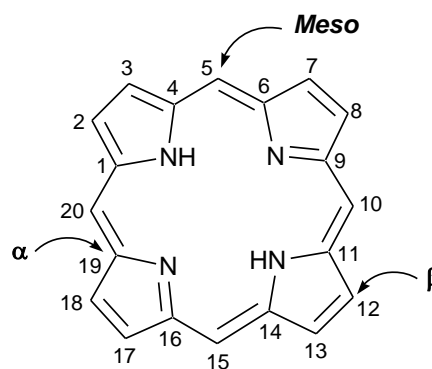


Figure 1. Porphine Macrocycle.

Phthalocyanines

Phthalocyanines (PCs, figure 2) are closely related to porphyrins; they are intensely coloured symmetric, aromatic macrocycles. They form coordination complexes with a wide range of metals (*via* the central cavity), yielding intensely coloured blue-green compounds, and have widely been used as colourants. More recently PCs have been used as photoconductive materials in laser printers and the light absorbing layer in recordable compact discs. They are also used as photosensitisers in phototherapy; as fluorescent reporters *in vitro* and *in vivo*; as non-linear optical materials; and as industrial catalysts [16-22].

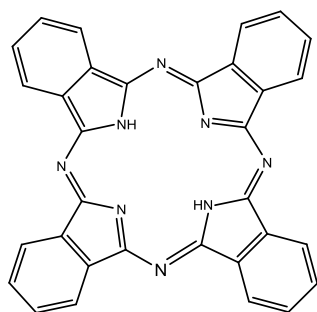


Figure 2. Phthalocyanine (PC).

PCs have an extended conjugate pathway relative to porphyrins – a benzene ring is fused to the β -positions of each of the four pyrrolic sub-units. These benzene rings act to strengthen the absorption of the chromophore at longer wavelengths (670-780nm), with respect to porphyrins. The absorption band of PCs is almost two orders of magnitude stronger than the highest Q band of haematoporphyrin (figure 3). These characteristics, along with the ability to selectively functionalise their peripheral structure, make PCs favourable photosensitiser candidates. PCs demonstrate stronger absorption of red light (than Photofrin®), allowing more effective light penetration of tumours and have shown promise as second generation photosensitisers [7, 9, 23].

Phototherapy: History

Porphyrins and PCs have been widely investigated for use in photodynamic therapy (pdt). Pdt is used clinically in the treatment of a number of medical conditions, including age-related macular degeneration (AMD), some cancers, skin conditions and for antiviral, antimicrobial and antibacterial applications including sterilisation of blood plasma and water [3-5,

7, 14, 24-30]. The first recorded use of “phototherapy” dates back over 4000 years to the ancient Egyptians while contemporary pdt was first reported in the late 19th century by Finsen *et al.* [3, 4, 13-15, 24, 28, 31, 32]. Finsen was later awarded the Nobel Prize (1903) for his work in pdt. However, it was not until 1995 that a suitable photosensitiser was approved (Photofrin®, by the Food and Drug Administration (FDA), USA) for clinical use against certain cancers [4, 5, 14, 24, 25, 27, 28, 32-34]. Pdt is minimally invasive and shows negligible toxicity thus offering advantages for both the patient and physician over traditional cancer treatments such as delicate surgery, or painful and tiring radio- and chemo-therapy. Lengthy recuperation periods are also minimised, along with minimal formation of scar tissue and disfigurement. However, pdt is not without its drawbacks – it is associated with generalised photosensitisation of cutaneous tissue, this is a major limitation in the potential efficacy of pdt [3, 24, 27, 28]. The principle behind pdt is based on a multi-stage process (figure 4) whereby (i) a photosensitiser is administered to the patient (systemically or topically) in the absence of light. When the optimum ratio of photosensitiser in diseased *verses* healthy tissue is achieved (ii) the photosensitiser is activated by (iii) exposure to a carefully regulated dose of light, which is shone directly onto the diseased tissue for a specified length of time. The activated photosensitiser then reacts with molecular oxygen generating reactive oxygen species (ROS) *in situ*, evoking a toxic response in the tissue, culminating ultimately in (iv) cell death [4, 5, 35]. The success of pdt lies in the prolonged accumulation of the photosensitiser in diseased tissue, relative to more rapid clearance from healthy tissue. The selectivity of pdt is based on the ability of the photosensitiser to preferentially accumulate in the diseased tissue and efficiently generate singlet oxygen (the cytotoxic species), inducing cell death.

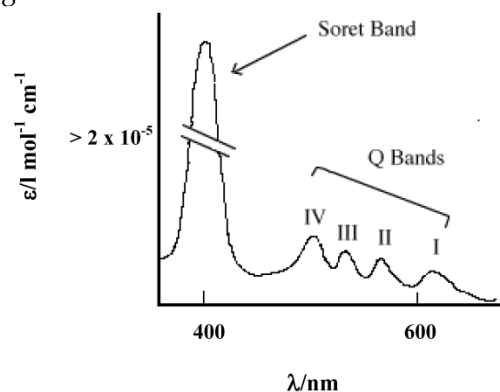


Figure 3. Typical Porphyrin Absorption Spectrum (Etio type).

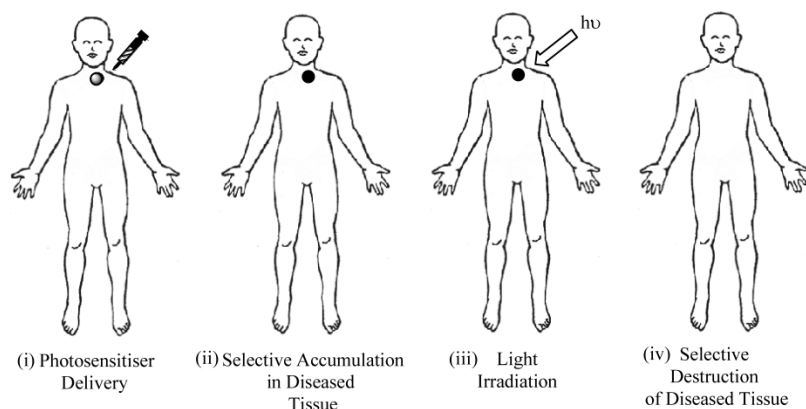


Figure 4. Clinical Procedure For Pdt.

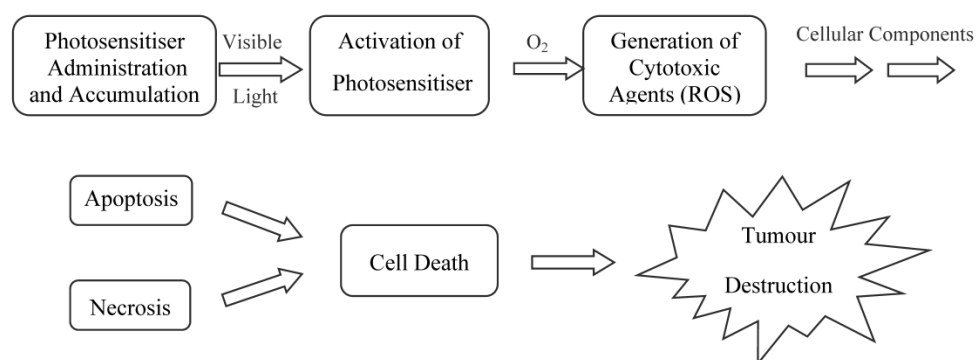


Figure 5. Photosensitiser Initiated Cell Death.

Photosensitisers

A photosensitiser is a molecule which when excited by light energy can utilise the irradiating energy to induce photochemical reactions producing lethal cytotoxic agents; these ultimately result in cell death and tissue destruction (figure 5). Photosensitisers are absorbed into cells all over the body and alone are harmless, *i.e.* in the absence of light and oxygen they have no effect on healthy or abnormal tissue: it is only their activated forms that have a cytotoxic effect [26, 27]. Ideally, photosensitisers should be retained by diseased tissue for longer periods of time in comparison to healthy tissue; thus, carefully timed light exposure is vital to ensure photosensitiser activation only occurs once the ratio of photosensitiser in diseased tissue is greater than that present in healthy tissue; thereby minimising unwanted healthy cell damage.

The nature of pdt requires efficient localisation of a photosensitiser in target tissue in order to achieve a satisfactory response [4, 14, 25, 28, 33, 36-43]. Pdt can offer an enhanced therapeutic effect *via* preferential uptake of the photosensitiser by: (i) the morphology

of the target tissue; (ii) specific illumination of target tissue; (iii) strategic timing of the applied light dose; (iv) topical application of the photosensitiser; and (v) chemical manipulation of the structure of the photosensitiser.

Photosensitiser localisation in tissues and cells plays a significant role in the mechanisms and efficacy of cell death crucial for effective pdt. Pdt works by inducing the formation of cytotoxic agents which readily attack neoplastic cells, a response known to be affected *in vivo* by the complexity of biological systems [4, 14, 25]. Any number of subcellular targets can be attacked during pdt, including mitochondria, lysosomes, plasma membranes and nuclei - the exact subcellular localisation of the photosensitiser can govern whether cell death occurs *via* necrosis or the preferred mode of death, apoptosis [4, 14, 25, 28, 36-43]. ROS have a short half-life and act close to their site of generation; it is therefore hypothesised that the type of photodamage incurred in irradiated photosensitiser-loaded cells depends upon the exact subcellular localisation of the photosensitiser [5, 14, 25, 28, 33, 38-42]. Different substituted photosensitisers have significantly different biodistribution patterns,

thus clinical activity is to a great degree dependent on the physicochemical characteristics of the molecules used [5, 14, 25, 28, 29, 33, 38-48].

Ideal photosensitisers – although a number of different photosensitising compounds, such as methylene blue (7-(dimethylamino)-N,N-dimethyl-3H-phenothiazin-3-iminium chloride, MB), rose bengal (4,5,6,7-tetrachloro-2',4',5',7'-tetraiodofluorescein disodium salt) and acridine (2,3-benzoquinoline) (figure 6) are known to be efficient singlet oxygen

generators (and therefore potential pdt agents) the vast majority of successful pdt photosensitisers are based upon the tetrapyrrole chromophore (figure 1); in particular porphyrin, chlorin, and bacteriochlorin (BC) derivatives (figure 6). These cyclic tetrapyrroles have an inherent similarity to the naturally occurring porphyrins present in living matter - they have no or minimal dark toxicity and, over the years, tetrapyrrolic chemistry has been well researched and developed [3-5, 24, 26, 27, 38-40, 43-52].

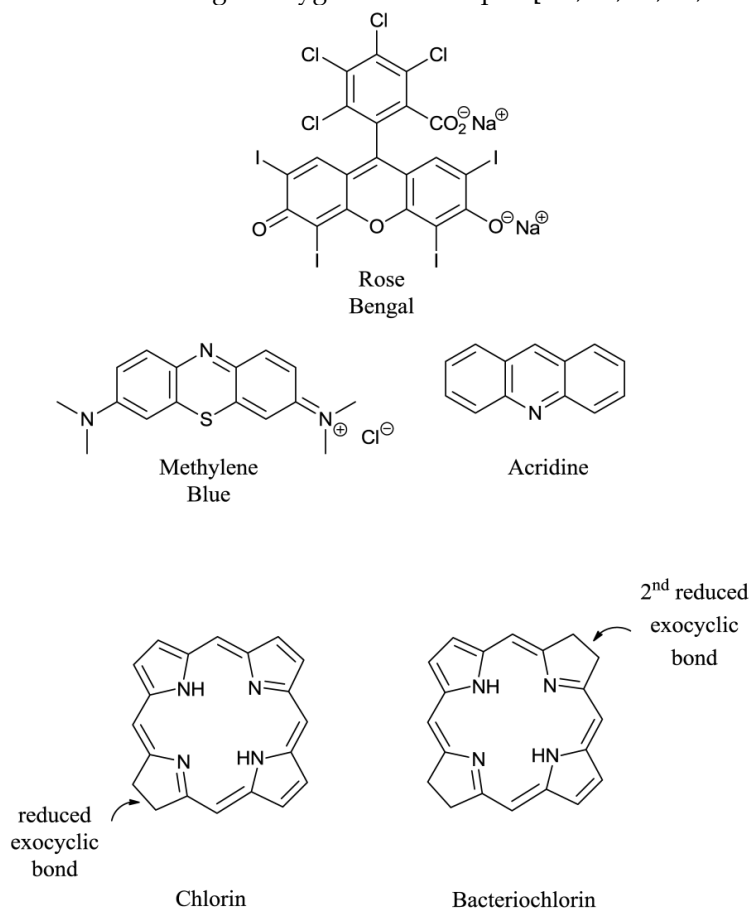


Figure 6. Examples of Non-Porphyrin and Porphyrin Based Photosensitisers.

Photochemistry

Photochemical Processes

Only when a photosensitiser is in its excited state ($^3\text{Psen}^*$) can it interact with molecular oxygen ($^3\text{O}_2$) to produce ROS. ROS include singlet oxygen ($^1\text{O}_2$), hydroxyl radicals ($\cdot\text{OH}$), and superoxide (O_2^-) anions and are widely accepted as the active cytotoxic agent in pdt. These toxic species interact with cellular components including unsaturated lipids; amino acid residues and nucleic acids (figure 7); with ensuing oxidative damage resulting in apoptotic or necrotic cell

death. Oxidative damage is limited (due to the short lifetime of ROS) to the immediate area (approximately 20nm) surrounding the excited photosensitiser. Singlet oxygen (the predominant ROS in pdt) can only interact with molecules and structures within this radius and is known to initiate a large number of reactions with biomolecules, including amino acid residues in proteins, such as tryptophan; unsaturated lipids like cholesterol and nucleic acid bases, particularly guanosine and guanine derivatives - the latter base is more susceptible to attack by singlet oxygen [3-5, 24, 27, 36, 40, 48-50, 53-58].

Photochemical Mechanisms

When a chromophore, such as a porphyrin, absorbs a photon of electromagnetic radiation (EMR) in the form of light energy, an electron is promoted into a higher-energy molecular orbital; hence, the chromophore is elevated from the ground state (S_0) into a short-lived, electronically excited state (S_n) composed of a number of vibrational sub-levels (S_n') (figure 8). The excited chromophore can lose energy by rapidly decaying through these sub-levels *via* internal conversion (IC) to populate the first excited singlet state (S_1), before quickly relaxing back to the ground state: the excited electron depopulates the excited singlet state (S_1) and return back to the ground state (S_0) by losing the absorbed energy *via* fluorescence ($S_1 \rightarrow S_0$). Singlet state lifetimes of excited fluorophores are very short ($\tau_{fl} = 10^{-9} - 10^{-6}$ seconds) since transitions be-

tween the same spin states ($S \rightarrow S$ or $T \rightarrow T$) conserve the spin multiplicity (spin) of the electron and are considered "allowed" transitions according to the Spin Selection Rules [27, 50]. Alternatively, an excited singlet state electron (S_1) can undergo spin inversion and populate the lower-energy first excited triplet state (T_1) *via* intersystem crossing (ISC), a spin-forbidden process, since the spin of the electron is no longer conserved ($S \rightarrow T$). The excited electron can then undergo a second spin-forbidden inversion and depopulate the excited triplet state (T_1) by decaying back to the ground state (S_0) *via* phosphorescence ($T_1 \rightarrow S_0$). Owing to the spin-forbidden triplet to singlet transition, the lifetime of phosphorescence ($\tau_p = 10^{-3} - 1$ second) is considerably longer than that of fluorescence.

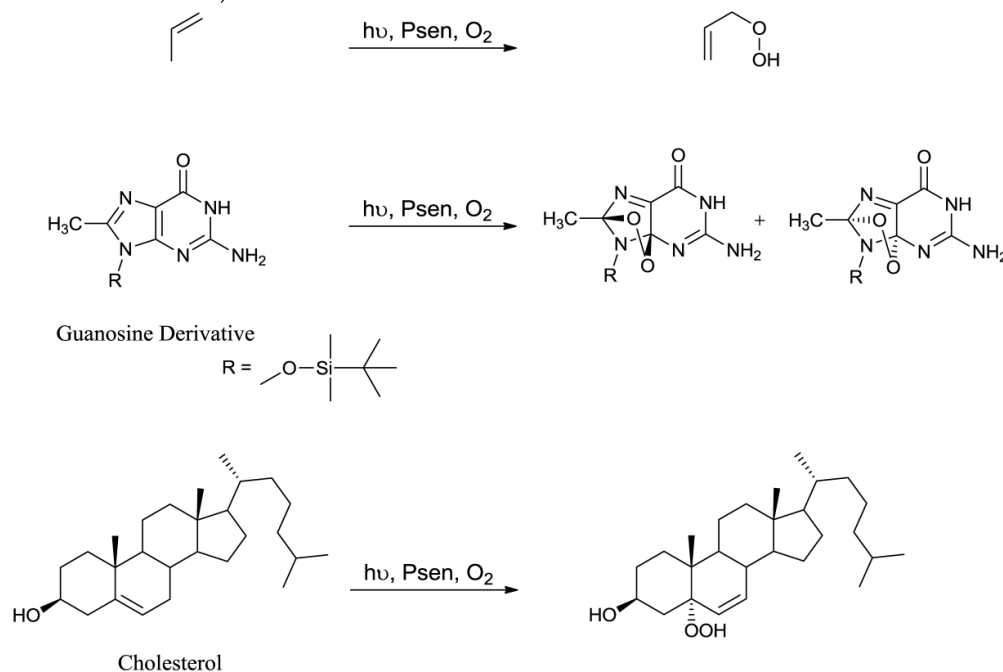


Figure 7. Examples Of Typical Singlet Oxygen Reactions.

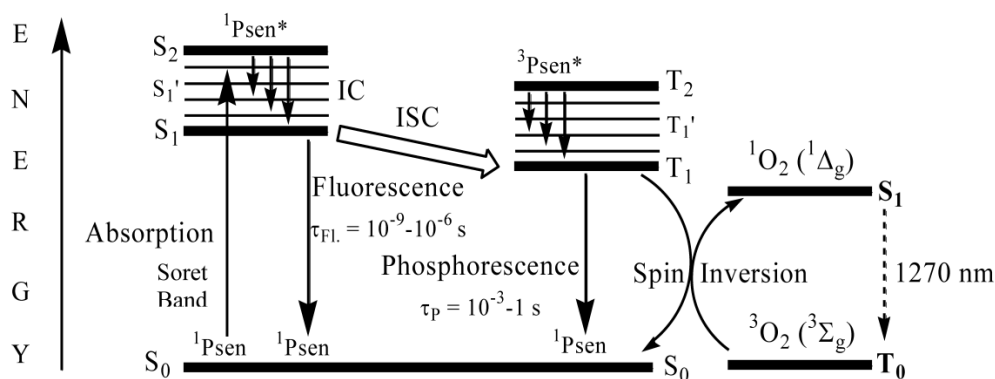


Figure 8. A Simplified Jablonski Diagram.

Photosensitisers And Photochemistry

Excited state porphyrins ($^1\text{Psen}^*$, $S_{>0}$ or $^3\text{Psen}^*$, $T_{>0}$) are relatively efficient at undergoing ISC and can have a high triplet-state (quantum) yields (Φ_T 0.62 (tetraphenylporphyrin (TPP), methanol), 0.75 (TPP, liposome, D_2O) and 0.71 (tetrasulphonated TPP, D_2O) [49, 50]. The longer lifetime is sufficient to allow the excited triplet state photosensitiser to interact with the surrounding biomolecules [4, 5]. Excited triplet-state photosensitisers can react in two ways defined as Type I and Type II processes. Type I processes involve the excited triplet photosensitiser ($^3\text{Psen}^*$, T_1) interacting with readily oxidizable or reducible substrates; whereas, Type II processes involve the interaction of the excited triplet photosensitiser ($^3\text{Psen}^*$, T_1) with molecular oxygen (3O_2 , $^3\Sigma_g^-$) (figure 8) [4, 5, 9, 25-29, 49-59]. The highly-reactive oxygen species (1O_2) produced *via* the Type II process act near to their site of generation with a typical lifetime of approximately 40ns in biological systems [3, 5, 14, 53]. These interactions cause damage and potential destruction to cellular membranes and enzyme deactivation, culminating in cell death [35-37, 50, 53]. It is highly probable that in the presence of molecular oxygen, both Type I and II pathways play a pivotal role in disrupting both cellular mechanisms and cellular structure as a direct result of the photoirradiation of the photosensitiser molecule. Nevertheless, there is considerable evidence to suggest that the Type II photo-oxygenation process predominates in the role of cell damage, a consequence of the interaction between the irradiated photosensitiser and molecular oxygen [3, 4, 24, 40, 50, 59, 60]. It has however, been suggested that cells *in vitro* are partially protected against the effects of pdt by the presence of singlet oxygen scavengers, such as histidine, and that certain skin cells are somewhat resistant to pdt in the absence of molecular oxygen; further supporting the proposal that the Type II process is at the heart of photo-initiated cell death [5, 46, 59-62]. The efficiency of Type II processes is dependent upon the triplet state lifetime (τ_T) and the triplet quantum yield (Φ_T) of the photosensitiser, both parameters have been implicated in the effectiveness of a photosensitiser in phototherapeutic medicine; further supporting the distinction between Type I and Type II mechanisms. However, it is worth noting that the success of a photosensitiser is not exclusively dependent upon a Type II process taking place - there are a number of photosensitisers whose excited triplet lifetimes are too short to permit a Type II process to occur, for example, the copper metallated octaethylbenzochlorin photosensitiser (figure 9) has a triplet state lifetime of less than 20ns and is still deemed

to be an efficient photodynamic agent [46].

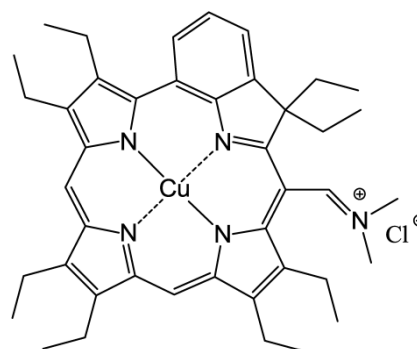


Figure 9. Copper Octaethylbenzochlorin.

First-Generation Photosensitisers

The first reported use of pdt in the treatment of solid tumours came in the early 20th Century by von Tappeiner's group in Munich, Germany - patients with skin carcinomas were successfully treated with the fluorescein-based dye eosin (figure 10) [3, 25, 29, 32, 63]. Shortly after, fellow German physician Meyer-Betz reported the major stumbling block of pdt - acute cutaneous photosensitisation. After injecting himself with the photosensitiser haematoporphyrin (Hp) Meyer-Betz swiftly experienced a general skin sensitivity upon exposure to sunlight; a problem that still exists [3, 14, 24, 25, 27]. Further research into Hp and the purified derivative (HpD) in tumours resulted in the first clinically-approved photosensitiser, Photofrin[®] (figure 11). Photofrin[®] was approved by the Canadian Health Agency in 1993 for use against bladder cancer and later in Japan, America and parts of Europe for use against certain cancers of the oesophagus and non-small cell lung cancer [4, 5, 13, 14, 24, 25, 27, 28, 32-34]. However, Photofrin[®] has well-documented problems - in addition to patients exhibiting prolonged photosensitivity, the drug itself has a weak long-wavelength absorption (630nm) [14, 25, 28, 33]. Research into improved photosensitisers saw the development of second-generation photosensitisers, including Verteporfin[®] (Visudyne[®]) and third-generation photosensitisers focused on targeting strategies, such as antibody-directed photosensitisers and photosensitiser-loaded nanocarriers [4, 14, 24, 26, 32, 64, 65]. Combined diagnostic and therapeutic modalities have begun to emerge creating theranostic tools for use in identifying (imaging) and treating diseased states: are these the next generation of pdt agents [28, 66-69]? The ability to "switch on" a cytotoxic effect, and combine photosensitisers with imaging modalities such as magnetic resonance imaging

(MRI) and radioimaging, makes pdt particularly attractive as the therapeutic partner in theranostic agents. The use of single agents/entities has the added benefit of ruling out variability in localisation; uptake; pharmacokinetic; and pharmacodynamic patterns of the agent (present when separate entities are used) at any stage during the theranostic treatment; stress on the body's clearance system is also minimised when a single agent rather than multiple agents are administered. A further advantage of using small molecule multimodal agents is their clearance by the renal system -avoiding toxicity associated with long-term liver retention [70].

tissue that could be treated; research focused on developing agents with higher absorption wavelengths. Increasing the absorption wavelength and having a higher extinction coefficient in the red/near-infrared region of the electromagnetic spectrum (EMS, 600-850nm) allows deeper penetration of illuminating light into the skin, thus increasing the depths at which tumour cells can be targeted. The range of photosensitisers approved for clinical use includes porphyrins, chlorins, texaphyrins, porphycenes, purpurins and phthalocyanines (figures 11 and 12) [2-5, 7, 9, 12, 13, 15, 23, 24, 26, 28-30, 32-34, 43-45, 48-50, 61, 64, 65].

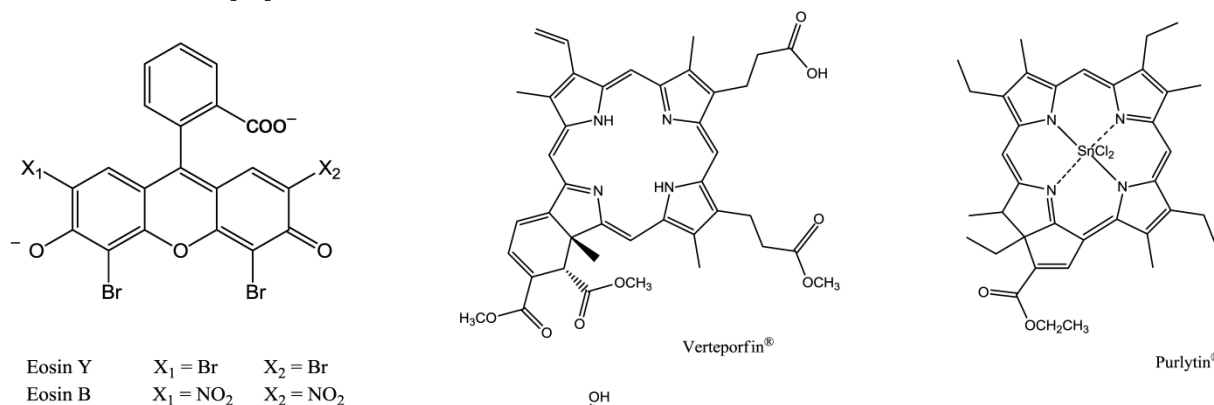


Figure 10. Eosin.

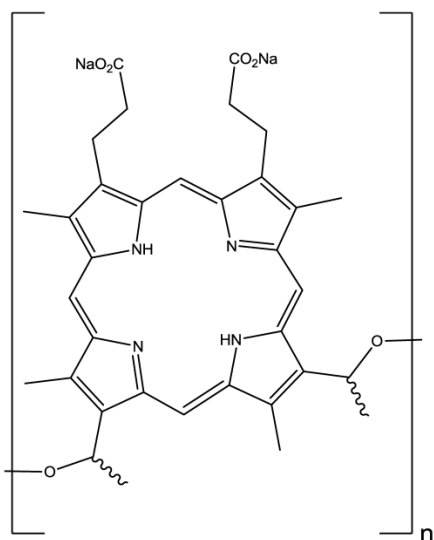
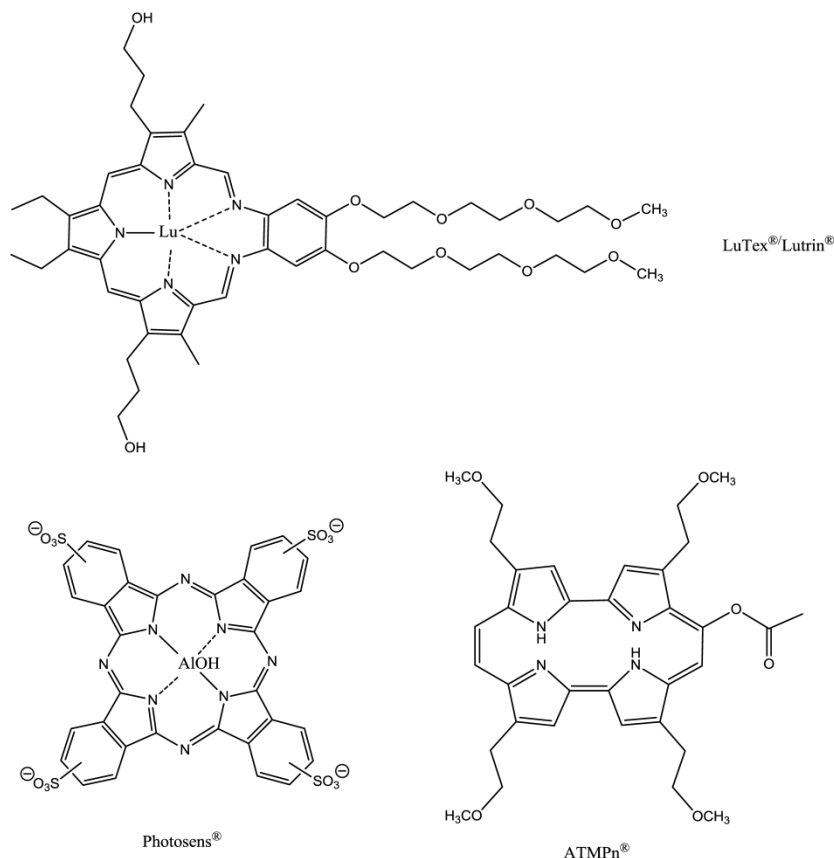


Figure 11. HpD, Photofrin®, n= 1-9.



Second-Generation Photosensitisers

Second-generation photosensitisers were developed in order to increase the power and efficiency of pdt and broaden the type of diseased

Figure 12. Clinically Approved Photosensitisers.

The prodrug 5-aminolaevulinic acid (δ -aminolaevulinic acid, ALA, marketed as Levulan[®]) generates the photosensitiser protoporphyrin IX (PPIX), *via* the haem biosynthetic pathway, when internalised by cells and is used in the imaging and treatment of superficial tumours. It has also been used as a topical treatment for dermatological conditions (psoriasis, Bowen's disease and acne). ALA derivatives are used in the clinic for imaging and treatment of basal cell carcinomas and other skin lesions (Metvix[®], a methyl ester derivative), Benvix[®] (a benzyl ester derivative) and Hexvix[®] (a hexyl derivative) have also been employed in the treatment of gastrointestinal cancers and in the diagnosis of bladder cancer [4, 7, 14, 24, 25, 29, 50, 71]. The ability of small molecule ALA derivatives to penetrate the skin selectively where tumours are present and both fluoresce and photosensitise the tumours *via in situ* production of PPIX makes them ideal theranostic agents. A benzoporphyrin derivative, monoacid ring A (BPD-MA, trade name Visudyne[®], Verteporfin[®] for injection) was developed and approved for use in wet age-related macular degeneration (wAMD) and cutaneous non-melanoma skin cancer. The success of Verteporfin[®] could be attributed to the red-shifted and intensified long-wavelength absorption maxima (approximately 690nm) - light can penetrate 50% deeper into the skin at this wavelength in comparison to Photofrin[®] [4, 7, 14, 25, 27, 29, 72-74]. Tin etiopurpurin (Purlytin[®], figure 12), a chlorin-based photosensitiser, is a derivative of the porphyrin chromophore with a reduced exocyclic double bond and an intensified long-wavelength absorption - the tin atom chelated in the central cavity further increases the red shift (20-30nm) of the drug (650-680nm). Purlytin[®] has been approved (USA) for cutaneous metastatic breast cancer, Kaposi's sarcoma in patients with AIDS and for the treatment of psoriasis and restenosis [4, 7, 14, 25, 27, 29, 50, 75, 76]. Tetra(*m*-hydroxyphenyl)chlorin (*m*THPC, Foscan[®]/Temoporfin[®], USA and Europe) has been evaluated for use in the pdt of head and neck cancers as well as gastric and pancreatic cancers, hyperplasia, field sterilisation after cancer surgery and for the control of antibiotic-resistant bacteria (USA, Europe and the Far East). Advantages of Foscan[®] are the low drug and light doses required to achieve suitable photodynamic responses - Foscan[®] is approximately 100 times more photoactive than Photofrin[®], although patients can remain photosensitive for up to 20 days (the length of photosensitivity varies between the second-generation photosensitisers from 1-2 days (Verteporfin) to up to 2 weeks (Purlytin) [4, 7, 14, 24, 25, 27, 29, 50, 71, 77, 78]. First-generation photosensitisers can render patients photosensitive for 90

days. Lutetium texaphyrin (Lutex[®]/Lutrin[®]), an expanded porphyrin with a penta-aza core, exhibits strong absorption in the 730-770nm region of the EMS, a region where tissue transparency is optimal. Lutex[®] has been approved for the treatment of breast cancer and malignant melanomas (USA). Antrin[®], a Lutex[®] derivative, has undergone trials for the prevention of restenosis, while Optrin[®], a second derivative, has been in trials for the management of AMD [4, 7, 14, 24, 25, 29, 50, 76, 79-82]. Texaphyrins have also been developed for use as radiosensitisers and chemosensitisers - a gadolinium complex has been investigated as a MRI contrast agent. 9-Acetoxy-2,7,12,17-tetrakis(β -methoxyethyl)-porphycene (ATMPn[®], porphycenes are structural isomers of porphyrins), absorption maxima ~640nm has been evaluated against psoriasis *vulgaris* and superficial non-melanoma skin cancer (USA) [4, 7, 83-86]. Zinc phthalocyanine (CGP55847) has undergone clinical trials against squamous cell carcinomas (SCC) of the upper aerodigestive tract (Canada) [4, 7, 24, 76, 87-93]. A sulphonated aluminium PC derivative (Photosens[®], Russia) entered clinical trials against skin, breast and lung malignancies and cancer of the gastrointestinal tract [4, 7, 24, 94-96]. Sulphonation of the PC significantly increases PC solubility in polar solvents including water, circumventing the need for alternative delivery vehicles. A silicon PC complex (PC4) has been evaluated for the sterilisation of blood components (USA), and against breast, colon and ovarian cancers and gliomas [4, 7, 97-103]. A drawback of metallo-PCs can be their tendency to aggregate in aqueous buffer (pH 7.4), leading to a decrease or total loss of their photochemical activity; detergents can limit this behaviour [7, 76]. Tetraazaporphyrins, porphyrazine (PZ, figure 13) derivatives, have been evaluated against Chinese hamster lung fibroblast cells; the PZs that exhibited the greatest induction of dark toxicity include the metallated cationic complexes PdPZ⁺, CuPZ⁺, CdPZ⁺, MgPZ⁺, AlPZ⁺ and GaPZ⁺ [7, 76].

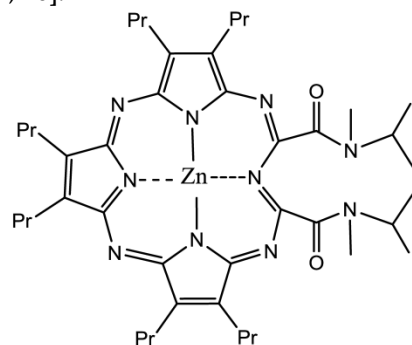


Figure 13. Zinc-Metallated Porphyrazine.

Naphthalocyanines (NCs, figure 14) are extended PC derivatives and absorb at even longer wavelengths (740-780nm) than PCs, further increasing the depth photosensitisers could effectively be used at. The absorption region of NCs makes them particularly promising agents for pdt of highly pigmented tumours, such as melanomas, which can present significant problems with the transmission of visible light. The emission from NCs in the near-IR also gives them great potential as *in vivo* imaging agents. However, NCs are generally less stable than their PC counterparts - they readily decompose in the presence of light and oxygen (two of the vital components for pdt), and metallo-NCs, lacking axial ligands, have a tendency to form H-aggregates in solution; the aggregates are photoinactive. Kenney *et al.*, van Lier *et al.* and Wöhrle *et al.* have mainly dominated the research into NC based photosensitisers [4, 7, 75, 76, 91, 104-115].

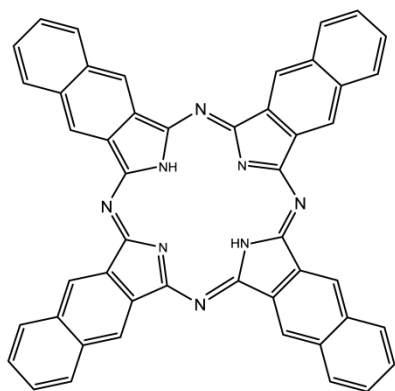


Figure 14. Naphthalocyanine (NC).

Changing the peripheral functionality of the photosensitiser macrocycle can have an effect on the potential pdt efficacy of the molecule. Diamino platinum porphyrins exhibit higher anti-tumour activity, demonstrating the combined effects of the cytotoxicity of the platinum complex and the pdt activity of the porphyrin species [7, 76, 116]. Cationic PC derivatives have also shown potential - positively charged species are believed to localise in the mitochondrion - organelles key to cell survival and the site of oxidative phosphorylation [76, 78, 91, 92]. Zinc and copper cationic species have been investigated although the cationic ZnPC was found to be less photodynamically active than its neutral counterpart *in vitro* against V-79 cells. Water-soluble cationic porphyrins bearing nitrophenyl, aminophenyl, hydroxyphenyl, and/or pyridiniumyl functional groups exhibit varying cytotoxicity towards cancer cells *in vitro*, depending on the nature of the metal ion (Mn, Fe, Zn, Ni), and on the number and type of functional groups present (figure 15). The manganese pyridiniumyl derivative has shown the greatest photodynamic activity, while the nickel analogue is photoinactive [76, 92, 118]. Another metallo-porphyrin complex, the iron chelate, was found to demonstrate greater photoactivity (towards HIV and simian immunodeficiency virus in MT-4 cells) than the manganese complexes; the zinc derivative was found to be photoinactive (figure 15) [76, 117].

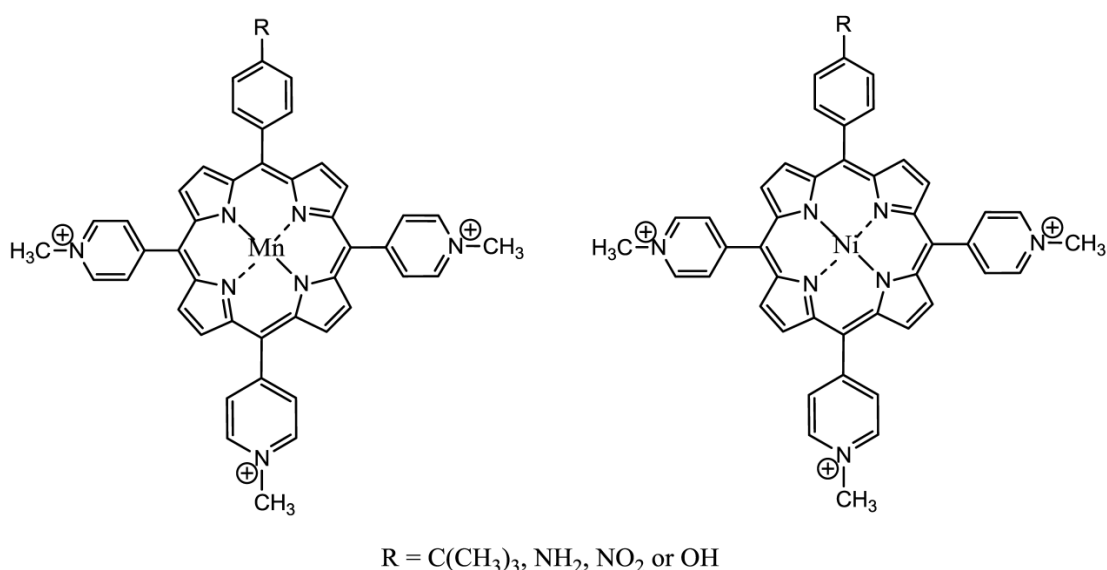


Figure 15. Water-Soluble Cationic Metallated Porphyrins.

The hydrophilic sulphonated porphyrins and PCs (AlPorphyrin and AlPC) have been evaluated for photodynamic activity. The disulphonated analogues (with adjacent substituted sulphonated groups, figure 16) exhibited greater photodynamic activity than their di- (symmetrical), mono-, tri- and tetra-sulphonated counterparts [7, 50, 93].

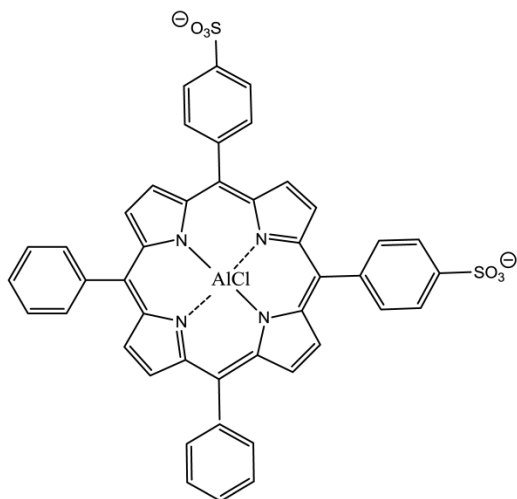


Figure 16.
5,10-Di-(4-sulphonatophenyl)-15,20-diphenylporphyrinato aluminium chloride.

Third-Generation Photosensitisers

The poor solubility of many first- and second-generation photosensitisers (in aqueous media, particularly at physiological pH) prevents their intravenous delivery directly into the bloodstream. It is advantageous if delivery models can be developed which facilitate the transportation of these potentially useful photosensitisers to target tissue/sites. Research has mainly focused on developing systems to effect greater selectivity and specificity on the photosensitiser in order to enhance cellular uptake.

Targeting Strategies

Reported hypotheses suggest the accumulation of photosensitisers in the mitochondria efficiently triggers apoptosis (preferred mode of cell death), therefore, the efficacy of a photosensitiser potentially could be improved by mitochondrial targeting. Alternatively, the cell nucleus is the cellular organelle that is most sensitive to phototherapy damage, hence nuclear damage can lead very quickly to cell death; this implicates the nucleus as a desirable photosensitiser target in PDT [14, 24, 114, 115, 119]. The intracellular localisation of a photosensitiser is not a static

process and may change during irradiation, for example, photoinduced lysosomal damage can cause lysosomes to rupture releasing any lysosomally-localised photosensitiser into the cytoplasm. To date, many photosensitisers have been non-site specific drugs, *i.e.* they do not target specific substrates or sites in their "free-state", highlighting the need for site-specific/selective photosensitisers and the development of targeting strategies [5, 24-26, 38, 39, 120]. One such set of examples are the photosensitiser bioconjugates which contain a receptor-targeting moiety (and a photosensitiser): a move that is in line with the "magic bullet" theory suggested in the early 20th century by Paul Ehrlich [121]. Ehrlich's notion of, "a compound which would have a specific attraction to disease-causing microorganisms by seeking them out and destroying them (whilst avoiding other organisms and having minimal undesired/harmful effects on the patient)", could be theoretically achieved using antibody conjugates [121-123]. Antibodies work by selectively targeting complimentary biomarkers expressed on the surface of cells; tumour cells are known to over-express certain biomarkers on their surface (such as certain antigens) against which antibodies can be raised and subsequently conjugated to a photosensitiser; facilitating the directed targeting of the photosensitiser towards specific bioreceptors with high degrees of affinity and specificity, thus making antibodies ideal targeting candidates. Free photosensitisers typically achieve ratios of only 2-5:1 (tumour to normal tissue) - improving this ratio could significantly reduce the dose of photosensitiser necessary for a PDT effect to be observed [124].

Targeting Moieties

A number of small biologically active molecules have been successfully conjugated to porphyrins, for example steroids, peptides and antibodies [3, 25, 28]. Active targeting/active uptake requires that target molecules be recognised by specific intermolecular interactions and shuttled across the cell membrane by receptors. Thus, molecules may be targeted towards these receptors by appending the appropriate substrate moieties to them. Passive uptake involves diffusion at some point in the process and results from non-specific cell-molecule interactions. The lipid membrane core dictates that the more lipophilic a molecule, the lower the barrier to traversing the cell membrane, whereas amphipathic molecules normally bind at the interface or polar region and have greater barriers in crossing the membrane [125]. Antibodies have been used in a range of techniques such as: (i) antibody-directed enzyme prodrug therapy (ADEPT) [126-132]; the use of a deactivated toxin or prodrug

which can be converted into its active form by an enzyme covalently bound to a suitable monoclonal antibody, thus “switching on” activity at the target cells; and (ii) antibody-directed abzyme prodrug therapy (ADAPT) [133, 134]. ADAPT is similar to ADEPT with the exception that ADAPT uses catalytic antibodies or abzymes, which can be engineered to catalyse the activation of the prodrug but minimise the immune response. Additional targeting and localising biomolecules have been employed in targeting therapy to achieve the “magic bullet” notion.

Serum Albumin

Serum albumin is the most abundant protein in humans – it is approximately ten times the total concentration of all other lipoproteins found in the blood [3, 6, 14, 24, 25, 135, 136]. Over 60% of the protein is found in interstitial fluid – fluid which surrounds cells and acts as a medium to provide nutrients to and remove waste products from the cells. Serum albumin is unique in its ability to bind, covalently or reversibly, with a large number of ligands with a high degree of affinity. It has been reported that photosensitisers possessing a high affinity for serum albumins could be efficient pdt agents; tumour cells have a higher rate of serum albumin turnover due to their increased metabolism and rate of proliferation [135]. One of the first studies into albumin binding with respect to targeted-pdt centred on the non-covalent binding (NCB) of an unsubstituted ZnPC (figure 17) to bovine serum albumin (BSA). Results were promising – tumour regression was observed (EMT-6 mouse mammary tumours on Balb/c mice and T380 human colon carcinomas on nude mice) with no hepatic toxicity. However, further tests indicated that, post-intravenous administration, the ZnPC redistributed towards the high density lipoprotein (HDL) fraction of the serum [135]. To circumvent this behaviour research concentrated on the covalent binding of photosensitisers to albumin [135]. Physically-modified albumin is targeted by scavenger receptors that are expressed in high concentrations on macrophages. The macrophages bind a broad range of different ligands and transport them to subcellular compartments; oxidised low density lipoprotein (LDL) and maleylated BSA readily bind to macrophages while native proteins do not. Estimates suggest that in several cancers greater than half of a tumours mass is of macrophage lineage giving the potential for targeting photosensitisers to the tumour by targeting macrophages. Reports suggest tumour-associated macrophages accumulate greater concentrations of photosensitiser than neighbouring tumour cells with a 9-fold increase observed for por-

phyrins. Results for other photosensitisers (porphyrins, PCs, chlorins) conjugated to albumin (BSA and maleylated BSA) have shown promise against a range of tumour cell-lines (human colon carcinoma HT29 tumour cells and J774 macrophage cell line from Balb/c mouse tumour cells). Albumin-conjugated photosensitisers have also shown promise in the treatment of arterial occlusion (inhibition of intimal hyperplasia and decreased restenosis post-initial disease therapy) and as agents to induce photodynamic tissue adhesion *via* tissue soldering [119, 135-141].

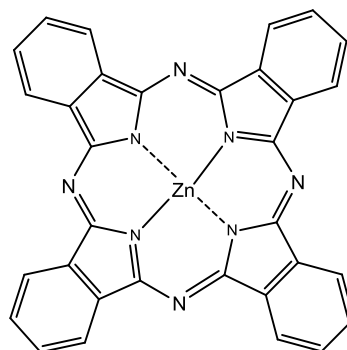


Figure 17. Unsubstituted ZnPC.

Low Density Lipoprotein Conjugates

Lipoproteins are naturally occurring particles composed of a hydrophobic lipid core (esterified cholesterol molecules), surrounded by an outer shell of polar lipids (phospholipids and unesterified cholesterol) and apoproteins (B-100 apolipoprotein). They are biocompatible, biodegradable and non-immunogenic species that serve as the main vehicle for transporting cholesterol molecules to mammalian cells [6, 119-137, 142-146]. Lipoproteins have two main roles: to solubilise highly hydrophobic lipids and regulate the passage of specific lipids into and out of particular cells and tissue. This movement occurs *via* a process of specific receptor binding in the plasma membrane of non-hepatic cells, internalising through endocytosis to form a vesicle within the cell: apolipoproteins control the recognition and binding of the LDL receptor and lead to receptor-mediated endocytosis [4]. They fuse with lysosomes and hydrolyse the protein component of the LDL. LDL receptors (apo B/E receptors) are overexpressed on malignant cells [142]. Cholesterol, a key component of all eukaryotic plasma membranes, is essential for the growth and viability of cells in higher organisms hence in tumour and tumour vasculature cells the LDL receptors are also overexpressed [3, 14, 25, 119, 135]. Such chemistry highlights the potential of LDL

as a carrier vehicle for targeted drug delivery. Depending on the photosensitiser-LDL binding site – either within the hydrophobic core or within the matrix of the apolipoprotein outer shell – the photosensitiser-LDL conjugates are believed to target the cellular or vascular components of the tumour, further supporting the idea of targeted drug delivery [119]. Research has identified further advantages of LDL targeted drug delivery in pdt; post-irradiation, LDLs are highly oxidised - the oxidised species are cytotoxic towards endothelial cells, thus the photodynamic action of the targeted system may be increased [135]. Reported results of photosensitiser-LDL conjugates to date differ, both in terms of association of the photosensitiser with the lipoprotein and the photodynamic effect observed. 2 types of LDL binding are recognised – non-covalent and covalent [135]. Germanium (IV) octabutoxyphthalocyanine administered *in vivo*, via Cremophor EL, demonstrated prolonged serum retention and stronger association with LDL in comparison to liposome-delivered PCs [135]. Similar results were observed with tin etiopurpurin. Haematoporphyrin (an amphiphilic compound) was bound to human LDL and delivered to human HT1080 fibroblast cells; accumulation of the complex in the cells was identified as a result of a high affinity for LDL receptors. In comparison, a hydrophobic zinc PC-LDL complex was internalised into the cellular environment *via* non-specific endocytosis – the poor affinity for the LDL receptor was a result in the changes of the apolipoprotein B structure induced by complexation of the ZnPC with the LDL. Sulphonated TPPs yield different results dependent on their chemical structures; the monosulphonated and adjacently disulphonated species have been identified as strongly associating with LDLs - up to 250 molecules of the latter porphyrin-LDL complex, per LDL, resulted in unchanged LDL receptor recognition in a human hepatoma (Hep G2) cell line. *In vivo* studies suggest that LDLs can incorporate up to 1000 photosensitiser molecules and still be recognised as native LDLs [135]. Naturally, improved incorporation of photosensitisers into the LDL structure is anticipated to improve pdt efficiency and overall therapeutic outcome. For ZnPC, non-covalent complexation of the photosensitiser to the LDL, prior to intravenous administration, enhanced both tumour uptake and photodynamic activity of the photosensitiser in comparison to liposomes (dipalmitoylphosphatidylcholine) [135]. LDL-Hp complexes have shown different subcellular localisation properties in comparison to albumin-Hp complexes – LDL complexes exhibited selective accumulation in sites such as the mitochondria, whereas the albumin complexes have demonstrated preferential

accumulation in the vascular stroma. Such differences in delivery and localisation properties could be utilised for the desired mode of tumour control: albumin delivery for extracellular tumour cell damage and LDL transport for a more direct cell death mode [135, 141]. The binding of photosensitisers to serum proteins is generally determined by photosensitiser hydrophobicity – moderately hydrophobic photosensitisers show preferential transport *via* albumins in the bloodstream, highly hydrophobic photosensitisers bind more predominantly with lipoproteins, specifically LDLs [146], thus there is potential to use LDL in the targeted delivery of hydrophobic and amphiphilic photosensitisers in pdt.

Epidermal Growth Factor

The epidermal growth factor (EGF) receptor is also often overexpressed in several tumour types, such as squamous cell carcinomas, highlighting the potential of photosensitiser bioconjugates with the EGF [135, 136, 147]. EGF is internalised into the cell *via* receptor-mediated endocytosis [147]. To date, this strategy has not been thoroughly investigated; only one research group has reported (in 1999) data on the photosensitiser-EGF model [148]. Lutsenko and colleagues focused their research on aluminium and cobalt disulphonated PCs. They observed the photosensitiser-bioconjugates displayed a greater degree of photoactivity than their non-conjugated analogues, with a 4.5-fold increase in the photocytotoxicity of the cobalt PC-EGF conjugate compared with the aluminium PC-EGF complex. Animal studies (C57B1/6 mice) on the murine melanoma cell line B16 using the CoPC-EGF model exhibited promising results – the mean life spans and survival times of the tumour-bearing mice were increased [148]. Further work needs to be undertaken on EGF conjugates to fully evaluate their potential as pdt targeting agents.

Sugars

Coupling of sugars to photosensitisers has also shown promise in the selective targeting of tumour/diseased cells [9, 125, 149, 150]. Tumour cells have high energy requirements and their proliferation is often dependent on glucose uptake – elevated glycolysis rates are observed in cancer cells in comparison to healthy cells. Glucose traverses the cell membrane *via* receptor mediated endocytosis [125, 149, 150]. Porphyrin-saccharide bioconjugates have demonstrated greater binding affinities for cancer cells – cancer cells overexpress glucose transporter receptors [150]. Two main types of sugar-porphyrin/PC molecules have been investigated: those where the sugar moiety is attached to the pe-

riphery of the porphyrin/PC structure through a linker group and those where the sugar is fused directly to the porphyrin macrocycle [150]. A number of research groups have looked at glycosylated porphyrins (figure 18).

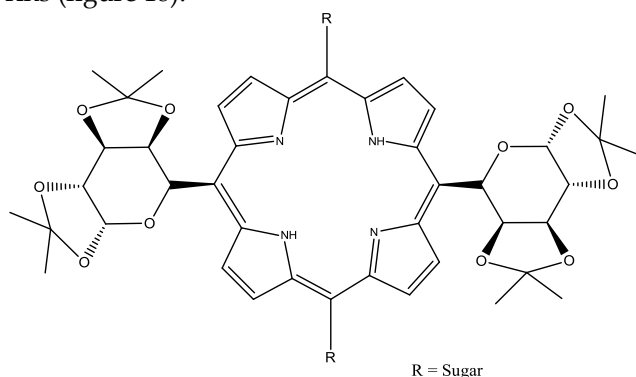


Figure 18. Glycosylated Porphyrins.

A common problem with these porphyrins is the hydrolysis of the sugar component - porphyrins bearing sugars appended *via* O-glycoside linkages undergo hydrolysis under physiological conditions (by enzymatic and non-enzymatic acid/base reactions) and therefore have short half-lives [125]. To overcome this problem, researchers have looked at developing porphyrins-saccharide species conjugated through C- or S-glycoside linkages; synthetic yields for these compounds were often poor and led to work focusing on the improved synthesis and pdt profile of S-glycoside linked porphyrin-saccharide conjugates bearing four sugar moieties: 5,10,15,20-tetrakis(4,1'-thio-glucose-2,3,5,6,-tetrafluorophenyl)porphyrin (P-Glu₄) and 5,10,15,20-tetrakis(4,1'-thio-galactose-2,3,5,6,-tetrafluorophenyl)porphyrin (P-Gal₄) [125]. Tetrapentafluorophenyl porphyrins (TPPF₂₀) can be readily synthesised in large quantities (*via* Adler or Lindsey routes) and are commercially available, making them an interesting porphyrin of choice for research purposes. The P-Glu₄ and P-Gal₄ saccharide-porphyrin photosensitisers exhibited enhanced binding to a human breast cancer cell line over non-sugar porphyrin derivatives, such as tetra(4-methoxyphenyl)porphyrin. Results further demonstrated preferential uptake and an enhanced pdt effect for the glucose analogue (P-Glu₄) in comparison to the galactose derivative (P-Gal₄) [125]. Observations of lower photosensitiser (P-Glu₄) uptake in normal rat fibroblast (3Y1) cells than in the transformed (3Y1^{v-Src}) cells were reported, highlighting the potential of photosensitiser-sugar conjugates in targeted cell attack [125]. Hirohara and colleagues observed the pdt efficacy of five different

glucosylated fluorophenylporphyrins: the *trans*-di(S-glucosylated) porphyrin demonstrated outstanding photocytotoxicity (twenty-fold higher than other S-glucosylated porphyrins tested and a three-fold increase in uptake) in HeLa cells [149]. Tomé and co-workers evaluated the antiviral activity of a number of *meso*-tetraarylporphyrins appended with carbohydrates. They reported elevated inhibitory effects on viral replication, against herpes simplex virus types 1 (HSV-1) and 2 (HSV-2) in Vero cells, for porphyrins bearing fully unprotected sugar moieties on the periphery of the porphyrin molecule [151]. The fluorinated glycoporphyrin analogue demonstrated antiviral activity of 40% towards HSV-1 and 50% against HSV-2 [9, 151]. Vedachalam *et al.*, Banfi *et al.* and Ferrand *et al.* report that diarylporphyrin sugar derivatives are more effective at inducing photodynamic cell death in human colon adenocarcinomas than the corresponding tetraarylporphyrin analogues [150, 152, 153]. A *meso*-bisglycosylated diarylporphyrin has been synthesised and its photodynamic potential explored. The bioconjugate was reported to localise in lysosomes, unlike other photosensitiser-sugar loaded complexes which have exhibited preferential localisation in the mitochondria or endoplasmic reticulum - the authors attributed lysosomal localisation to the sugar proportion of the bioconjugate [150]. Work to improve cellular uptake, decrease aggregation and increase hydrophilicity of PCs has been undertaken. Alvarez-Mico and colleagues have reported the synthesis of an anomeric glycoconjugate of PCs, while Lee *et al.* describe the synthesis and *in vitro* photodynamic activity of a silicon PC appended with galactose [154, 155]. Lee and colleagues observed increased solubility in most organic solvents, minimal aggregation and high photodynamic activity for the galactose-PC compound against the human HepG2 hepatocellular carcinoma cell line [154, 155]. They also observed very high quantum yields of singlet oxygen formation (Φ_{Δ}): 0.94, 0.79, 0.82 and 0.88 in dimethyl formamide. Analogues of Si(IV) PC conjugated through axial coordination with ligands such as polyethylene glycol (PEG) generally have singlet oxygen quantum yields in the range 0.16-0.52 [147, 155]. Ribero and colleagues report the preparation and evaluation of glycoconjugated PCs - a cyclic glucose heptamer PC [156]. They observed that the β -cyclodextrine moiety imparted a greater degree of solubility on the conjugate in water, however in aqueous solution the conjugate co-exists in its monomeric and oligomeric forms [156]. NC-saccharide conjugate chemistry is also being developed: peripherally substituted tetraglucose Zn(II) NCs have been synthesised by Iqbal and colleagues; however, solu-

bility issues are hindering their evaluation as potential pdt agents [157]. Therefore they have begun to focus their work on incorporating more than four sugar units into the NC-glucose complex to increase the hydrophilicity of the molecule. It appears the potential pdt efficacy of saccharide-photosensitiser conjugates is dependent on the sugar moiety and the photodynamic profile of the photosensitiser; the position and nature of the attachment of sugars to photosensitisers are also important factors in their role as pdt agents.

Antibodies

The term photoimmunotherapy (PIT) is used in reference to pdt utilising photosensitiser-antibody conjugates [3, 14, 25, 65, 122-124, 142, 158-164]. A range of antibody-photosensitiser conjugates have been trialed for pdt including - (scFv) bound to hydroxyl and pyridiniumyl porphyrins [64, 65, 159, 161], and monoclonal antibody (MAb) conjugates of cationic porphyrins [64, 65, 161, 162]. The two main antibody species that have been investigated are MAb and scFv [159, 160, 163]. A number of photosensitiser-MAb conjugates have been evaluated against a

range of targets including oncofoetal antigens; receptors for signal transduction pathways; and growth factor receptors. However, the conjugation of the photosensitisers to the MABs was not efficient: MABs were initially appended to porphyrins *via* activated esters and carbodiimide coupling chemistry to porphyrins bearing multiple carboxy groups and the free amines within the MAb structure, such methodology gives rise to antibody crosslinking issues and/or changes in the photophysics of the photosensitiser [159, 163]. Coupling to polymeric carriers has also been used to increase photosensitiser loading and conjugate solubility. Sutton and colleagues developed a porphyrin molecule (figure 19) that incorporated a reactive isothiocyanate (NCS) group designed to allow conjugation to biomolecules under very mild conditions, with no intermediates or by-products [165]. The synthesised porphyrin underwent bioconjugation through direct reaction of the single reactive isothiocyanato group and the primary amino group present on the side chain of lysine residues; negligible non-specific binding was observed (figure 19) [64, 65, 159].

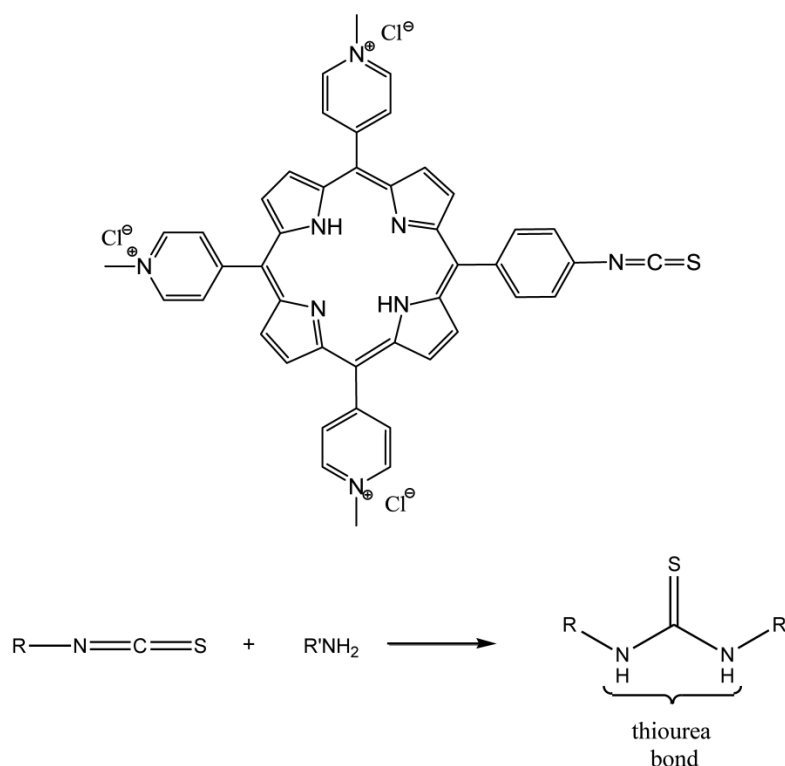


Figure 19. NCS Porphyrin And Isothiocyanate-Amine Coupling Reaction.

Hudson and colleagues directly compared the efficacy of internalising conjugates with conjugates that remained surface bound. Their work focused on conjugating the water-soluble isothiocyanato porphyrin with MAb 35A7 (non-internalising), FSP 77 (internalising) and 17.1A antibodies; the bioconjugations were performed under ambient conditions with antigen binding remaining intact. *In vitro* results suggested 16-fold less of the 5-(4-isothiocyanatophenyl)-10,15,20-tri-(3,5-dihydroxyphenyl)porphyrin (PS1)-FSP 77 MAb conjugate was needed in comparison to the unconjugated porphyrin to yield the same inhibitory concentration (IC_{50}) in the hybrid human ovarian carcinoma (SKOv3-CEA-1B9) cell line [64]. The results reported by Hudson and colleagues added weight to those reported by Carcenac and coworkers: the use of internalising MAb-photosensitiser conjugates has advantages over the use of non-internalising MAbs or free photosensitisers [166]. *In vivo* Hudson *et al.* were able to demonstrate that the PS1-FSP 77 MAb conjugate had biodistribution values comparable with those for the unconjugated MAb in Swiss nude mice subcutaneously implanted with the appropriate antigen expressing cell lines. Hudson and colleagues further reported that the least substituted analogues of 5-(4-isothiocyanatophenyl)-10,15,20-tris-(4-N-methylpyridiniumyl)porphyrin trichloride (PS2)-MAb conjugates had tumour uptake values similar to the native unconjugated antibodies. Hudson *et al.* and Pardridge *et al.* observed that when the substitution of the MAb with the photosensitiser increased, tumour and other organ uptake decreased significantly [64, 167]. Pardridge and colleagues noted that increasing the MAb cationic charge reduced its serum half-life to as low as 5% of the unmodified native antibody [167]. Hudson and colleague's biodistribution data, for the respective conjugate systems, demonstrated retention of MAb pharmacokinetics following substitution of PS1 and to a lesser degree PS2. Tumour/normal tissue ratios (for colon carcinomas) were exceptionally high - 33.5 for PS2-35A7MAb conjugate; data from other groups for unconjugated photosensitisers report ratios ranging between 2 and 4 [64]. There have been fewer reports of hydrophilic PC-MAb conjugates in the literature. Duan and colleagues reported a ZnPC bearing alkoxy substituents conjugated to a MAb while another article describes the first coupling of AIPC(SO₂Cl)₄ to an antibody (E7) - the bioconjugate was reported to increase photocytotoxicity in human bladder carcinoma in comparison to the free photosensitiser [147, 168, 169]. Phototoxicity in the human bladder carcinoma cell line 647V was dose-dependent - at equimolar PC doses the liposomal analogue of the conjugate was

13-fold more effective. Immunofluorescence studies identified specific cell surface localisation and internalisation. Carcenac and colleagues reported results for a AIPCS4-MAb (FSP77, internalising MAb) bioconjugate selective towards ErbB2 on a SKOv3-CEA (CEA - carcinoembryonic antigen) cell line, they found that in comparison to an earlier bioconjugate they had prepared composed of a non-internalising MAb (35A7), the reported growth inhibition after a 20 hour incubation period at a dose as low as 0.04 μ gmol⁻¹ with the AIPCS4-MAb (FSP77) system was 51% in comparison to a 68% growth inhibition with the AIPCS4-MAb (35A7) conjugate under the same conditions, clearly highlighting advantage of an internalising MAb over a non-internalising MAb bioconjugate [147, 170]. Vrouenraets and colleagues describe the coupling of a AIPCS4 to MAbs (U36, E48 and 425) *via* a tetraglycine derivative (AIPC(SO₂N_{gly})₄). They reported having trouble conjugating a second MAb to the photosensitiser due to hydrolysis of the ester groups. The PC-MAb (425) conjugate exhibited the greatest photocytotoxicity against the A431 cell line and selective tumour targeting in nude mice [170]. Vrouenraets and colleagues further report, *in vitro*, photocytotoxic evaluation of *m*THPC and PC-MAb conjugates using five head and neck SCC cell lines; PC in its free form was ineffective but when coupled to MAbs it presented high effectiveness [147, 171]. A recent article by Mitsunga colleagues describes a PC-based photosensitiser coupled to a MAb targeted against epidermal growth factor receptors: promising results have been observed - cell death was induced immediately after irradiating target cells with near-IR light [164].

There are notable drawbacks to using MAbs - they are relatively large and bioconjugate size limits the passage of the photosensitiser-MAb into solid, deep-seated and poorly vascularised tumours. In comparison to MAbs, scFv fragments are antibody fragments that are smaller in size but since they retain the same binding specificity as the larger MAbs they penetrate tumour cells more deeply and effectively [159]. Other antibody fragments that have been investigated include Fab fragments [172]. scFv are observed to clear more effectively from the circulatory system than MAbs because of their lack of an Fc domain, they also exhibit lower kidney uptake. Staneloudi and colleagues reported the preparation of photosensitiser-scFv conjugates utilising the novel NCS porphyrin developed by Sutton *et al.* [159]. Neri and colleagues published research into the targeted delivery of a photosensitiser (tin(IV) chlorin e₆) by a phage-derived antibody fragment (anti-fibrogen antibody L19) in the PIT of endothelial cells in an ocular

model [173]. Staneloudi and colleagues used the same two water-soluble porphyrins they had optimised in the MAb studies and colorectal tumour-specific (LAG3) scFv fragments that had been isolated from a phage antibody display library. They found that at higher molar loading concentrations (20:1 and 40:1 PS:scFv, in comparison to 5:1) the level of binding between the scFv and cell line was reduced or destroyed – suggesting that scFv were more susceptible to interference from antigen binding sites than their MAb counterparts. They reported that conjugation between the more hydrophobic PS1 and scFv was unsuccessful but conjugation between PS2 and the scFv had occurred. PS1 gave significant non-covalent binding, with excess porphyrin reportedly blocking the scFv antigen binding site. Preliminary evaluation of the PS2-scFv bioconjugates showed selective cytotoxicity towards antigen-positive cell lines [64]. A recent perspective by Bullous and colleagues reviews photosensitiser-antibody conjugates in depth [163]. Transferrin, insulin and steroid molecules coupled to photosensitisers have also shown promise as third-generation tumour-targeting systems [135, 147]. Lovell and colleagues have recently published a thorough review on the use of activatable photosensitisers as imaging and therapeutic (theranostic) agents [68]. When in its native state, a photosensitiser's imaging

and phototoxicity properties are quenched, molecular activation of the photosensitiser unquenches its photochemical capabilities, thereby facilitating the photosensitisers role as an imaging and therapeutic agent. Activation is specific to each photosensitiser type and disease and can be achieved *via* a number of routes including environmental factors (such as solvent hydrophobicity and pH); enzymatic means (certain enzymes are overexpressed in specific diseases); nucleic acid mechanisms; and the synthesis of photosensitisers with cleavable bonds [68].

Delivery Vehicles

The poor solubility of many photosensitisers in aqueous media prevents their intravenous delivery directly into the bloodstream. It would therefore be advantageous if a delivery model could be conceived which would allow the transportation of these (otherwise potentially useful) photosensitisers to the site of diseased tissue. Delivery vehicles have been investigated to circumvent the solubility problems of some of these photosensitisers, the main cargo-carrier systems investigated, beside the liposomes already discussed, include emulsions and nanoparticle carriers. PEG and Cremophor EL are two of the more common systems used for the emulsification process, although

a number of other agents have been investigated [14, 25, 33, 34, 42, 174-181]. Cremophor, moleculsol and γ -cyclodextrin have all been compared against one another for the effective delivery of the hydrophobic porphyrin derivative tin etiopurpurin (Purlytin®) [3, 4, 14, 24, 25, 27, 28, 33, 42]. The three emulsifying agents (administered in an aqueous ethanolic solution) all exhibited a greater degree of intracellular localisation relative to that of the “free” ethanolic solution. Results suggested that a lower intracellular concentration of photosensitiser was required to effect cell death when an emulsifying agent was used - a direct consequence of more effective photosensitiser accumulation.

Liposomal Encapsulation

Lipophilic photosensitisers may be encapsulated within the inner hydrophobic region of a liposomal delivery vehicle, while the outer hydrophilic layer (soluble in aqueous media), allows transportation of the photosensitiser towards the target site [14, 182]. Tin-etiopurpurin, benzoporphyrin derivatives and zinc PCs have all been successfully encapsulated in order to demonstrate this technique [4, 14, 42]. Liposome-associated photosensitisers have exhibited greater efficiency and selectivity towards tumour targeting (demonstrated by improved accumulation of the photosensitiser in tumour cells) compared with the same photosensitiser administered in a homogeneous (aqueous) solution [14, 24] - the improved uptake is thought to be the result of the LDL receptor mechanism discussed earlier [24, 49].

Tetrapyrrolics As Imaging Agents

Porphyrinic molecules show potential not only as photosensitisers but their unique luminescent properties make them useful imaging agents too. Porphyrins can be excited by visible light; emit in the red or near-IR regions of the EMS and are advantageous in cellular studies in comparison to those with shorter excitation wavelengths - lower wavelength light (ultra-violet light) can lead to cell damage and cellular autofluorescence can interfere with fluorescence investigations. The ideal fluorophore should also be one with a high quantum yield of fluorescence (Φ_{fl}); a large Stokes shift; minimum photobleaching; and have a high affinity for the target species. Such multimodal agents have been utilised as image guidance tools and hence are useful in setting and adjusting the parameters needed during pdt [7, 28, 183-195]. Porphyrinic photosensitisers may also be radiolabelled and coupled with MRI imaging agents to provide multifunctional probes for positron emission tomography (PET) and MRI imaging in addition

to having therapeutic applications [7, 28, 68, 196-199].

Fluorescence Imaging

In the laboratory fluorescence imaging can be used for studying basic pdt mechanisms; understanding pdt-tissue interactions; developing models of disease; and as a marker of therapy response [7, 28, 68, 183-200]. Fluorescence imaging agents that can be activated around 400nm are extremely useful in diagnostic imaging; the low fluence rates needed to activate the photosensitiser at this wavelength cause little or no cytotoxicity [194]. The history and applications of fluorescence imaging in relation to photodetection have been thoroughly reviewed by Ackroyd and colleagues (2001) [200].

Fluorescence Imaging In The Clinic

Bronchoscopes allow a physician to visualise mammalian airways observing the presence of any diseased tissue. Early versions of the apparatus were rigid metal tubes which required the patient to be sedated/anaesthetised in order to minimise discomfort and relax the airway reflexes. The use of these early versions carried specific risks to the patient such as scratching or tearing of the airway tissue and damaging the vocal cords. Excessive bleeding and pneumothoraxes were further potential complications encountered when biopsies were taken with the apparatus. In 1966 the Japanese physician Ikeda developed the first flexible fibre optic bronchoscope allowing better visualisation of the airways; the flexibility of the scope tip allowed a physician to see deep into the bronchi of the lungs [201, 202]. In the late 1980's Lam and colleagues (MacAulay, Palcic and Jaggi) at the British Columbia Cancer Centre in Canada invented the highly sensitive fluorescence bronchoscopy technique (LIFE-Lung) based on the natural fluorescence (autofluorescence) of bronchial tissue to aid the detection and localisation of pre-invasive and early stage lung cancers - they were awarded the Friesen-Rygiel Award for Outstanding Canadian Academic Discovery (1999) for the invention [191, 203-205]. In 2002 Lam was awarded the Gustav Killian Medal by the World Association of Bronchology for pioneering contributions in the field of early lung cancer diagnosis. The LIFE-Lung (light-induced fluorescence emission) imaging device is now used in over 150 major medical clinics worldwide. LIFE-Lung, originally marketed by Xillix, is based on the principle of naturally occurring fluorescence, *i.e.* when tissue is exposed to light the native fluorophore's fluoresce - no exogenous fluorophores/photosensitisers (drug-induced fluorescence (DIF)) have been administered to the patient for the (auto)fluorescence signal

to appear. The traditional bronchoscopy technique relies on illuminating an area with broad spectrum (white) light and observing the reflected light; when tissue containing abnormal cells is exposed to the light, the physician is able to observe autofluorescence and identify abnormal tissue. However, this subjective approach is generally restricted to the identification of gross macroscopic changes in a lesion - white light bronchoscopy cannot show neoplastic or early neoplastic changes [185]. The optical properties of human tissue are dominated by endogenous light absorbing chromophores, which absorb in the 250-500nm spectral region of the EMS and exhibit fluorescence emission over the 300-700nm range. Complex tissue such as bronchial mucosa is made up of different cell types (epithelial, connective and vascular); total fluorescence emission is made up from each individual chromophore, each with its own unique and characteristic spectra (spectral content and intensity - fluorescence quantum yield); this composite emission is termed autofluorescence and generally covers a broad spectral band, although characteristic features tend to be lacking [185]. Autofluorescence can be enhanced by the addition of exogenous chromophores, such as photosensitisers, facilitating the monitoring of drug localisation properties; the technique is termed photodynamic diagnosis (pdd) and relies on the selective uptake and retention of photosensitisers within abnormal tissue, enhancing the image contrast between the healthy and abnormal tissues. DIF is generally greater in intensity than autofluorescence and displays characteristic luminescence features [28, 185, 188, 193, 194, 198]. Autofluorescence bronchoscopy has been commonly used in observing/imaging the lungs, bladder, ovaries, skin, brain and gastrointestinal tract [28, 185-194]. Reviews by Ethirajan *et al.*; Allison *et al.*; Moghissi *et al.*; and Celli *et al.* cover the topic in more detail - Ethirajan *et al.*'s. and Celli *et al.*'s. reviews are particularly thorough [28, 183, 186, 194]. It is worthy to note Celli and colleagues refer to "pdd" as "photosensitiser fluorescence detection" (PSFD) rather than diagnosis - diagnosis could be interpreted as the ability to grade and stage tumours, as opposed to detect them; photodynamic implies generation of ROS [194]. Therefore, for technical clarity in the remainder of this review, the term PSFD will be used instead of pdd.

Lam *et al.*'s. LIFE-Lung system uses a Cd-He laser (excitation 442nm, blue light) and an optical multi-channel analyser detection system to provide real-time video imaging capabilities. When exposed to blue light normal bronchial mucosa tissue emits a green-coloured fluorescence signal; the presence of dysplasias or carcinomas is observed through a red-

dish/brown fluorescence signal from the abnormal tissue. The spectral differences are due to the chemical constituents of the respective tissue histology – one hypothesis is that the connective tissue beneath the epithelial of the bronchial mucosa displays a more intense fluorescence signal in comparison to the fluorescence signal from the epithelial cells, therefore when exposed to blue light, the green fluorescence emission from the connective tissue underneath the healthy epithelial dominates the observed signals. In the case of neoplastic changes in tissue, the epithelial layer is thicker and contains a lower concentration of fluorophores, hence a reduction in the intensity of the fluorescence signal observed from the connective tissue, there is also a relative shift in the spectral emission from green (healthy) to red (abnormal) [186]. The LIFE-Lung system can be used by physicians in adjunct to the conventional white light examination technique; autofluorescence is more than four times more sensitive in identifying morphological changes specific to pathological progression than the white light used in traditional bronchoscopy and can detect lesions as small as 1mm and only a few cells thick, thus a more definitive identification of lesions can be made [186, 206]. Prior to the clinical implementation of autofluorescence it was necessary for a patient to undergo a number of bronchoscopy procedures whereby multiple biopsies were taken in order to appropriately identify and localise lesions present with occult cancer [186]. Lam and colleagues report an increase in the sensitivity in identifying and localising intra-epithelial neoplastic lesions by a factor of 6.3 when autofluorescence and white light illumination are used as complimentary imaging methods in comparison to using white light alone; sensitivity was increased by a factor of 2.7 when invasive carcinomas were also present [186, 193, 207]. A number of different systems have now been developed for autofluorescence imaging all based on laser or filtered high intensity arc lamp illumination. LIFE-Lung was marketed by Xillix (Canada) in 1993; the D-Light system, marketed since 1995 by Stortz (Germany) can be manually switched between white light and blue light modes; the SAFE system (versions 1000 and 3000) marketed by Pentax (Japan) since 2006 incorporates a single action image switching and simultaneous display; the Evis Lucera Spectrum Autofluorescence by Olympus was also brought to the market in 2006 and comprises of three signals which induce autofluorescence by blue and reflected (550-610nm) light; ONCO-Life (Novadaq Technologies, Canada) also combines fluorescence and reflectance imaging; the combination of fluorescence and reflectance imaging is aimed at reducing the number of false-positives

reported; it can be difficult to distinguish fluorescence emission produced from increased vascularity (associated with airway inflammation) to that produced from pre-invasive lesions [186, 189]. The quantification of the reflectance (red) and fluorescence (green) intensity signals allows the red:green ratio (R/G), termed the colour fluorescence ratio (CFR), to be determined for the area being examined [189, 191, 192]. The resulting CFR assists the physician in making a more confident and precise identification of abnormal tissue (moderate dysplasia and/or carcinoma *in situ* that has begun to progress) for biopsy; Lee and colleagues report a good correlation between the CFR-identified abnormal tissue and histological-verified diseased tissue [189]. Updated versions of the LIFE-lung (LIFE-Lung II) with a filtered Xe lamp to produce blue light and with two image-intensified charge-coupled device sensors to capture emitted fluorescence: one in the green region (480–520nm) and the other in the red region (≥ 625 nm) and the Evis Lucera system (with narrow-band imaging capabilities) are now available [186, 189]. The significant and rapid improvement in fluorescence imaging technology has increased the number of body areas physicians are able to take biopsies from without the need for surgery. New technology is focusing on high definition optical systems with recording options facilitating the ability of a team of medics to view live images (not just the physician) and for the team to view the images at a later date when planning treatment regimens [185].

History Of Fluorescence Imaging

Observation of autofluorescence in tumour localisation is not a modern interest and dates back to 1924 when Policard observed the fluorescence (brown/red) of malignant tumours - characteristic Hp fluorescence was observed when rat sarcomas were illuminated with ultraviolet light, demonstrating the preferential accumulation of a photosensitiser in cancerous tissue [185, 194, 208]. These observations were supported by the studies (1940's) of Auler and Banzer and Figge and colleagues who evaluated the tumour-localising properties of several porphyrin and metallo-porphyrin compounds [209, 210]. The latter group's studies revealed that all of the porphyrin species investigated emitted localised fluorescence from tumour tissue but not from healthy tissue upon ultraviolet illumination, with the exception of lymphatic; omental; faetal; placental; and traumatised regenerating tissue. A clinical study of PSFD was undertaken in the 1950's by Figge and colleagues utilising the Hp hydrochloride salt to demarcate benign and malignant tumour tissue; fluorescence from the

photosensitiser was evident in a greater percentage of malignant tumour tissue than benign tissue and the intensity of the fluorescence signal increased with increasing photosensitiser concentration, to the extent that solid tumours could be observed through intact skin [211]. DIF was first used in the clinic (Mayo Clinic, USA) in the 1960's when Lipson and colleagues used a fluorescence endoscope to view HpD differential fluorescence between tumour and healthy tissue [212, 213]. The same decade saw Sutro and colleagues report the observation of contrasting fluorescence signals from excised human breast cancer tissue (purple/red emission) to healthy surrounding tissue (green fluorescence) [214]. Further clinical studies were undertaken with HpD in the fluorescence detection of cervical and lung cancers; head and neck tumours; and a number of bladder malignancies - the one large-scale study (226 patients) conducted by Gregorie and colleagues concluded with disappointing results: only 76.3% of the patients with confirmed malignant neoplasms displayed positive tumour fluorescence [215]. The late 1970's and early 1980's witnessed a number of groups conduct detailed investigations into the uptake and pharmacokinetic profiles of HpD-based PSFD and pdt [216, 217]. Gomer and Dougherty conducted detailed tissue timing and distribution studies in healthy and malignant tissue and reported higher concentrations of HpD in tumour tissue compared to cutaneous tissue or muscles of mouse models bearing a mammary carcinoma; the highest concentrations of HpD were in the liver, kidneys, spleen and lungs [216]. Jori and colleagues reported in a similar study that relative to the HpD in the liver, only small concentrations of HpD were metabolised by tumour cells in a rat ascites hepatoma model [217]. Both groups reported that time windows (Gomer and Dougherty 24 hours, Jori and colleagues 12 hours) existed during which the higher accumulation of HpD in the tumour tissue relative to surrounding healthy tissue allowed for tumour destruction with minimal toxicity to the healthy tissue. Kessel's investigations, along with those by Unsöld and colleagues, identified the issue of HpD impurity as a limiting factor in its ability to accurately and reliably identify the boundaries of diseased tissue in detection and/or surgical guidance [218, 219]. However, Balchum *et al.*, Hyata *et al.* and Cortese *et al.* employed HpD to induce fluorescence as a means of locating early endo-bronchial tumours in the clinic in the 1980's [220-222]. Moghissi and colleagues highlighted in their 2008 review (on fluorescence bronchoscopy) that over 200 articles had been published on fluorescence bronchoscopy (since the 1980s) and autofluorescence (since 1992) [186]. Fluorescence imaging has

now become well-established and is routinely used in a number of clinical and medical applications/situations, including in the identification of neoplastic changes; localisation and topographic distribution of neoplastic lesions; fluorescence-guided local cancer therapy for airway; dermatological; bladder; and brain cancers [28, 183, 185-194]. In oncology, the use of fluorescence detection has significantly enhanced the diagnostic process and has seen a range of minimally invasive procedures and intervention methods introduced into cancer treatment and management, particularly in the identification and localisation of pre- and early cancerous lesions as well as image-guided therapy [28, 183-194].

Lung cancer is the most common cancer in men in the industrial world and the most common cause of death amongst all cancers in men and women in the UK, Europe and USA. Surgical resection is the treatment of choice for all histological varieties of lung cancer, except the small-cell type. There is a definite relationship between the stage of cancer at diagnosis and outcome in terms of survival. For patients with early stage I cancer a greater than 70% chance of a 5 year survival rate can be achieved, however, in the absence of a reliable screening programme, less than 15% of patients are diagnosed at this stage [186]. In the majority of cases, over 80% of lung cancers are inoperable at presentation, limiting treatment options and the potential of achieving a "cure" [186, 189]. Central-type lung cancer at its initial development is radiologically occult (presentation of clear chest x-rays/CT scan) [186]. Chest x-rays have previously failed to identify up to 77% CT-detected cancers [190]. Although, it may (with great difficulty) be possible to detect the disease with white light bronchoscopy, the use of blue light more readily discriminates lesions from normal tissue; these differences are more visible by a factor of 7 in comparison to white light - this was reported for all "reviewed" cases of autofluorescence *versus* white light bronchoscopy [186]. Autofluorescence bronchoscopy has also been successfully used for staging cancer - 9.3% of patients who were identified for surgical resection showed additional lesions in pre-surgery autofluorescence bronchoscopy [223]. Furthermore, autofluorescence bronchoscopy has shown greater reliability than sputum testing in diagnosis - sputum testing was reported to have missed 100% of the lesions in a clinical study [224]. Unfortunately, autofluorescence isn't without drawbacks - its specificity is much lower than that of white light bronchoscopy; there are recordings of false positives in autofluorescence bronchoscopy; there is difficulty distinguishing airway inflammation from pre-invasive lesions based on the visual grading of

tissue fluorescence, this can result in excessive biopsies; longer procedural times; a greater risk of complications; and greater cost, it is therefore good practice to employ autofluorescence bronchoscopy as an adjunct technique to white light bronchoscopy [186, 189]. In the post-surgical surveillance and monitoring of post-pulmonary resection patients (resection performed with curative intent), 12% of a group of 25 patients and 6% of a group of 51 patients developed intra-epithelial neoplasia solely diagnosed by autofluorescence [225, 226]. When a patient is subject to monitoring, if lesions (early and recurrent) are identified and are in the early stages of the disease, it has been postulated that any further lesions found in follow-up protocols can be treated with endoluminal pdt with curative intent [186, 227, 228] - there is widespread acceptance of pdts safety and efficacy in a bronchoscopic application for broncho-pulmonary malignant neoplasia [188].

Fluorescence Imaging, Guided Resection And Pdt - A Theranostic Approach To Disease

In the early stages of lung cancer pdt can provide long term survival opportunities (potential cure); in the mid-stages, where the extent of the disease can be more accurately diagnosed with fluorescence imaging and endoscopic ultrasonography, results can match those of surgical resection [188]. Systemic photosensitiser administration, followed by bronchoscopic illumination is used to achieve cancer necrosis; a combination of imaging and pdt (theranostics) can therefore provide improved therapeutic strategies for lung cancers [188]. The combination of the modalities can also help in laboratory-based disease research; fluorescence imaging can be utilised in studying basic pdt mechanisms; understanding pdt tissue interaction; developing disease models; and as a marker to therapy response [194]. The two modalities (fluorescence imaging and pdt) work on the same basic principles - illumination and photochemistry but differ greatly in their desired outcome - fluorescence imaging has minimal/no cytotoxicity due to the low fluence rate used to generate light activation, whereas in pdt, where a cytotoxic effect is the goal of the treatment, a high fluence rate is used to generate the singlet oxygen necessary to elicit cell death [194]. Both the uniqueness and major advantage of using fluorescence imaging and pdt in combination with each other is that the same entity can act as both the imaging and therapeutic agent, the only known exception to this is **TOOKAD®**, the palladium-complexed bacteriochlorophyll (figure 20); **TOOKAD®** has a negligible fluo-

rescence quantum yield [229, 230]. This emphasises the potential of fluorescence imaging in pdt for the diagnosis, guided therapy and monitoring of surgery (or in other therapies) - the therapeutic outcome in the treatment of disease can be made more robust by utilising all of the available forms of imaging and guidance techniques/technologies. Such theranostic modalities are likely to become more routinely used in the treatment and management of diseases in the future [194].

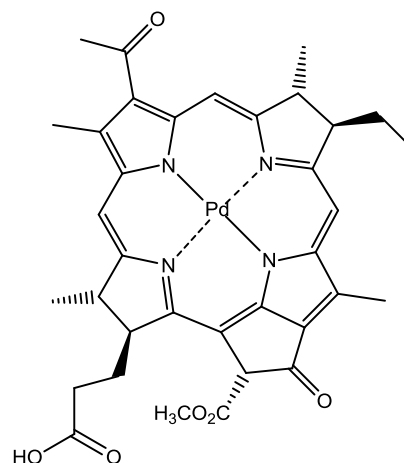


Figure 20. **TOOKAD®**

A number of different imaging systems exist which are capable of observing molecular, structural and functional parameters of the mammalian body. The type of imaging system is chosen depending on the spatial scale of the entity to be imaged and the source of contrast enhancement. For example, imaging at the molecular level, involving small molecules and proteins (ranging from 10ppm-10nm), can be achieved with spectroscopy-based techniques including MRS (magnetic resonance spectroscopy), PET and optical spectroscopy; such imaging techniques facilitate the visualisation, characterisation and quantification of biological targets and processes at a cellular level; particularly useful for the imaging of singlet oxygen [194]. Microscopy, surgical microscopy, endoscopy, ultrasound and fluoroscopy techniques can be used for imaging organelles; cells; tissue matrices; physiological ducts; and tissue layers ranging in size from 50nm-100mm and are valuable platforms in surgical-guidance, therapy monitoring and dosimetry procedures [194]. When images of body organs and the whole body are required tomographic techniques such as computerised tomography (CT) and MRI are employed [194]. Imaging at the molecular level provides the ability to monitor *in vivo* responses to pdt in near/real-time [194]. In many situations, the

outcome of an oncological treatment is only known at a much later date when the patient is undergoing post-sampling protocols or when the disease may have progressed/recurred due to incomplete removal and/or poor treatment response; online and/or early monitoring approaches are invaluable in developing strategies to combat inadequate treatment responses - one strategy is the use of image-guided surgical-resection (achieved with autofluorescence bronchoscopy and/or DIF) [194]. Due to the propensity of photosensitisers to preferentially accumulate in neoplastic tissue their fluorescence properties makes them inherently well-suited for the selective visualisation of tumours using the fluorescence contrast between healthy and diseased tissue to demarcate the boundaries around diseased sites. The ability to accurately define the margins of a tumour is a crucial step in the optimisation of surgical resection; a cancer-free margin around the cancerous tissue that is being excised is a major predictive factor in the success of the treatment and the long-term outcome for the patient [28, 183, 194]. Particular care must be taken not to remove too much healthy tissue - this is most apparent in brain surgery, for example, if 1mm of tissue were unnecessarily excised motor skills could be detrimentally affected with severe implications to the patient's quality of life [194]. The suitability of PSFD for clinical translation has allowed its use for selective identification of cancerous lesions in a broad range of anatomical sites including the lungs, bladder, brain, skin, breast and female reproductive tract [28, 183, 185, 188, 191, 193, 194, 198]. The limitation of PSFD, particularly, in comparison to PET, MRI and CT, is the inherent surface sensitivity of the technique; PET, MRI and CT are able to provide structural details that are not achievable with PSFD - the detection sensitivity of PSFD decreases during the resection process as the volume of non-resected disease diminishes - the sensitivity of fluorescence imaging is not affected [194]. PSFD had its first widespread and successful implementation in identifying diseased tissue after Kennedy and Pottier introduced an alternative approach of enhanced endogenous protoporphyrin (PPIX) production in the haem cycle of tumours in the early 1990s [231, 232]. The strategy is based on the *in situ* conversion of ALA, a non-photoactivatable precursor, into PPIX, a naturally occurring photosensitising species *via* the cellular haem biosynthesis pathway (Figure S1/scheme 1). In the synthetic pathway iron is inserted into the PPIX cavity to form haem; the ferrochelatase enzyme that catalyses this chelation is down-regulated in many tumours and as a result iron is chelated into the PPIX cavity at a relatively low rate and is unable to com-

pensate for the excess PPIX formed - significant accumulation of PPIX in neoplastic tissue occurs as a result following administration of exogenous ALA. The rates of ALA uptake in healthy *versus* neoplastic tissue are thought to be comparable; it is the differential rates of ALA conversion and resulting accumulation of PPIX that are the primary force behind favourable tumour selectivity [194, 233]. PSFD has proved a powerful tool in the detection and guided resection of bladder cancer and has been reviewed by Witjes and Douglass [194, 234]. Bladder cancer is the fourth most common malignancy in men and the industrial world; it has a high rate of recurrence and is a very costly cancer to treat and monitor [235-237]. A critical factor in predicting disease recurrence is the detection of carcinomas *in situ* (CIS); these flat lesions are particularly difficult to detect with white light due to the poor contrast they generate [194, 236]. Levulan® has proved successful in the fluorescence identification of numerous bladder lesions that were not detected by white light bronchoscopy; the detections were 100% supported by histological validation [194, 238-241]. In the follow-up assessment of patients with fluorescence imaging, the superior sensitivity of the modality led to a reduced rate of early recurrence of superficial bladder cancer in comparison to white light evaluation [242]. In a phase III trial, comparing transurethral guided resection using ALA *versus* white light cystoscopy, 61.5% of the patients in the PPIX fluorescence endoscopy group were tumour-free at the follow-up assessment in comparison to only 40.6% in the white light group [243]. The hexylester derivative of ALA, Hexvix®, has been used to achieve greater tissue penetration depths into the urothelial layers and a more homogeneous distribution in malignant tissue; Hexvix® produced a stronger fluorescence intensity at a lower dose following a shorter incubation time [244]. Fluorescence-guided resection (FGR) has also been used in the treatment of brain cancer; when ALA-induced PPIX was used in a guided resection study 63% of the patients achieved complete resection through contrast enhancement. A phase III trial was terminated at the interim analysis of 270 patients, when 65% of those in the FGR group (procedure followed by standard adjuvant radiotherapy) were free of residual disease at the post-operative 6 month assessment (by MRI), compared with 36% in the white light group. It is noted that the survival curves for the patients in both groups converged after 15 months [194, 245]. Foscan®, particularly suited to imaging and treating bulky brain tumours due to its depth of light penetration, has been evaluated by Zimmermann and colleagues for the FGR of malignant gliomas; in 138 tissue specimens

from 22 of the patients, a sensitivity and specificity of 87.9% and 95.7% were achieved [194, 246]. In 10 of the 22 patients, malignancies were not identified by white light examination but were exclusively identified by PSFD [194, 246]. Foscan® has exhibited further advantages over ALA-induced PPIX in that after several minutes of illumination it does not undergo photobleaching. To date, FGR has been invaluable in improving the extent to which tumour tissue can be removed but is now beginning to show promise in cases where a tumour cannot be completely removed because it has infiltrated functional brain tissue; the residual tumour tissue can be treated with pdt. In a

standard treatment protocol, surgical resection is followed by adjuvant radiotherapy, however, when FGR is used instead of white light, the photosensitiser is already present in the tissue at the time of resection; a logical extension of the procedure would be to use pdt to selectively destroy any residual disease in the resection bed - a great example demonstrating the promise of theranostic regimens. Kostron and colleagues reported results from a study on FGR with adjuvant pdt in a group of patients (26) with malignant brain tumours using m-THPC; an increase in median survival from 3½ months to 9 months was achieved [247].

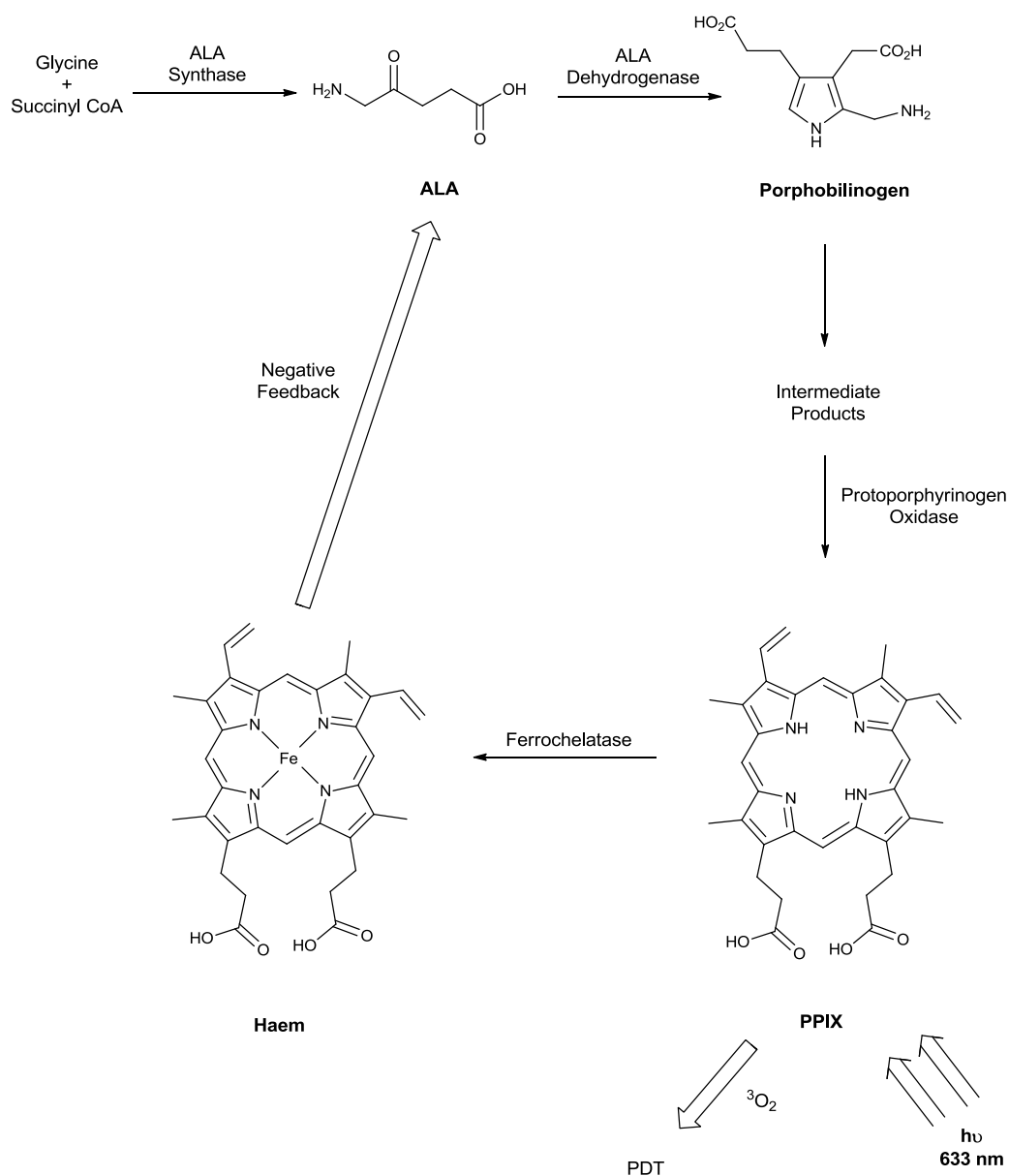


Figure S1. Scheme I. Simplified Haem Biosynthesis.

In 2007, Stepp and colleagues also reported an evaluation of FGR in combination with adjuvant pdt in the treatment of malignant glioma. When ALA was used the assessment showed healthy brain tissue was practically free from ALA [248]. The most extensive work in image-guided resection and the pdt of gliomas is by Wilson and colleagues [249-252]. Their "point and shoot" system initially used Photofrin[®], before moving on to ALA. They demonstrated that their intra-operative fluorescence imaging system not only improved tumour resection but allowed pdt of the residual tumour [249-252]. Bogaards and colleagues have investigated the impact of low light doses over extended periods of time *via* implanted diodes, as opposed to the conventional methodology of a single light dose at a higher fluence rate [251]. Gibbs-Strauss and colleagues have investigated measuring the fluorescence of PPIX through the cranium with the idea that more frequent screenings can take place non-invasively [253]. Reddy and colleagues have undertaken pre-clinical studies on nanoparticles with increased specificity (through a targeting peptide) for both imaging (MRI) and the pdt of brain tumours. They monitored the pharmacokinetics and distribution of the nanoparticles within a 9L rat glioma model and reported a pronounced increase in the survival rate of the animals in the targeted-nanoparticles therapy group; a survival probability of approximately 0.4 at 60 days was achieved post-treatment compared to death within 20 days for the control groups [254]. To date, ALA-induced PPIX FGR in brain tumours has been the highest impact application of PSFD.

DIF has been utilised in ovarian cancer; ALA/Hexvix[®]-induced PPIX has been used to image lesions in ovarian cancer undetected by white light imaging, the intensity ratio of neoplastic to healthy tissue was approximately 4:1 (optical biopsied lesion size was as small as 1.0mm (0.3-2.5mm) and 1.5mm (0.5-2.9mm) for white light) [255, 256]. Over 70% of patients presenting with ovarian cancer have late stage symptoms, leading to the high mortality rate observed with the disease. These patients undergo surgical debulking and cycles of chemotherapy, there is also a high likelihood of disease recurrence resulting in a 5 year survival rate of 31%, this can be increased to a 93% chance of survival after 5 years when the disease is diagnosed early and has not spread to regional and distant sites [194]. Ovarian cancer presents particular challenges in its thorough imaging and diagnosis – the disseminated disease has microscopic tumour nodules implanted throughout the peritoneal cavity. These nodules can be missed during surgical debulking and escape detection by traditional

laparoscopic second-look procedures; PSFD shows great potential in the more thorough imaging/detection of the microscopic diseased nodules [257-259]. In a clinical study (29 patients) using ALA-induced PPIX, the ovarian cancer nodule detection sensitivity was 92%, a huge improvement over traditional white light imaging. The same study also identified that in 13 patients where the disease had been confirmed histologically or cytologically, 4 patients had lesions that were detected only by fluorescence imaging [260]. Zhong and colleagues combined PSFD (Visudyne[®]) with high-resolution fluorescence microendoscopy to detect (*in vivo*) nodules of a disseminated ovarian cancer in the peritoneal cavity of mice on the order of a few tens of micrometres [261]. Zhong *et al.* used PSFD to conduct baseline imaging to assess the disease state immediately before intra-peritoneal therapeutic radiation, Visudyne[®] was then activated and treatment response assessed in follow-up imaging several days later allowing the quantitative reporting of treatment response. The data revealed that the tumour nodules continued to grow unchecked in untreated mice while in the treatment group a significant reduction in tumour volume was observed. The observation highlights the promise photosensitiser-based fluorescence shows in monitoring pdt response in outcome assessments post-therapeutic intervention [261]. Further studies are required to indicate the true value of the modality in reporting treatment outcome.

The accessibility of skin lesions and the ease of topical photosensitiser application has seen the integration of PSFD and pdt in the imaging and treatment of dermatological conditions, including SCC, basal cell carcinoma (BCC), Bowen's disease (SCC *in situ*), Paget's disease and the guidance of Moh's surgery [194]. Pdt (using ALA) was successfully demonstrated in the treatment of superficial BCC and SCC in 1989; Kennedy, Pottier and Pross reported that the topical application of ALA was suited to delineating malignancies of the skin due to the preferential uptake of ALA in abnormal keratin cells *versus* normal keratin cells, enhancing the fluorescence emission contrast of abnormal tissue [232]. Photosensitiser fluorescence imaging has been used to try and increase PPIX-based fluorescence tissue contrast in healthy skin in seven patients with nodular BCC; SCC *in situ*; or cutaneous T-cell lymphoma. Andersson-Engels and colleagues used a multi-channel fluorescence imaging system to collect PPIX fluorescence emission (635nm), autofluorescence (470 and 600nm) and photobleached product emission (670nm) from cancerous lesions and surrounding normal tissue pre- and post-pdt [262, 263]. The data was used to deconvolute background

autofluorescence from tumour-based PPIX fluorescence on a pixel-by-pixel basis. Andersson-Engels *et al.* have also used fluorescence imaging to demonstrate the potential of tracking the accumulation of photodegraded products during pdt. Further studies are needed to corroborate verification of tumour margins and pdt treatment response using multi-channel PSFD. Hewett and colleagues have demonstrated the ability to monitor the kinetics of PPIX photobleaching pre-, during and post-pdt of superficial skin cancer *in vivo* using a multi-spectral fluorescence imaging system with an integrated excitation source – they varied rate of light delivery and fraction schedule to optimise treatment outcome [264]. The study demonstrated rapid photobleaching early in the pdt treatment, indicating light doses should be delivered at a slower rate or fractionated over the course of the treatment to achieve greater consistency in the therapeutic effect. Hewett and colleagues attempted to use PPIX-induced fluorescence contrast and autofluorescence from the surrounding tissue to more accurately delineate the lesion margins. In understanding the importance of the role of ALA-induced PPIX synthesis and distribution in abnormal *versus* normal tissue in PSFD, pdt and therefore treatment outcome, Martin and colleagues examined the macroscopic heterogeneities in PPIX distribution in patients (20% ALA applied topically to 16 patients) with BCC [265]. Significant heterogeneities in PPIX fluorescence patterns were observed, suggesting no preferential selectivity of the photosensitiser for BCC over healthy tissue. Martin *et al.* purported any macroscopic selectivity could be attributed to the increased stratum corneum surrounding the diseased tissue as well as tumour thickness effects. Their study emphasises the usefulness of PPIX-induced fluorescence in the treatment of malignant cutaneous lesions or superficial BCC but highlights that in the treatment of deeper lesions optimisation of ALA formulation and delivery is important. The need to improve selectivity and homogeneity of photosensitisers in diseased tissue has been addressed by Fritsch and colleagues [266]. They compared ALA- *versus* Metvix[®]-induced PPIX production in human solar keratoses to surrounding healthy skin. Higher levels of total PPIX accumulation was observed in the skin keratosis cells *versus* healthy cells for ALA compared to Metvix[®]. Selectivity of Metvix[®] for skin keratoses cells over healthy cells was significantly greater than with ALA. Distribution analysis revealed that 82% of the porphyrins in skin keratoses were specifically composed of PPIX in comparison to 89% in normal skin cells when incubated with Metvix[®]. PPIX represents 90% of

ALA-induced porphyrin metabolites in both healthy and diseased cells. Moan and colleagues investigated the use of a second ALA derivative, Hexvix[®], in relation to ALA and Metvix[®] in the treatment of dermatological conditions [267]. They found that the PPIX concentrations needed to induce half the maximum PPIX-induced fluorescence were 2% (ALA), 8% (Metvix[®]) and 1% (Hexvix[®]) when the pro-drugs were applied at 0.2%, 2.0% or 20% w/w, highlighting the potential of achieving a similar fluorescence outcome (PPIX concentration) for Hexvix[®] at an eighth of the concentration needed by Metvix[®] in healthy cutaneous tissue. Kuijpers and colleagues have evaluated the response rates of ALA and Metvix[®] pdt of BCC and acne *vulgaris* to report that there was no differential outcome in the two photosensitiser pro-drugs [268, 269]. A greater incidence of severe side effects was reported for ALA-pdt than Metvix[®]-pdt [270]. This is perhaps surprising given that there is a marked contrast in the PSFD of bladder cancer where the ALA-derivative Hexvix[®] is preferred and widely accepted in the imaging protocol rather than ALA [194]. Redondo and colleagues conducted a clinical pilot study into the use of Metvix[®]-induced PPIX fluorescence for the guidance of Moh's surgery in the delineation of BCC; they compared the margins identified by Metvix[®]-induced PPIX PSFD; white light imaging; and histopathology evaluation [271]. The margins in the diseased *versus* healthy tissue in 14 out of 20 patients determined by PSFD corresponded exactly to the gold-standard histopathological evaluation (haematoxylin-eosin staining). This allowed the step-wise excision of diseased tissue until the presence of the healthy tissue was verified (histologically). In half of the patients the diseased regions determined by PSFD (and confirmed by histology) were larger than those determined by white light imaging. It was noted that PSFD did identify 3 false-negative results and 3 false-positive results; 2 of them from recent scar tissue [271].

The outcome of oral cancer in terms of survival/cure is also determined by the stage of the cancer at the time of diagnosis: a 5 year survival rate of 82% for early stage cancer, reduced to 53% for regional spread cancer and considerably lower at 23% for distant spread cancers [272]. Leuning and colleagues evaluated the use of ALA-PSFD in the detection of small lesions/early-stage cancer and observed that ALA-induced PPIX fluorescence identified a group of patients with dysplasia; carcinoma *in situ*; primary tumour; secondary carcinoma; and tumour branches that were not detected by white light examination [270, 273]. Subsequent studies by the group added further support to the use of combining PSFD and

autofluorescence together and observed that the ability to demarcate neoplastic regions was independent of disease stage - an additional benefit of PSFD [274]. Ebihara and colleagues reported that in a hamster cheek pouch model of oral cancer fluorescence emission from PPIX can differentiate between the different stages of pre-malignancy and malignancy [275]. Duska and colleagues have reported that in cervical malignancies oral administration of ALA overcame the penetration and distribution inhomogeneity experienced with topically delivered ALA [194, 276].

Fluorescence Imaging, Site-Activatable Constructs And Pdt - A Theranostic Approach To Identify And treating Diseased Tissue

Non-specific localisation of photosensitisers often leads to sub-optimal treatment outcomes and unwanted toxicity in healthy tissue; targeting strategies and the synthesis of target-activated photosensitisers have been investigated to try and address this short-coming. Site-activated photosensitisers achieve specificity for tumour tissue by selective activation of the entity in the diseased tissue by tumour-specific agents [194]. Applications of such entities in imaging and pdt have been reviewed by Stefflova [277]. The principle of the constructs is based on energetically quenching a photosensitiser by placing two photosensitisers within close proximity to each other (self-quenching) or a dye (energy-transfer). If the chemical bonds holding the photosensitiser and quencher together are broken the photosensitiser will no longer be quenched and will become fully activated [194]. Weissleder carried out the early work in this area by developing protease-activated near-IR probes for cancer imaging [278]. The group went on to report the conjugation of a chlorin photosensitiser (C₆) onto a polylysine backbone [279]. The photosensitisers were held in close geometry to each other in order to facilitate efficient self-quenching, preventing energy transfer between the photosensitiser and molecular oxygen. In the presence of tumour-associated enzymes (for example cathepsins), the peptide linkages of the polylysine backbone were cleaved and the "degraded" probes became highly phototoxic and fluorescent. Weissleder and colleagues went on to evaluate (*in vivo*) the novel theranostic construct for pdt efficacy and imaging using fluorescence molecular tomography to determine the distribution of C₆ in tumours; the target tissue was visualised and the local drug concentration quantified before selective therapy was applied [279]. Lovell and colleagues have reported establishing the correlation

between photosensitiser fluorescence quenching and singlet oxygen quenching; implying that fluorescence intensity can be used as an indicator for the status of singlet oxygen production by a photosensitiser [280]. Zheng and colleagues put this notion into practice by introducing several Förster/fluorescence resonance energy transfer (FRET)-based target-activatable constructs consisting of a photosensitiser and quencher - the authors termed the constructs "photodynamic molecular beacons" [281]; the feasibility of the construct was demonstrated using an apoptotic factor-cleavable linker - as already mentioned apoptosis is the preferred mode of cell death in pdt, thus an apoptotic factor-cleavable linkage carries implications in the molecular imaging of pdt-induced apoptosis [281]. The construct wasn't selective for tumour cells but the selectivity will undoubtedly be fully addressed in the near future. One solution would be to photodynamically activate a photosensitiser with the matrix metalloproteinase MMP-7 - an important tumour biomarker [281]. Zheng and colleagues have also demonstrated the potential of target-activatable constructs in the treatment of pathogens - a phenothiazinium-based target-activated construct has been developed against β -lactam producing phenotypes in an approach termed "see and treat" [282].

Imaging And Monitoring - Time Gated Fluorescence, PET, MPE, OCT And MR Imaging

It can be difficult to determine specific dosimetry in pdt due to the non-linear relationship between light dose, irradiation time, photosensitiser and molecular oxygen concentrations. During the administration of light (in pdt) there are a number of photophysical, metabolic and molecular changes occurring within the target tissue, each change providing a unique signal. Several techniques for measuring effective dose-response relationships online exist including measuring a photosensitiser's fluorescence and dynamic properties during photobleaching. Time-gated fluorescence imaging is one example used to detect cancerous tissue and monitor the emission of disulphonated aluminium PC (AlS₂PC) during pdt of MS-2 fibrosarcomas [283, 284]. The technique reports differences in spatial variation to response - some mice displayed enhanced fluorescence emission while others exhibited a decrease in fluorescence intensity - however, further investigations are needed to fully evaluate this technique for use in dosimetry studies [284]. The Lecomte group (Sherbrooke, Canada) observed (1999 and 2006) online changes in tumour metabolism using dynamic PET in rat and mouse

mammary tumours [285, 286]. They were able to report dynamic changes in perfusion rates and metabolic activity in the pdt of tumours. PC-based photosensitisers were irradiated for 30 minutes or 2 hours during the PET protocol. Three distinct phases of cellular metabolism were identified as being related to therapeutic or biological factors. Within the first 3 minutes of a radiolabelled agent (fluoro-2-deoxy-D-glucose) being administered the imaging scans indicated tumour perfusion – the 3-15 minute time period was associated with the type of tumour death (direct cell killing or indirect cellular necrosis) occurring; tumour uptake after 15 minutes was correlated to cellular metabolism and reflected the efficacy of the photosensitiser [285, 286].

PET imaging is relatively new in pdt and is still in its infancy but shows promise in the ability to visualise real-time changes in treatment parameters allowing an optimal therapeutic outcome to be achieved. The technique can be used to image the whole body and has been used to detect hyper-metabolic cancers; it has proved sensitive enough to detect cancers ranging from lung, breast, colorectal, pancreatic, head and neck and malignant lymphoma and melanoma, it has also been used in identifying unknown primary tumours in patients [28, 194]. The technique can provide quantitative drug biodistribution data – a parameter not achievable with optical imaging platforms [70]. Blood flow dynamics have been studied using fluorescence imaging, laser speckle imaging and Doppler optical computed tomography (OCT) in the prediction of vascular occlusions as a signal for photodynamic therapeutic end point [287-294]. Fluorescently-labelled antibodies (against endothelial cells CD32 and platelet aggregation CD41) in combination with a cell permeability/viability indicator have been used to image immediately before and post-6 minute illumination period of pdt performed with Verteporfin® [295]. The ability to measure therapeutic signals in real-time during light application potentially offers the physician the ability to appropriately adjust the therapy during the treatment procedure [194]. In pdt, monitoring photosensitiser fluorescence may facilitate immediate changes to be made; whereas during PET real-time assessment cannot be made – fluoro-2-deoxy-D-glucose's metabolism is a direct result of pdt and cell death may not be observed until hours or days after the treatment has finished [194].

Fluorescence imaging, PET, CT, MRI, angiography and OCT have all been used in the assessment of the therapeutic outcome of pdt [194]. The modalities image tissue before and after pdt for evidence of cell death - necrosis, apoptosis and blood

vessel occlusion. MRI of the tissue has been based on contrast-enhancement MRI analysis of T₁-weighted and T₂-weighted relaxation times; apparent diffusion coefficient maps; and longitudinal changes in tumour volume [194]. There is a good spatial correlation between MRI-determined necrosis and histopathological analysis of tissue when images are obtained a short time after pdt – due to the onset of fibrosis there is little or no correlation when the images are taken after a longer period of time [194, 296-298]. Changes in vascular perfusion and permeability can be observed in as little time as 1 hour post-pdt; permeability changes are believed to be indicative of the success of pdt [299, 300]. Tumour necrosis and the absolute volume of the tumour can be monitored using radioisotopes with PET or autoradiography. Moore and colleagues reported that PET can follow tumour volume and surviving fractions with the same degree of accuracy as high-resolution MRI [301]. Angiography has routinely been used to monitor choroidal neovascularisation (CNV) from AMD in the clinic, most commonly with fluorescein but indocyanine green has been used; there have been suggestions that the texaphyrin LuTex® may also be used [194, 302].

The drawbacks associated with fluorescence imaging have so far been limited to the depth at which it can penetrate tissue – a few hundred millimetres. For the detection of flat lesions this limitation presents no problems but restricts the use of the modality in imaging abnormal tissue at greater depths. This can be readily overcome by using a multimodal protocol whereby a second imaging platform, capable of observing structures deep inside tissue, such as OCT, is used to compliment fluorescence imaging. Imaging at deeper penetration depths may also be addressed using other non-invasive modalities including PET, MRI and multi-photon excitation (MPE) [28, 194].

MPE can be used for deep tissue imaging; visible light that results in fluorescence emission from a photosensitiser typically penetrates only a few hundred millimetres into tissue, restricting PSFD to superficial tumour identification [194]. One solution could be to use MPE where a molecule can be promoted into the same excited state as in single photon excitation through simultaneous absorption of two or more lower-energy photons, provided the sum of the energy equals the energy of the electronic transition states. Advantages of MPE in imaging in general have been reviewed and the application of MPE in pdt follows the same basic principle [303]. Lower energy near-IR photons are subject to less scattering in the tissue and have reduced tissue absorption indicating MPE can intrinsically probe deeper (centimetre

depths) into a tissue sample in comparison to visible light, allowing 3-dimensional tumour margins to be precisely defined below the surface of the tissue. MPE-pdt has been investigated with HpD and Photofrin® - a drawback is that the porphyrin photosensitisers that are used in the clinic have very low two-photon absorption cross-sections (10GM; 1GM = $1^{-50}\text{cm}^4\text{s}/\text{photon}$) and thus necessitate impractical light doses (6300Jcm^2) to achieve a 50% cell kill [194, 304-306]. Research efforts for the application of MPE-PSFD and pdt are focusing on developing photosensitisers with enhanced two-photon excitation properties [194]. Alternatively, photosensitisers could be appended to chromophores with strong two-photon absorption properties and transfer the required energy *via* FRET [306-308]. MPE could potentially be used for deep measurements and 3-dimensional imaging of blood vessel oxygenation in healthy and diseased tissue. Photosensitiser triplet state lifetime (τ_T) measurements through delayed fluorescence alongside singlet oxygen phosphorescence could be used to give a more complete idea of photosensitiser dosimetry [194].

All clinically approved photosensitisers lack efficacy in the absence of molecular oxygen. Higher light does can lead to rapid consumption and depletion of local oxygen concentration; lower dose rates or fractionated light delivery is therefore more beneficial and may lead to superior treatments; this behaviour varies greatly between different photosensitisers and tissues [194]. Imaging molecular oxygen can be difficult, particularly in tumour tissue where high spatial and temporal accuracy are difficult to measure, pdt can also readily consume all available molecular oxygen if the optical fluence and photosensitiser concentration lead to high rates of molecular oxygen consumption; understanding the behaviour of tissue oxygenation from a spatial and temporal perspective may help improve the efficacy of pdt [194]. In large regions of tumours there can be a molecular oxygen pressure near to or at zero, in other regions this pressure can be quite high making the quantification of tissue oxygen concentration a difficult process to undertake [194]. While global oxygen measurements can be achieved with good repeatability (surface oxygen partial pressure (pO_2) sensors), measurement on the microscopic level where there is a transient pO_2 , are much more difficult to undertake [309, 310]. OCT, an optical analogue of ultrasound, has found success as an imaging method for the online monitoring and assessment of pdt response in ophthalmology; the technique is very effective in diagnosing retinal detachment, multiple sclerosis-related eye disease, glaucoma and AMD (types I and II) [194]. OCT was

first used to monitor the response of AMD and its associated neovasculature and is being studied as a tool for monitoring vascular pdt effects - pdt has been used as the first line of treatment (imaging) in over two million patients with AMD [194]. The technique typically uses light in the 850-1350nm region of the EMS; therefore OCT can be used to image tissue pre-, during, and post- pdt treatment. The contrast in OCT comes from the refractive index changes at reflective surfaces, the OCT system does not have molecular sensitivity; this hurdle can be overcome by using OCT in combination with other imaging modalities where rapid structural contrast is collected alongside fluorescence [194]. OCT can image in 3-dimensional by collecting individual images in the xy plane of the subject at different depths, making OCT volumetric imaging almost an order of magnitude faster than even video-microscopy. OCT can image beyond 1.5mm deep into tissue - a depth comparable to that of pdt-induced necrosis. The depth (axial) resolution is decoupled from the lateral resolution, allowing for subcellular millimetre resolution, hence imaging deep into a sample [194].

MRI is usually the method of choice for many imaging needs and relies on contrast-enhancing agents to improve the inherent contrast between healthy and diseased tissue; agents normally used contain paramagnetic ions - the most widely used ion is gadolinium (Gd(III)) - Gd(III)-based agents approved by the FDA are Magnavist®, Omniscan® and Prohance® [7, 28]. The plasma clearance rates for these agents is typically of the order of 15 minutes or less; this limits the usable time frame for data acquisition in MRI which can take between 5 and 15 minutes [28]. Tumour selectivity of these agents is dependent upon perturbations in normal vascular permeability - small foci of metastatic tumour cells, particularly those in normal sized or minimally enlarged lymph nodes, may not be detected by current methods [28]. Improvements can be made by slowing down *in vivo* tumour clearance rates or by binding (selectively or non-selectively) the contrast-enhancement agents to a tumour target. The groups of Hoffman and Pandey have investigated one such solution - tumour-avid porphyrins; the gadophrin-2 conjugate has been widely studied and determined to be necrosis-avid [311]. Pandey's group (Roswell Park Cancer Institute, USA) have extensively investigated multimodal contrast agents based on photosensitiser conjugates [198, 312]. The conjugates can be utilised in pdt, as medical imaging contrast agents (PET or MRI), and/or in fluorescence imaging allowing tissue imaging (pre-, during and post-pdt) to assess treatment outcome. Work has been conducted to generate a con-

trast-enhancement agent which can target living tumour cells, particularly those that are actively undergoing metabolic processes [28]. One such conjugate comprises of a photosensitiser (3-vinyl-3-[1-(hexyloxy)ethyl]pyropheophorbide *a* (HPPH)) appended to a MRI contrast agent (Gd(III)-aminobenzyl-diethylenetriaminepentaacetic acid (DTPA)) *via* a tris(polyethylene glycol)monomethyl-ether linkage in a liposomal formulation. This conjugate enhanced tumour localisation (imaged by MRI) by a 10-fold lower dose than Magnevist® while maintaining its pdt efficacy [28, 194]. A second agent developed by Pandey and his group is a PET-active photosensitiser achieved by labelling HPPH with ¹²⁴I which demonstrated 100% tumour-free progression 60 days after pdt [28, 194].

Radioimaging

Porphyrins are excellent metal chelators and very efficient at delivering radioisotopes, one example is a copper porphyrin-peptide-folate (⁶⁴Cu-PPF) compound [199]. This complex is a PET imaging agent targeted against folate receptor positive tumours and has been evaluated as a PET probe for cancer imaging. The ⁶⁴Cu-porphyrin is extremely stable and attempts at using it in tumour localisation studies were first reported in the late 1950's; the use of PET radioisotopes in identifying the localisation of brain tumours was reported in the early 1950's [313, 314]. Wilson and colleagues attempted to detect brain cancers using ⁶⁴Cu-porphyrins and PET imaging in the 1980's but had limited success due to poor tumour localisation properties and poor spatial resolution of the available PET systems [315, 316]. More recent studies by the Wilson group have focused on utilising their pyro-folate receptor targeting conjugate technology and incorporating ⁶⁴Cu into the porphyrin moiety [199]. Porphyrins are known to have a stable ⁶⁴Cu-chelating ability; ⁶⁴Cu-porphyrin has minimal toxicity; the half-life of the radioisotope and the porphyrins pharmacokinetics are compatible; and the chelation of the ⁶⁴Cu ion does not alter the biodistribution properties of the porphyrin [315]. Such a system is envisaged to become a novel-cancer-targeting PET imaging probe - facilitating the monitoring of porphyrin tumour uptake in patients undergoing pdt by pre-treatment PET imaging and facilitating the prediction and quantitative measurement of photosensitiser uptake/accumulation in tumours, hence aiding treatment planning and monitoring [199]. The same group have reported a multimodal bacteriochlorophyll theranostic probe - the optical properties of bacteriochlorophylls are significantly red-shifted, thus it is a very attractive agent for optical imaging

(near-IR wavelengths provide deeper tissue penetration) [70]. Early bacteriochlorophyll pdt and imaging studies were limited due to the chromophores unstable nature, however TOOKAD® has been developed and shown promise as a bifunctional imaging and pdt theranostic agent; it has been used as a pdt agent in the treatment of prostate cancer [70]. Wilson and colleagues extended their targeted PPF probe to create a multifunctional targeted bacteriochlorophyll probe suited to the imaging of deep-seated tumours [70]. They reported that a bacteriochlorophyll-peptide-folate moiety (BPF) better delineates tumour margins within the surgical resection bed, ensuring complete tumour resection and aids intra-operative detection of small metastatic lesions [70]. Copper can also increase the stability of bacteriochlorophyll molecules, therefore insertion of ⁶⁴Cu into the bacteriochlorophyll central cavity may further stabilise the chromophore, making ⁶⁴CuBPF an effective and highly stable PET probe. PET imaging studies have not demonstrated ideal tumour delineation, although some ⁶⁴Cu-BPF tumour accumulation was observed [70].

PET imaging with ¹⁸F-fluorodeoxyglucose (FDG) has been developed to quantitatively assess local glucose metabolism - malignant tumours exhibit increased glucose metabolism, therefore, quantification of FDG uptake using PET may help to differentiate between benign and malignant tumours; determine the degree of malignancy; evaluate the effectiveness of chemo- or radio-therapy and predict treatment prognosis [317]. Drugs labelled with ¹¹C and ¹⁸F are the most commonly used PET isotopes, however, their short half-lives limits their use in studies involving MAbs and photosensitisers which have long accumulation times (hours), therefore ¹²⁴I has been deemed to be a more suitable candidate ($t_{1/2}$ - 4.2 days) [28]. There are only a few reports of pdt with various ¹⁸F based radiotracers (FDG, 9-(4-¹⁸F-fluoro-3-hydroxymethylbutyl) guanine (F-FHBG) and 3'-deoxy-3'-¹⁸F-fluorothymidine (FLT)) [301, 318-321]. Radiolabeling techniques with ¹²⁴I are well defined and complexes with good radiochemical purity and in good yields can be afforded; ¹²⁴I labelled photosensitisers have been utilised to monitor cellular events post-pdt in mice [322]. Pandey and colleagues have also studied ^{99m}Tc complexes of their HPPH-photosensitiser system in rats bearing Ward colon tumours at 4 and 24 hours post-injection; it was observed that the ^{99m}Tc half-life (6 hours) was incompatible with the HPPH ($t_{1/2}$ - 24 hours) accumulation time [323]. Suggestions have been made that the longer lived ¹¹¹In isotope may be more suitable ($t_{1/2}$ - 72 hours) [324]. The ¹¹¹In-HPPH analogue was reported

to be more than 40-fold effective *in vitro* and 8-fold more effective *in vivo* with limited skin photosensitivity [324].

An alternative approach to increasing photosensitiser-tumour specificity is the use of nanotechnology – nanoparticles are particularly well-suited to incorporating multimodal theranostic entities (targeting, imaging and therapeutic), each with their own separate domain, into a single particle platform [194, 197]. One such targeted example by Reddy and colleagues has already been mentioned [254]. These nanosystems are not without drawbacks though – there are transitional issues such as transport barriers; drug uptake; and distribution hurdles that need addressing, along with studies evaluating their long-term effects.

Nanosized Carriers

Nanosized vehicles work on a similar principle to liposomes: they can be composed of an outer hydrophilic and inner hydrophobic region (capable of encapsulating hydrophobic photosensitisers within their inner matrix); thus, facilitating the transportation of photosensitisers in biological environments. They have been developed as an alternative carrier system to liposomes in an attempt to overcome a number of disadvantages associated with liposomal formulations: it has been suggested that only a small fraction of the chosen photosensitiser can be effectively incorporated into liposomes and that the limited lifetimes associated with liposomes results in their structural degradation over time [325]. It has also been hypothesised that the type of vehicle used in photosensitiser delivery can influence the distribution of the photosensitiser within the body's serum. Thus, the transport mechanisms and kinetics of the photosensitiser to the target tissue, as well as the subcellular distribution of the photosensitiser are affected. It would appear delivery *via* lipid-based vehicles shows enhanced binding of the porphyrin (photosensitiser) to the lipoproteins, in particular, orienting towards LDL, possibly resulting in the selective release of the photosensitiser into neoplastic tissue [14].

Nano-Delivery

There is concern however, that although the use of these nanosystems may increase the therapeutic effect observed as a result of photodynamic therapy, a number of the carrier systems may inadvertently decrease the singlet oxygen quantum yield of the encapsulated/associated photosensitiser [24]: the singlet oxygen generated by the photochemical reaction would have to diffuse out of the carrier system (singlet oxygen has a narrow radius of action), if the singlet oxygen has a reduced sphere of action it may not

reach the target tissue and elicit the desired effect, thus reducing the therapeutic effect of the photosensitiser. Furthermore, if the size of the carrier system is not sufficiently small or does not fully dissolve/disperse in physiological media, the incidence/exciting light may not be effectively absorbed; the resultant light scattering may be significant, thus reducing the singlet oxygen yield.

Why Nanosized Vehicles?

Nanotechnology is a rapidly expanding and powerful discipline capable of measuring, manipulating and manufacturing materials at the atomic, molecular and supramolecular levels. This new field is bringing together scientists, engineers and physicians in an interdisciplinary manner to develop new platforms for novel complimentary imaging and diagnostic tools; thereby, propelling crucial work at the cellular and molecular levels, as well as mediating the creation of more effective therapeutic delivery platforms. Together these developments hold the potential to facilitate dramatic advances in biomedical sciences; the market alone for molecular imaging was estimated to be worth \$45 billion (USA dollars) in the year 2010 [326-333]. Molecular imaging is beginning to emerge as a complimentary technique to structural and functional imaging; it allows a wider picture of the body's biological response to treatment to be captured. Molecular imaging can be used to elucidate biological mechanisms induced by pdt; imaging dynamic molecular events *in vivo* allows the real-time imaging of critical pdt parameters, including optimal photosensitiser delivery time, dosage and the appropriate delivery vehicle for molecular targeted therapeutic agents, therefore allowing the more effective combination of therapies in pdt, hence limiting the photosensitiser's associated intrinsic toxicity. It is also critical in studying tumour cells that have survived sub-lethal pdt and in determining if they are able to cope with further rounds of the therapy [194]. Imaging specific molecular disease targets should allow the earlier diagnosis and more thorough assessment of cancer patients [198].

Nanospecies (NS) of many different compositions and for a variety of applications have been described in the literature [66, 328-381]. These species are generally, but not exclusively, synthesised from polymers and due to their minute size are comparable to biological molecules [325, 347, 367-369]. Through the ability to fine-tune both their physical and chemical properties, a range of versatile NS can be synthesised with varying sizes, compositions and surface chemistries [66, 67, 68, 326, 332, 334, 336, 342, 344, 346, 347, 349, 356, 364, 368, 382-387]. The ability to create

species with nanometre dimensions brings with it the potential to bring about life-changing advances in both science and medicine. The design and synthesis of novel NS can have a broad and dramatic effect in the fields of: biological sensing/detection/imaging; targeted diagnostics/delivery; drug delivery/disease therapy; forensic science; and in the field of engineering [66, 67, 68, 325, 326, 329-332, 336-338, 340, 344-347, 349, 351, 353, 355-357, 361-367, 380, 382, 383, 387, 389-400]. The potential to increase the knowledgebase around intricate and complex cellular mechanisms offers huge promise, particularly in the field of disease states. By gaining direct information on intracellular trafficking and molecular functions it may be possible to gain a better understanding of disease mechanisms and therefore, tailor disease management to treat the cause, rather than the symptoms, of a disease. An example of the application of NS in disease therapy is the concept of nano-sized carriers; this type of system offers the ability to more efficiently deliver therapeutic agents to the disease site: thereby, minimising the required administration dose; systemic side effects; and the toxicity commonly associated with drugs in their free state. NS of this type have been increasingly sought in the management of cancers (especially in conjunction with pdt) and for the delivery of gene-therapy agents. Typically, such strategies have been based on those investigated for photosensitiser-targeting moieties described above. Magnetic NS have also been developed and shown potential in facilitating the detection and treatment of some diseases. They have been linked to: the *in vivo* detection of cancer; drug delivery; for use in the photodynamic treatment of cancer; and in the delivery of insulin [332, 347, 353, 380]. Magnetic NS can act as imaging contrast (MRI) agents to: enhance the detection of diseased tissue; in targeting strategies; and in the near-IR management of tumours - reports suggest a nearly fifty percent increase in the magnetic susceptibility of these systems compared to the gadolinium chelates approved for MRI [197, 332, 333, 348, 349, 353, 355, 364, 380, 381, 383, 384, 390, 394, 398]. Furthermore, NS have recently shown some promise in the field of forensic science [400].

Synthetic Materials And Techniques

The ability to synthesise NS from a range of materials and techniques is particularly important when considering the end application and, if applicable, the route of species administration. It is desirable in imaging and therapeutic studies to control and limit the cellular uptake and intracellular localisation of the NS used. One way of achieving this is to selectively direct NS to the specific area/site of interest. This can be

achieved by chemically modifying the surface of NS in a number of ways; namely, through the incorporation of a range of functional groups [66]. For example, by conjugating the NS to a target-specific molecule (such as an antibody), the system can be selectively directed towards sites of interest. Such systems can offer reduced side effects from drug delivery and surgical procedures, making them suitable for a range of different biomedical situations. Due to their size NS can be dispersed in aqueous media [66]; show low toxicity; exhibit prolonged circulation in the blood system; are biodegradable (days to months); can be readily modified to incorporate surface functionality; encapsulate various guest molecules; their size can be varied with relative ease; and polylactic acid; polyglycolic acid; and poly (lactide-co-glycolide) have been established for use in humans [325]. The types of functional groups that can be incorporated onto the NS surface are numerous and include hydroxyl (OH), sulphonate (SO_3^-), carboxylic acid (COOH) and amino (NH_2) groups, as well as bio-reactive groups. Some NS have been reported to selectively localise within specific subcellular compartments/areas, while others appear to show no specificity for one intracellular site over another. NS internalisation can be enhanced by targeting them against internalising receptors, such as a CD19 surface antigen which is expressed on a β -cell lymphoma cell-line and a folate receptor (folate-binding protein). Localisation in a specific intracellular region/subcellular compartment can be particularly important with nanosensors fabricated for studying intracellular signaling mechanisms or imaging [60]. Localisation can also be important in drug delivery systems. Tumours express a greater degree of specific ligands at their surface and nanosystems which are selectively targeted towards these ligands have been shown to accumulate at higher concentrations at the periphery of solid tumours (known as the "binding site barrier") rather than at deeper depths; therefore, minimising diffusion of the NS into the deeper tumour regions. This effect can have a significant impact on the management of tumours and on the initial administration concentration of the drug-loaded vehicle. It is also important to bear in mind the heterogeneous nature of the tumours; certain regions of the tumour will have a greater number of ligand receptors, whilst other areas may not express these receptors at all.

Theranostics - A 21st Century Biomedical Imaging And Therapeutic Platform

The term theranostic refers to the dual diagnostic and therapeutic utility of a compound or methodology and was first used by Funkhouser in 2002 [401].

Theranostics entities simultaneously deliver imaging and therapeutic agents within the same “dose”; the functionality of the system can be readily “switched” between imaging (diagnostic) and therapeutic platforms, facilitating the improved detection and treatment of disease. These novel entities can further offer the potential of site-specific biomedical imaging and treatment *via* targeted delivery. To date, theranostic research has predominantly focused on and been evaluated (*in vivo*) against cancer and atherosclerosis disease types.

History Of Theranostics

The research and development of third- and fourth-generation photosensitisers highlighted the potential a single multimodal (imaging and therapeutic) platform could have in the detection and treatment of disease – such systems negate the need for multiple agents to be administered individually, circumventing variability issues in the uptake; localisation; and pharmacokinetic and pharmacodynamic behaviour of the imaging/therapeutic agents in their free-states – any toxicity associated with the agents in their free-states is also lost. The intracellular biodistribution issues when non-targeted multiple entities are administered have already been noted. DIF (discussed earlier) used for the guidance of surgical resection of cancerous tissue and in setting and adjusting parameters for and during pdt is an example of a theranostic therapy successfully used in the clinic. Being able to “switch” between an imaging state and a therapeutic/cytotoxic state in a single modality lends itself particularly well to photosensitisers and imaging modalities such as fluorescence-, magnetic resonance-, radio- and nuclear imaging and treatment modalities such as photodynamic, photothermal and photoacoustic therapies, as well as hyperthermia, gene and nuclear- and chemo-therapy [402]. There are a number of platforms that are particularly suited to bringing imaging and therapeutic agents together in a single entity; these include nanoagents (nanobiayls, magnetofluorescent-, mesoporous- and photon-up-converting nanoparticles (NPs), carbon nanotubes, quantum dots (QDs) and liposome-like porphysomes – each platform with its own unique properties, advantages and disadvantages [403-411].

Nanoagents As Theranostic Platforms

The physical properties (including small size (for efficient cell uptake) and facile surface functionalisation (for appending targeting moieties)) of NPs make them attractive candidates for theranostic applications, particularly high surface-to-volume ratios (high loading potentials) and the ability to encapsulate in-

dividual entities together in the same protected environment, thereby minimalising cellular immunostimulation and toxicity of the entities in their free states towards cells. Furthermore, the ability to increase the target-to-background contrast for/in imaging applications and the local concentration of the therapeutic agent at the target site (ultimately reducing systemic toxicity) are extremely versatile properties with respect to structural modifications and the type of cargo the nanoagents can be loaded with.

A range of nanoagents are currently being studied as theranostic platforms and include nanobiayls; macrophage-avid- and mesoporous silica NPs; carbon nanotubes; and novel porphysome vesicles [403, 404, 407-409, 411]. Kelkar and Reineke have thoroughly reviewed the developments of a broad range of theranostic agents with applications in the fields of pdt, chemo-, gene-, hyperthermia and radiation therapy and MRI, nuclear and near-IR imaging strategies [402].

Nanobiayls

Theranostic gadolinium-based perfluorocarbon NPs have been developed and successfully evaluated against detecting, characterising, treating and monitoring angiogenesis in pre-clinical models of cancer and atherosclerosis [403]. However, a serious and unexpected side effect (nephrogenic systemic fibrosis (NSF)) of gadolinium blood pool agents has recently been observed amongst a number of renal and liver-transplant patients [412]. NSF is a serious complication which causes patients to develop thickening of the skin and connective tissue, and in some cases, bone fractures. NSF has been reported to progress rapidly, with reports that it can be fatal in approximately 5% of sufferers [412]. It is therefore important to consider alternative paramagnetic contrast agents for use in MRI. One of the first alternatives investigated was the lanthanide metal manganese. Manganese was chosen for its favourable efficiency in R_1 enhancement and because it is a natural cellular constituent, often a co-factor for enzymes and receptors [403, 413]. Manganese blood pool agents, such as mangafodipir trisodium, have been approved as hepatocyte-specific contrast agents with transient side-effects due to dechelation of the manganese ion from the linear chelate. Release of manganese (caused by disruption of the vesicles) allowed MR detection of sites where vesicles such as $MnSO_4^{3c}$ or Mn-DPTA were non-specifically entrapped [403]. Pan and colleagues have developed theranostic targeted Mn(III)-labelled nanobiayls based on the novel Mn(III)-protoporphyrin chloride contrast agent and

chemotherapeutic drugs (doxorubicin and camptothecin) for the imaging and treatment of vascular targets [403]. The nanobiaryl entities are produced from the molecular self-assembly of amphiphilic branched polyethylenimine, forming inverse micelles and taking on a toroidal (do-nut, "biaryl") shape; the nanobiaryls have desirable tunable particle sizes and low polydispersity indices [403]. The biaryl geometry drives the increased stability of the nanobiaryl and presents kinetically stable, porphyrin-coupled Mn(III) complexes directly to the surrounding water environment. Pan and colleagues evaluated (*in vitro*) the imaging component of the nanobiaryls against fibrin (a critical component of intravascular thrombosis) by targeting them towards (avidin-biotin interactions and MAbs (biotinylated fibrin-specific, NIB5F3). The resultant MR images of the clot samples showed marked contrast enhancement of the fibrin-targeted Mn(III)-nanobiaryls, with no contrast improvements from the two control experiments (non-target and metal-free nanobiaryls) [403]. Pan and co-workers further evaluated (*in vitro*) the potential of their nanobiaryls as drug carrier vehicles, with the hydrophilic and hydrophobic drugs doxorubicin and camptothecin, respectively. Results demonstrated loading efficiencies of approximately 98% and 99% and drug release values of 12% and 20% over three days, supporting the group's hypothesis that nanobiaryls offer great potential as biomedical theranostic platforms [403].

Macrophage-Targeted Theranostic Nanoparticles

Atherosclerotic vascular disease (myocardial infarctions and cerebrovascular accidents) is a leading cause of death worldwide. Atherogenesis is an insidious process that occurs over many years, hence there is a vital need to diagnose and treat sub-clinical and high risk atherosclerotic plaques prior to their sub-clinical manifestations [414]. Macrophages have been identified as key biological, imaging and therapeutic targets in atherosclerosis [404, 414-418]. Research has begun into the investigation of anti-macrophage therapies, including the systemic modulation of macrophage activity and localised pdt, the latter involves de-bulking of atherosclerotic plaques *via* angioplasty [404, 419]. The benefit of using pdt is the localised and selective destruction of the target area. A number of photosensitisers have demonstrated preferential uptake in atherosclerotic plaques, purported to be a result of the interactions between the relatively hydrophobic nature of the porphyrin and the lipid-rich core of the atheroma [420-426]; the most studied photosensitiser Antrin® is

currently in clinical trials against coronary artery disease [427, 428]. McCarthy and colleagues hypothesised that by building on the already existing field of photosensitiser-NP pdt agents, they could increase the efficacy of pdt by conjugating photosensitisers to macrophage-avid magnetofluorescent NPs [342, 350, 429-431]. McCarthy *et al.* had previously reported the enhanced uptake (*in vivo*) of a dextran-coated magnetofluorescent NP in atherosclerotic plaques, in addition to specificity of the agent for macrophages [405, 406, 432]. McCarthy and colleagues further identified the need for the magnetofluorescent NPs to be detectable by MRI and catheter-based fluorescence imaging - achieved by incorporating a magnetic core (iron oxide) and fluorescent dye (Alexa Fluor® 750) respectively within the NP [404]. The potent chlorin photosensitiser

5-(4-carboxyphenyl)-10,15,20-triphenyl-2,3-dihydroxychlorin (Φ_{Δ} 0.65) was appended to the surface of the iron oxide NP. There was approximately 100nm difference between the longest wavelength of absorption of the photosensitiser and Alexa Fluor®, minimising the energy transfer between the two chromophores when the theranostic agent was excited at the therapeutic wavelength (650nm); hence minimising cell death when the intracellular distribution of the theranostic agent was being imaged. The theranostic magnetofluorescent NPs were detectable by MRI and fluorescence imaging and did not demonstrate significant dermal-localisation. The evaluation (*in vitro*) of the agent demonstrated that when murine macrophage cells (RAW 264.7) were illuminated at 750nm, under conditions comparable to intravital fluorescence imaging of atherosclerosis (0.8mW total power, scanning laser, 512 x 512 pixels, 3min 45s acquisition), minimal cell death was observed. The theranostic NPs were observed to be no more toxic to macrophage cells than the control photosensitiser-free NPs, however, when the system was therapeutically irradiated, dose-dependent phototoxicity was observed - complete cell killing was achieved in transformed human macrophage (U937) cells 1 hour post-incubation and irradiation (0.2mg Fe per mL, irradiation with 646nm laser) [404].

McCarthy and colleagues report that their system should enhance the pdt of various diseases including atherosclerosis and in-stent restenosis and have significant *in vivo* applicability with high macrophage uptake; efficient cell killing; safe monitoring of the spatial distribution of the agent *in vivo* by MR; and near-IR fluorescence imaging [404].

Mesoporous Silica Nanoparticles

Ohulchanskyy *et al.* reported the synthesis of a

novel silica-based (ORMOSIL) NP which covalently incorporated a photosensitiser (iodobenzylpyrophephorbide) for the pdt of colon cancer in 2007 [433]. Zhang and colleagues also reported the use of silica in the formulation of silica-coated NPs (photon up-converting NPs) in 2007 for the theranostic imaging and pdt of breast cancer cells with the non-porphyrinic photosensitiser merocyanine 540 [408, 434]. More recently (2009), Cheng *et al.* have reported the synthesis of mesoporous silica (MPS) NPs comprised of highly-ordered, hexagonal pores with mean particle diameters of 70-100nm. These NPs are readily modified and taken up by breast cancer cells; offer payload protection; and low cytotoxicity towards cells. To date, MPS NPs have been functionalised for use in chemical catalysis, drug delivery, cell labelling and the controlled release of therapeutics [435-445].

The large surface areas offered by MSP NPs enable the high-loading concentration of photosensitisers per particle and the efficient delivery of large concentrations of photosensitisers, thereby reducing the energy of photoirradiation needed to achieve efficient oxidative cytotoxicity - avid cell-uptake enables significant intracellular accumulation of photosensitiser for optimal pdt [407]. Cheng and colleagues appended a phosphorescent Pd-porphyrin photosensitiser onto the nanochannel surface of a MSP NP. Pd-TPP is conventionally used for oxygen sensing and imaging - tissue oxygen distribution is measured *via* oxygen-dependent quenching of phosphorescence [446, 447] - the long-lived triplet state of Pd-TPP is produced with a unity quantum yield, while the concentration of singlet oxygen generated in pdt depends on the accessibility of the excited Pd-TPP to oxygen. The energy of photoirradiation needed in phosphorescence imaging is typically 10^{-4} to 10^{-5} times that used in pdt [446, 448], therefore the concentration of singlet oxygen generated *via* Pd-TPP during oxygen sensing/imaging from phosphorescence quenching is much less than that produced during pdt. Hence, when Pd-TPP is irradiated with respect to imaging energy requirements, the singlet oxygen produced has a negligible therapeutic effect. This can be readily changed by simply altering the energy parameters used to irradiate the chromophore, thus the Pd-TPP can readily be "switched" from being a phosphorescent oxygen sensing/imaging probe to a pdt agent. Cheng *et al.* chose MSP NPs for their facile uptake into cells *via* endocytosis and reported that breast cancer cells (MDA-MB-231) transfected with their pdt-MSP NPs underwent significant morphological changes and cell death post-irradiation (532nm, 1.2Jcm^{-2}) [407]. Cheng and colleagues hypothesise that their multi-

modal Pd-TPP-MSP NP is a promising platform for cancer theranostics.

Carbon Nanotubes

Advances in photoacoustic imaging and photothermal therapy techniques based on the non-radiative conversion of absorbed energy in thermal and accompanying acoustic phenomena has demonstrated great potential in various spectroscopic sensing/imaging and therapeutic applications [449]. Endogenous biomolecules and exogenous contrast agents have successfully been used in photoacoustic imaging and photothermal therapies. The exogenous contrast agents have even been based on small molecule optical dyes, such as Evans blue, indocyanin green and MB, and synthetic NPs, including gold and carbon-based ones [409]; NPs offer advantages over biomolecules since they typically exhibit strong optical absorption and photostability properties [409]. Carbon nanotubes (CNTs) have demonstrated numerous biomedical applications over the years as single-walled and multi-walled nanotubes (SWNT and MWNT, respectively) [409]. The ability to absorb light over a broad range of wavelengths (UV, visible, near-IR and microwave) lends CNTs as natural contrast agents for photoacoustic and photothermal techniques [409]. Zharov and colleagues were the first to demonstrate (*in vitro* and *in vivo*) the use of CNTs as photoacoustic contrast agents in 2007. The group were able to detect circulating CNTs alone or *via* circulating *Staphylococcus aureus* (*S. aureus*) and *Escherichia coli* (*E. coli*) labelled with CNTs in flowing blood using a novel photoacoustic/photothermal flow cytometry system [450]. They also reported the application of two-colour photoacoustic flow cytometry (in real-time) for *in vivo* identification of CNTs in lymph flow [451]. de la Zerda and colleagues went on to image (photoacoustically) CNTs by molecularly targeting (using arginine-glycine-aspartic acid peptides) SWNTs to tumour neovasculature in living mice [452]. Research has continued into the use of CNTs for photoacoustic imaging, with a number of groups focusing on chemical modifications to enhance CNT photoacoustic signals [409]; the modifications include coating CNTs with organic optical dyes; gold with folates and antibodies for the molecular targeting of circulating tumour cells (CTC); and endothelial lymphatic receptors with potential lower toxicity or antibodies for targeting primary tumours [453-456]. About 90% of cancer deaths result from metastatic spread from the primary tumour; detection of CTCs is therefore a marker of metastases development and the efficiency of any therapy delivered. The sensitivity of the majority of current CTC assays is limited; de la

Zerda and colleagues believe they can increase the sensitivity of detection by assessing large volumes of blood *in vivo* [409]. Additional applications of CNTs include the photoacoustic detection of metastasis in sentinel lymph nodes and the identification of tumour-initiating cancer stem cells in circulation among bulk CTCs [455, 457, 458]. Photoacoustic and photothermal microscopy has been reported to demonstrate promise in studying the distribution of CNTs in histological samples [459].

The photoacoustic and photothermal effects of CNTs can be transferred into therapeutic use, including pulsed photothermal nanotherapy (nanophotothermolysis) with laser-induced nano- and micro-bubbles around overheated gold NPs, leading to tumour (and bacterial) cell death, as well as for targeting bones, atherosclerotic plaques, blood lymph vessels and thrombus [458, 460-468]. The pulsed-mode in laser treatment has the potential to precisely kill individual cancer cells with a spatial accuracy of a few millimetres, sparing healthy cells, unlike continuous-wave photothermal treatment [348, 366, 460, 469]. Photoacoustic imaging and photothermal therapeutic modalities are based on similar thermal effects, enabling their facile integration into a multimodal/functional theranostic system and facilitating the navigation, optimisation and monitoring efficiency of photothermal nanotherapy [409]. The photoacoustic and photothermal effects of de la Zerda *et al.*'s nanosystem can be amplified and the spectral peaks sharpened, increasing the sensitivity, specificity and capability of multiplex photothermal therapy by targeting multiple NPs with different optical spectra to different disease-associated biomarkers, thereby potentially offering personalised medicine [454, 470].

Several techniques have been developed to synthesise CNTs, including high-pressure carbon monoxide, chemical vapour deposition, arc discharge and laser ablation methods [471-474]. All of the atoms in SWNTs are exposed on the entities surface, thus generating very high surface areas (theoretically approximately $1300\text{m}^2\text{g}^{-1}$), facilitating efficient SWNT-optical radiation interactions [409]. SWNTs can be characterised by very broad and flat optical absorption spectra, spanning the UV, visible and near-IR regions of the EMS. SWNTs absorb the majority interacting photons, resulting in local heating of the NTs surrounding environment [450, 455, 465]. When an intense nanosecond laser pulse light is used as the incident light, the local heating leads to the emission of an ultrasound wave (the Photoacoustic Effect) [450-457, 475-478]. Semi-conducting SWNTs with small band gaps (approximately 1eV) exhibit fluorescence properties with excitation and emission

wavelengths in the near-IR range [409]; different excitation-emission wavelengths can be achieved with different SWNT chiralities [479]. The majority of light that interacts with SWNTs is absorbed but a small portion of the photons are scattered, leading to a distinctive Raman scattering spectrum – these unique spectra can then be used for (*in vivo*) detection and imaging [480-484]. The strong optical absorption characteristics of MWNTs also makes them attractive photoacoustic and photothermal contrast agents [465]; although MWNTs have pure optical absorption, they do not have the rich optical characteristics of SWNTs [409]. Drawbacks of CNTs are their relatively low near-IR absorption coefficients (with respect to other nanoagents such as goldNPs) and the high concentration of CNTs needed for effective photoacoustic and photothermal theranostic applications [409].

Functionalisation of CNTs is important, not only to increase their specificity for their chosen targets but CNTs in their “raw” state have hydrophobic surfaces and hence are not soluble in aqueous media (such as blood) [409]. Covalent and non-covalent surface functionalisation of CNTs has been reported in the literature [409]. Since “raw” CNTs are inert entities, covalent functionalisation typically involves creating defects in the sidewalls of the NT *via* oxidation [485-486]. However, this does not fully address the hydrophobicity issue as the oxidised CNTs aggregate in the presence of salts; remedies such as PEGylation are being explored [487-488]. A disadvantage of covalent bonds is their interference with the natural physical properties (Raman scattering and photoluminescence) of CNTs, something not apparent with non-covalent functionalisation [409]. In non-covalent functionalisation the surface the CNT is coated with amphiphilic surfactant molecules or polymers so that the hydrophobic surface of the NT is non-covalently attached to the hydrophobic tail of the surfactant. A number of investigations have utilised this π - π interaction to non-covalently bind porphyrins and pyrenes to NT surfaces [489-492]. SWNTs have also been radio-labelled with ^{64}Cu (for imaging tumour angiogenesis) [493]. Successfully attaching and evaluating porphyrinic-type molecules to CNTs has demonstrated the theranostic biomedical utility of these nanoagents. The CNTs and their hybrids (with increased photoacoustic and photothermal contrasts) have been evaluated for nanomedicine-related theranostics by de la Zerda and colleagues [409]; the CNT-based contrast agents facilitated minimally invasive, highly sensitive and target-specific multiplex detection and killing of solid and metastatic tumour cells and bacterial infections in static and dynamic conditions (for example blood and lymph flow) that had previously been dif-

difficult to accomplish with traditional methods [409].

Porphysomes

An alternative organic theranostic agent is based on the novel organic self-assembled porphyrin nanovesicles, known as porphysomes; these multimodal biophotonic contrast agents have been developed by Lovell and colleagues in response to the limitations (drug-loading limited to NP surface and concerns relating to long-term safety of the inorganic modalities) posed by optically active inorganic NPs [411, 494-497]. The biocompatibility and high-loading capacity of optically active organic NPs, including liposomes, micelles and polymersomes, have been evaluated in many human theranostic applications [497]. However, these organic agents are not without their own limitations - theranostic platforms in biophotonic techniques need to intrinsically absorb light in the near-IR region of the EMS. Lovell and colleagues have investigated and evaluated porphyrin conjugates and novel biophotonic tools utilising the unique light-absorbing properties of the porphyrin chromophore. Due to the lack of stability and solubility associated with many tetrapyrroles, Lovell and colleagues fabricated liposome-like NPs self-assembled from phospholipid-porphyrin conjugates (termed porphysomes) with good loading capacities; high absorption of near-IR light; structure dependent fluorescence quenching; and excellent biocompatibility - all features lending themselves to creating a biophotonic modality with diverse ranging applications [411].

The porphysome vesicles (100nm) were formulated by supramolecular self-assembly with the sub-units composed of porphyrin-lipid conjugates generated *via* an acylation reaction between lysophosphatidylcholine and pyropheophorbide. The hydrophobic chromophore was substituted in place of an alkyl side chain - maintaining the amphiphilic properties of the structure. The spherical conjugate then underwent self-assembly in aqueous media with extrusion to form the porphysome vesicles. TEM images revealed that the porphysome structure was comprised of two separate monolayers of material separated a 2nm gap. The porphysome vesicle exhibited two absorption peaks (400nm and 680nm (near-IR)). Lovell and co-workers also formulated red-shifted porphysomes (760nm) utilising sub-units of a bacteriochlorophyll analogue [411]. A further porphysome, with shifted optical density bands (440nm and 670nm), was generated by inserting metal ions into the porphyrin-lipid structure, demonstrating the ability of porphysomes to form metal-chelating bilayers [411]. The ability to readily alter the photo-

chemistry of the porphysome vesicles offers an imaging platform with potential in situations where specific operating wavelength(s) are required - such as when the operating wavelength(s) of given laser sources are required to be matched [411].

Porphysomes are highly self-quenched - energy that is normally dissipated to fluorescence and singlet oxygen formation is disseminated elsewhere. Upon exposure to laser illumination, thermal energy was released with an efficiency comparable to gold NPs (photothermally active inorganic NPs) - irradiation of standard liposomes generated no significant increase in the temperature of the solution [411]. Since photoacoustic signal generation is related to thermal expansion, porphysomes also generated photoacoustic signals proportional to concentration and detectable as low as 25pM (note, detection in this range was reported by Lovell *et al.* to be non-linear) [411]. Lovell and colleagues further reported that when a detergent is added to a solution of porphysomes (in order to disrupt the vesicles structure), an (unexpected) increase in absorption was observed while the photoacoustic signal decreased six-fold. In a control experiment with MB (a clinically used contrast agent), detergent was deemed not to have an effect on the photoacoustic signal of the dye, suggesting that the structurally-based self-quenching of porphysomes is requisite for nanoscale photoacoustic properties - a phenomenon of photoacoustic signal attenuation on detergent-induced porphysome dissociation [411].

Lovell and colleagues evaluated the capability of their nanovesicles to act as tomographic agents *in vivo* and observed that the local lymphatic system (of rats) become clearly detectable (photoacoustically) within 15 minutes of post-intradermal injection of porphysome vesicles - as the porphysomes drained to the lymph vessels and nodes they exhibited a strong photoacoustic signal, facilitating the visualisation of the first draining lymph node, the in-flowing lymph vessel and surrounding lymph vessels; the photoacoustic investigations (6.5ns pulse width, 10Hz laser) did not generate sufficient heat to cause damage to the surrounding tissue [411]. The fluorescence imaging capabilities of the system were assessed in mice bearing KB cell xenografts. Initially, a low fluorescence signal was observed 15 minutes post-injection, demonstrating the self-quenching of porphysomes *in vivo*, however, high tumour fluorescence was observed after two days as the porphysome vesicles accumulated in the tumour (the porphysomes used for fluorescence imaging were appended with a 1 molar % folate-PEG-lipid moiety for specific tumour uptake) and became unquenched [411]. The notion of porphysome quenching *in vivo* was more markedly

illustrated when Lovell and colleagues injected detergent-disrupted porphosomes into mice and reported observing higher initial fluorescence. Lovell and co-workers concluded that their observations and findings supported their hypothesis that porphosomes are intrinsically multimodal for both photoacoustic tomography and low-background fluorescence imaging. The group also assessed the appropriate factors relevant to clinical application of their porphosomes [411]. Porphosomes had been observed to be stable for months in aqueous media but demonstrated susceptibility to enzymatic degradation. On incubation with detergents and lipase the phospholipid structure of the porphosome was cleaved; the main aromatic product was pyropheophorbide, the starting material for the porphyrin-lipid porphosome vesicle [411]. Similar to chlorophyll, pyropheophorbide is known to be enzymatically cleaved into colourless pyrroles when incubated with peroxidase and hydrogen peroxide [498]. The degradation of porphosomes was verified by Lovell and colleagues: they monitored the loss of porphyrin absorption and confirmed pyropheophorbide could be efficiently degraded by peroxidase; the group concluded that, to their knowledge, the porphosomes they had fabricated were the first examples of an enzymatically biodegradable, intrinsically optically active NP [411].

In the thorough assessment of the porphosome vesicles Lovell and co-workers carried out a preliminary study to assess the potential toxicity of the vesicles and reported that mice treated with a high dose (1000mgkg^{-1}) of porphosomes remained healthy over a two week period [411]. Blood tests carried out post-euthanasia suggested that the hepatic function of the mice was generally normal (with the exception of elevated bile acid and alanine transferase levels less than twice the upper range of normal). Red blood cell counts and attributes were reportedly unaffected; the porphosome did not interfere with the physiological regulation of endogenous porphyrin (haem). The reported unaffected white blood cell count suggested that the porphosome vesicles were not immunogenic at the two week time point. Post-mortem histopathological examination of the liver, spleen and kidneys indicated good health of the respective organs [411].

Recognising the utility and capability of the large aqueous porphosome core towards cargo-loading and delivery and therefore as a theranostic platform, Lovell and colleagues investigated loading the potent chemotherapeutic drug doxorubicin into the porphosome core [411]. The group determined an active-loading technique (ammonium sulphate gradient method) coupled with cholesterol (50% molar ratio, cholesterol is known to enhance the loading of

compounds within phosphatidylcholine-based liposomes) achieved 90% loading of the anti-cancer drug into the porphosome core [411, 499]. The porphosomes maintained a self-quenching porphyrin bilayer. Lovell and colleagues demonstrated the biophotonic potential of their organic nanovesicles investigating them as agents for photothermal therapy. The group reported that porphosomes containing 30 molar % of cholesterol demonstrated favourable biodistribution following their systemic administration, with greater accumulation in the tumour tissue (KB tumour-bearing mice) and less accumulation in the liver, spleen and kidneys than observed with standard porphosomes. The tumour was irradiated for 1 minute post-24 hour administrated (injection) of the porphosomes and the tumour temperature monitored (*via* thermal camera); the tumour temperature rapidly rose to 60°C ; 20°C higher than the control mice where the tumours were injected with PBS. Following treatment, mice in both groups developed eschars on the tumours; the laser-alone and porphosome-alone control groups did not. The eschars healed after two weeks and the tumours in the porphosome-laser treated (photothermal) group were reportedly destroyed. Tumours in the control group of mice continued to grow rapidly [411].

Lovell and colleagues have been able to develop and successfully evaluate a porphyrin-based nanovesicle that generates large tunable extinction coefficients, structure-dependent fluorescence self-quenching and unique photoacoustic and photothermal properties, facilitating the sensitive visualisation of lymphatic systems; the near-IR fluorescence of low-background fluorescence imaging; and following active-loading and accumulation in tumour cells, the photothermal ablation of tumours, thus demonstrating the highly promising biomedical potential of their theranostic agent [411].

Porphyrinic-Based Photodynamic Inactivation Of Bacteria

Photosensitisers are also emerging as key therapeutic agents in other pathological areas too, most notably as antimicrobial agents. There is an increasing prevalence of antibacterial resistance among a number of pathogenic bacteria strains despite the advancement of antibiotics; among the most reported multidrug resistant bacterial strains are methicillin, mupirocin and vancomycin, hence the urgent need for alternative antibacterial therapies [500, 501]. One such therapy that is showing great promise is photodynamic inactivation (PDI), also referred to as photoantimicrobial chemotherapy (PACT). PACT is similar to PDT in that a photosensitising agent, light and molec-

ular oxygen are required to elicit an appropriate cytotoxic and thus photoinactivation process. To date, PACT has shown promise against antibiotic-resistant and antibiotic sensitive strains of methicillin-resistant *S. aureus* (MRSA) (strains of *S. aureus* are often implicated in cases of superficial and serious skin and soft tissue infections as well as infecting burns and other wounds) and has the potential to be used topically as a treatment modality for chronically infected wounds [502-515]. Biotargeting of photosensitisers in PACT has the ability to offer enhanced photodynamic tissue/cell killing in line with the increased selectivity offered by photosensitiser-bioconjugates in traditional pdt. Such photosensitiser bioconjugates have been prepared utilising the targeting ability of antibodies, a cell-penetrating peptide (TAT) and bacteriophages have been raised for PACT against *S. aureus*, MRSA, *Pseudomonas aeruginosa* (*P. aeruginosa*), *E. coli* and *Porphyromonas gingivalis* [511, 512]. PACT has a number of advantages over traditional antibiotics (i) PACT has a broad spectrum of action and has shown efficacy in the inactivation of many antibiotic resistant strains of pathogens (ROS are toxic to nearly all bacteria if sufficient ROS-induced damage is inflicted); (ii) PACT offers low mutagenic potential since it has been shown that bacteria cannot readily develop resistance to ROS; (iii) PACT has demonstrated greater photocytotoxicity against bacteria than mammalian cells, allowing the selective destruction of bacteria. PACT is showing potential towards local microbial infections such as skin associated bacteria; bacteria present in periodontal pockets; and the oral cavity. A number of agents have been prepared based on PACT for the treatment of acne *vulgaris* and infected leg ulcers [69, 500]. The NCS porphyrin developed by Sutton *et al.* has been used in the preparation of a PACT agent selective towards MRSA [501]. The NCS photosensitiser was coupled to a purified recombinant protein and evaluated *in vitro* for specific anti-MRSA cytotoxic potential [501]. Observation suggested a 66% reduction in MRSA growth in comparison with non-irradiated cells, highlighting the potential of PACT as a therapeutic model. Other photosensitiser conjugates have been prepared and evaluated. Biolitec AG has marketed a liposomal formulation of Temoporfin® under the registered name Fospeg®. When evaluated against *S. aureus* (in PACT) Fospeg® has proven to be effective in inducing phototoxic cell death [69]. Bombelli *et al.* have also developed a Temoporfin®-loaded cationic liposome with comparable bactericidal activity to the free photosensitiser [516]. Antimicrobial peptides (AMPs) are a further example of bacteria-targeting agents being investigated [69]. The cationic nature of AMPs facilitates their interac-

tion with negatively charged lipids in the bacterial membranes of both Gram-positive and Gram-negative bacteria, while amphiphilic properties allow penetration into bacterial membranes and the formation of membrane pores, culminating in damage to the integrity of the bacteria [69]. Yang *et al.* have recently reported the preparation of a novel bacteria-targeting liposomal formulation utilising such targeting moieties and evaluating the conjugate against MRSA resistant (*S. aureus*, Gram-positive) and *P. aeruginosa* (Gram-negative) pathogens [69]. They were able to observe greater uptake of the targeted AMP-Temoporfin® liposome in bacteria (*in vitro*) than in comparison to the unmodified liposome and the eradication of MRSA, however, to date, only a reduction of *P. aeruginosa* has been achievable under their investigative conditions [69]. There has been concern that some photosensitisers evaluated for PACT may have an adverse effect on neutrophils. Tanaka *et al.* have highlighted that optimal photosensitisers for use in PACT should destroy the target bacteria but spare neutrophils – the white blood cells that are paramount in fighting disease [517]. In the treatment of localised microbial infections PACT causes direct pathogen death but also affects host neutrophils that have been stimulated by PACT. In order to enhance the antimicrobial therapeutic efficacy of PACT, cytotoxic damage to neutrophils must be minimised. Tanaka and colleagues have evaluated cytotoxic effects of PACT on murine peripheral-blood neutrophils with a range of antimicrobial photosensitisers [517]. They compared Photofrin® and Laserphyrin® (mono-L-aspartyl chlorine e6 (NPe6), Talaporfin®) with non-porphyrinic photosensitisers – Erythrosine B, rose bengal, crystal violet, new methylene blue, toluidine blue-O and MB. Tanaka *et al.* found that the toluidine blue-O and MB photosensitisers had a negligible cytotoxic effect on neutrophils in comparison the porphyrin based Photofrin® and new methylene blue photosensitisers had a strong cytotoxic effect on neutrophils [517]. The group hypothesise that the degree to which different photosensitisers kill bacteria (particularly Gram-negative) varies considerably and that the effectiveness of the cytotoxic effect of photosensitisers against neutrophils must be considered when designing antimicrobial PACT protocols [517]. Gallium PCs have been prepared and investigated as potential PACT agents. Mantareva *et al.* evaluated two cationic Ga(II)PCs (tetra-methylpyridoxyl substituted GaPC and octa-methylpyridoxyl substituted analogue) against MRSA, *Enterococcus faecalis* (*E. faecalis*, also Gram-positive), *P. aeruginosa* and *Candida albicans* (*C. albicans*) (a fungus) in the planktonic phase [507]. The PACT activity of the two PCs was compared to MB

and a ZnPC with the same substitution pattern. Relatively high uptake concentrations were observed for the two GaPCs for the bacterial and fungal species, with the octa-substituted PC exhibiting higher uptake. Photodynamic inactivation of the pathogens was observed for all but the *E. faecalis* bacteria. Ragàs *et al.* reported the synthesis of a tri-cationic water soluble porphycene evaluated *in vitro* for PACT; 2,7,12-tris(α -pyridinio-*p*-tolyl)-17-(*p*-methoxymethyl) phenyl porphycene (Py₃MeO-TBPO) was tested against *S. aureus* 8325-4, methicillin-resistant *S. aureus* Xen 31, *E. faecalis* (ATCC29212) all Gram-positive bacteria and *Acinetobacter baumannii* (*A. baumannii*, ATCC 51393), *E. coli* (ATCC53868), *Proteus mirabilis* (ATCC51393), and *P. aeruginosa* (ATCC 19660) as Gram-negative bacteria. *C. albicans* (ATCC 18804) and *Candida krusei* (*C. krusei*, ATCC 6258) were the fungi used [510]. Ragàs *et al.* were able to demonstrate the high photodynamic activity of the porphycene photosensitisers against a broad spectrum of microbial cells *in vitro* and against infection in a third-degree burn model (*in vivo*) [510]. Yu *et al.* have investigated the synthesis of a group of novel quaternary ammonium cationic porphyrins and assessed their potential (*in vitro*) as PACT agents against *S. aureus*, *E. coli*, *P. aeruginosa* and *C. albicans* [505]. They observed antimicrobial activity was sensitive to the functional groups and metal ion present in the photosensitiser: activity was decreased with increasing electron withdrawing effect of the functional groups attached to the aromatic rings. The Gram-negative bacteria showed resistance to all of the synthesised porphyrins, however, two of the compounds did exhibit a degree of photoinactivation against the Gram-positive bacteria and the fungus. Research has been undertaken to observe the effect of the number of positive charges and the charge distribution in a porphyrin's structure in relation to photoinactivation of bacteria in the treatment of waste water [503]. Results suggested that cationic porphyrins bearing three and four charges are highly efficient in the photoinactivation of *E. faecalis* and *E. coli*. *Meso*-substituent groups on the porphyrin yield different effects on photoinactivation – the 5,10,15-tris(1-methylpyridinium-4-yl)-20-(pentafluorophenyl)-porphyrin triiodide photosensitiser achieves greater cell survival at lower light doses [503, 504]. These results demonstrate the potential PACT has as a modality for the treatment of infections that are becoming more and more resistant to conventional therapies. Huang *et al.* have reported on the potential of cationic BCs as photosensitisers for PACT [509]. They describe four BCs with 2, 4 or 6 quaternised ammonium groups or 2 basic amine groups and their

cytotoxic effect on *S. aureus*, *E. coli* and *C. albicans*. All four of the BCs exhibited high bactericidal activity against *S. aureus* and showed selectivity for bacteria over human cells (phototoxicity was assessed in human HeLa cancer cells). Increasing cationic charge on the BCs increased activity against *E. coli*. The only BC toxic towards *C. albicans* was the BC bearing the basic groups [509]. Hypothesises that PACT offers a treatment modality whereby the development of resistant strains of pathogens is minimised has been made by Giuliani *et al.* [506]. Preliminary investigations have been undertaken to support their theory - they have investigated three common pathogens and their potential to develop resistance to PACT photosensitisers. They targeted a novel tetracationic Zn(II)PC chloride (RLP068/Cl) against the pathogens *P. aeruginosa*, *S. aureus* and *C. albicans* *in vitro*. Results demonstrated the novel PC exhibited a concentration-dependent killing efficacy against the three pathogens associated with skin and soft tissue infections. Notably, photodynamic activity was retained against multidrug resistant strains of the pathogens evaluated. Giuliani and colleagues propose that the unique mechanism of action in PACT exhibits a low propensity for inducing resistance in the three clinically relevant human pathogens tested. Nanoparticle-photosensitiser delivery systems are being investigated as agents suitable for PACT, although to date not with porphyrin based photosensitisers [518].

Conclusion and Outlook

There is potential to increase the efficiency and effectiveness of treatments offered against disease management by using targeting modalities and drug-loaded vehicles; these strategies can be used as stand-alone tools or combined to form more potent systems (theranostics) to fight disease. Advances in porphyrinic photosensitiser chemistry over the past two decades have seen improved second-generation photosensitisers authorised for photodynamic anticancer therapy and the development of porphyrinic bioconjugates that have greatly enhanced a photosensitiser's selectivity for tumour cells; significantly reducing the acute/chronic cutaneous photosensitivity associated with first- (and second-) generation photosensitisers. Current research has focused on drug delivery methods to circumvent the need to disregard potential efficacious photosensitisers that have solubility issues. Porphyrin-based chemistry has emerged as a leader in the field of fluorescence-guided imaging and detection - photosensitiser fluorescence imaging has been increasingly used as a potent adjunct therapy in detecting cancerous tissue and in the fluorescence-guided resection of tumours –

greatly increasing a patient's quality of life and survival rates. The use of porphyrinic photosensitisers as theranostic agents also is beginning to show great potential – the capability of a single entity to act as a dual imaging and pdt agent holds significant benefits in the detection and treatment of cancers and other disease models. Furthermore, imaging combined with pdt has the potential to provide patient-customised treatments. The versatility of porphyrinic moieties in the imaging of cancer and other pathological conditions is further demonstrated by their use as radio-labelled imaging probes and in the development of contrast-enhancement agents for MRI and PET. Porphyrinic photosensitisers have recently been identified as strong candidates in the promising alternative treatment model (PACT) for treating microbial infections, especially those with antibiotic resistant strains.

It can be readily observed that there is a clear unequivocal deficit in the understanding of intracellular mechanisms and a need to develop a means by which these delicate and powerful events can be further visualised and understood. An enhanced comprehension of these mechanisms, in both healthy functioning cells and stressed and diseased states, could allow scientists and physicians to develop enhanced, eloquent and sensitive investigative techniques and strategies: empowering them with the potential to detect, control and eliminate cellular damage and disease. Such a physiological breakthrough would court major benefits in not only the health of the patient but financially too. One avenue would through the creation of a multimodal imaging, detective and therapeutic system developed *via* an interdisciplinary approach which brings together: (i) nanotechnology; (ii) porphyrinic chemistry; (iii) optical spectroscopies; and (iv) cell biology. Such a system potentially offers the ability to answer many of the mysteries surrounding the biological labyrinth of cellular functioning and life and facilitate the better management, treatment and possible control of diseases.

Abbreviations

A. baumannii: *Acinetobacter baumannii*; ADAPT: antibody-directed abzyme prodrug therapy; ADEPT: antibody-directed enzyme prodrug therapy; ALA: 5-aminolaevulinic acid/ δ -aminolaevulinic acid; AMD: age-related macular degeneration; AMP: antimicrobial peptides; ATMPn: 9-acetoxy-2,7,12,17-tetrakis-(β -methoxyethyl)-porphycene; BC: bacteriochlorin; BCC: basal cell carcinoma; Benvix®: benzyl ester derivative of ALA; BPD MA: benzoporphyrin derivative monoacid A; BPF: bacteriochlorophyll-peptide-folate; BSA: bovine serum albumin; C.

albicans: *Candida albicans*; CFR: colour fluorescence ratio; CGP55847: a zinc phthalocyanine derivative; CIS: carcinomas *in situ*; *C. krusei*: *Candida krusei*; CNT: carbon nanotube; CNV: choroidal neovascularisation; CT: computerised tomography; CTC: circulating tumour cells; DIF: drug-induced fluorescence; DTPA: (Gd(III)-aminobenzyl-diethylenetriaminepentaacetic acid; *Escherichia coli*: *E. coli*; *E. faecalis*: *Enterococcus faecalis*; EGF: epidermal growth factor; EMR: electromagnetic radiation; EMS: electromagnetic spectrum; FDA: Food and Drug Administration; FDG: ¹⁸F-fluorodeoxyglucose; F-FHBG: 9-(4-¹⁸F-fluoro-3-hydroxymethylbutyl) guanine; FGR: fluorescence-guided resection; FLT: 3'-deoxy-3'-¹⁸F-fluorothymidine; FRET: Förster/Fluorescence Resonance Energy Transfer; Gal: galactose; Glu: glucose; HDL: high density lipoprotein; Hexvix®: a hexyl derivative of ALA; Hp: haematoporphyrin; HpD: haematoporphyrin derivative; HPPH: 3-vinyl-3-[1-(hexyloxy)ethyl]pyropheophorbide *a*; HSV: herpes simplex virus; IC: internal conversion; IC₅₀: 50% cell kill; ISC: intersystem crossing; LDL: low density lipoprotein; LIFE: light induced fluorescence emission; Lutex®/Lutrin®: lutetium texaphyrin; MAb: monoclonal antibody; MB: methylene blue; Metvix®: a methyl ester derivative of ALA; MPE: multi-photon excitation; MPS: mesoporous silica; MRI: magnetic resonance imaging; MRS: magnetic resonance spectroscopy; MWNT: multi-walled nanotube; NC: naphthalocyanine; NCB: non-covalent binding; NP: nanoparticle; NS: nanospecies; NSF: nephrogenic systemic fibrosis; NT: nanotube; OCT: optical computed tomography; *P. aeruginosa*: *Pseudomonas aeruginosa*; PACT: photoantimicrobial chemotherapy; PC: phthalocyanine; PC4: a silicon PC complex; pdd: photodynamic diagnosis; PDI: photodynamic inactivation; pdt: photodynamic therapy; PEG: polyethylene glycol; PET: positron emission tomography; P-Gal4: 5,10,15,20-tetrakis(4,1'-thio-galactose-2,3,5,6,-tetrafluorophenyl)porphyrin; *P. gingivalis*: *Porphyromonas gingivalis*; P-Glu4: 5,10,15,20-tetrakis(4,1'-thio-glucose-2,3,5,6,-tetrafluorophenyl)porphyrin; PIT: photoimmunotherapy; *P. mirabilis*: *Proteus mirabilis*; PPF: porphyrin-peptide-folate; PPIX: protoporphyrin IX; PS1: 5-(4-isothiocyanatophenyl)-10,15,20-tri-(3,5-dihydroxyphenyl)-porphyrin; PS2: 5-(4-isothiocyanatophenyl)-10,15,20-tris-(4-N-methylpyridiniumyl) porphyrin trichloride; psen: photosensitiser; PSFD: photosensitiser fluorescence detection; PZ: porphyrazine; QD: quantum dots; ROS: reactive oxygen species; *S. aureus*: *Staphylococcus aureus*; scFv: single chain antibody fragments; SCC: squamous cell carcinoma; scFv: single chain antibody fragments; SWNT: single-walled

nanotube; THPC: tetra(*m*-hydroxyphenyl)chlorin; TPPF₂₀: tetrapentafluorophenyl porphyrins; TPP: tetraphenylporphyrin; wAMD: wet age-related macular degeneration; Φ_{Δ} : singlet oxygen quantum yield; Φ_{F} : fluorescence quantum yield; Φ_{T} : triplet quantum yield; τ_{T} : triplet state lifetime.

Competing Interests

The authors have declared that no competing interest exists.

References

- Anderson HL. Building molecular wires from the colours of life: conjugated porphyrin oligomers. *Chem Commun.* 1999; 23: 2323-2330.
- Milgrom LR. An introduction to the chemistry of porphyrins and related compounds. In: Milgrom LR, ed. *The Colours of Life*, 1st ed. New York: The Oxford University Press. 1997; 1, 16, 48-57; 70, 71, 78-80, 84 and 85.
- Sternberg ED, Dolphin D, Brückner C. Porphyrin-based photosensitizers for use in photodynamic therapy. *Tetrahedron.* 1998; 54: 4151-4202.
- Sharma WM, Allen CM, van Lier JE. Photodynamic therapeutics: basic principles and clinical applications. *Drug Disc Today.* 1999; 4: 507-517.
- Castano AP, Demidova TN, Hamblin MR. Mechanisms in photodynamic therapy: part one - photosensitizers, photochemistry and cellular localization. *Photodiagnosis Photodynamic Ther.* 2004; 1: 279-293.
- Castano AP, Demidova TN, Hamblin MR. Mechanisms in photodynamic therapy: part two - cellular signaling, cell metabolism and modes of cell death. *Photodiagnosis Photodynamic Ther.* 2005; 2: 1-23.
- Josefsen LB, Boyle RW. Photodynamic therapy and the development of metal-based photosensitizers. *Metal-Based Drugs.* 2008; doi:10.1155/2008/276109.
- Stylli SS, Howes M, MacGregor L, Rajendra P, Kaye AH. Photodynamic therapy of brain tumours: evaluation of porphyrin uptake versus clinical outcome. *J Clin Neurosci.* 2004; 11: 584-596.
- Goslinski T, Piskorz J. Fluorinated porphyrinoids and their biomedical applications. *J Photochem Photobiol C: Photochem Rev.* 2011; 12: 304-321.
- Dougherty TJ. An update on photodynamic therapy applications. *J Clin Laser Med Sur.* 2002; 20: 3-7.
- Kato H, Usuda J, Kato Y. Photodynamic therapy in lung cancer. In: Wang K-P, Mehta AC, Turner JF, ed. *Flexible Bronchoscopy*, 3rd ed. Oxford: Wiley-Blackwell; 2012; doi: 10.1002/9781444346428.ch20
- Lam M, Hsia AH, Liu Y, Guo M, Swick AR, Berlin JC, McCormick TS, Kenney ME, Oleinick NL, Cooper KD, Baron ED. Successful cutaneous delivery of the photosensitizer silicon phthalocyanine 4 for photodynamic therapy. *Clin Exp Dermatol.* 2011; 36: 645-651.
- Silva JN, Filipe P, Morlière P, Mazière J-C, Freitas JP, Cirne de Castro JL, Santos R. Photodynamic therapies: principles and present medical applications. *Bio-Med Mater Eng.* 2006; 16: S147-S154.
- Dougherty TJ, Gomer CJ, Henderson BW, Jori G, Kessel D, Korbek M, Moan J, Peng Q. Photodynamic therapy. *J Natl Cancer Inst.* 1998; 90: 889-905.
- Moreira LM, dos Santos FV, Lyon JP, Maftoum-Costa M, Pacheco-Soares C, da Silva NS. Photodynamic therapy: porphyrins and phthalocyanines as photosensitizers. *Aust J Chem.* 2008; 61: 741-754.
- Linstead RP. Phthalocyanines. Part I. A new type of synthetic colouring matters. *J Chem Soc (resumed).* 1934; 1016-17.
- Eichhorn H. Mesomorphic phthalocyanines, tetraporphyrins, porphyrins and triphenylenes as charge-transporting materials. *J Porphy Phthalocya.* 2000; 4: 88-102.
- Yourre TA, Rudaya LI, Klimova NV, Shamanin VV. Organic materials for photovoltaic and light-emitting devices. *Semiconductors.* 2003; 37: 807-815.
- Sekkat N, van den Bergh H, Nykong T, Lange N. Like a bolt from the blue: phthalocyanines in biomedical optics. *Molecules.* 2012; 17: 98-144.
- Beng YY, Gu DH, Wu YQ, Gan FX. High speed recording property of phthalocyanine thin film for compact disc recordable. In: Gan F, Li Z, ed. *Sixth international symposium on optical storage (ISOS 2002)*. Proceedings of the society of photo-optical instrumentation engineers (SPIE). Washington: SPIE, Bellingham. 2003; 5060: 63-66.
- de la Torre G, Classens CG, Torres T. Phthalocyanines: old dyes, new materials. Putting colour in nanotechnology. *Chem Commun.* 2007; :2000-2015.
- Zagal JH, Griveau S, Silva JF, Nykong T, Bedioui F. Metallophthalocyanine-based molecular materials as catalysts for electrochemical reactions. *Coord Chem Rev.* 2010; 254: 2755-2791.
- Spikes JD. Phthalocyanines as photosensitizers in biological systems and for the photodynamic therapy of tumours. *Photochem Photobiol.* 1986; 43: 691-699.
- Nyman ES, Hynninen PH. Research advances in the use of tetrapyrrolic photosensitizers for photodynamic therapy. *J Photochem Photobiol B: Biol.* 2004; 73: 1-28.
- MacDonald IJ, Dougherty TJ. Basic principles of photodynamic therapy. *J Porphy Phthalocya.* 2001; 5: 105-129.
- Svanberg K, Wang I, Colleen S, Idvall I, Ingvar C, Rydell R, Jocham D, Diddens H, Brown S, Gregory G, Montan S, Anderson-Engels S, Svanberg S. Clinical multi-colour fluorescence imaging of malignant tumours - initial experience. *Acta Radiol.* 1998; 39: 2-9.
- Bonnett R, Martinez G. Photobleaching of photosensitizers used in photodynamic therapy. *Tetrahedron.* 2001; 57: 9513-9547.
- Ethirajan M, Chen Y, Joshi P, Pandey RK. The role of porphyrin chemistry in tumour imaging and photodynamic therapy. *Chem Soc Rev.* 2011; 40: 340-362.
- Detty MR, Gibson SL, Wagner SJ. Current clinical and preclinical photosensitizers for use in photodynamic therapy. *J Med Chem.* 2004; 47: 3897-3915.
- Smetana Z, Ben-Hur E, Mendelson E, Salzberg S, Wagner P, Malik Z. Herpes simplex virus proteins are damaged following photodynamic inactivation with phthalocyanines. *J Photochem Photobiol B: Biol.* 1998; 44: 77-83.
- Edelson RL. Light activated drugs. *Sci Am.* 1988; 259: 68-75.
- Allison RR, Mota HC, Sibata CH. Clinical PD/PDT in North America: an historical review. *Photodiagnosis Photodynamic Ther.* 2004; 1: 263-277.
- Jori G. Tumour photosensitizers: approaches to enhance the selectivity and efficiency of photodynamic therapy. *J Photochem Photobiol B: Biol.* 1996; 36: 87-93.
- Decreau R, Richard MJ, Verrando P, Chanon M, Julliard M. Photodynamic activities of silicon phthalocyanines against achromic M6 melanoma cells and healthy human melanocytes and keratinocytes. *J Photochem Photobiol B: Biol.* 1999; 48: 48-56.
- da Silva EFF, Pedersen BW, Breitenbach T, Toftegaard R, Kuimova MK, Arnaut LG, Ogilby PR. Irradiation- and sensitizer-dependent changes in the lifetime of intracellular singlet oxygen produced in a photosensitized process. *J Phys Chem B.* 2012; 116: 445-461.
- Jiménez-Banzo A, Sagristà ML, Mora M, Nonell S. Kinetics of singlet oxygen photosensitization in human skin fibroblasts. *Free Radical Bio Med.* 2008; 44: 1926-1934.
- Kochevar IE, Redmond RW. Photosensitized production of singlet oxygen. *Methods Enzymol.* 2000; 319: 20-28.
- Morgan J, Oseroff AR. Mitochondria-based photodynamic anti-cancer therapy. *Adv Drug Delivery Rev.* 2001; 49: 71-86.
- Patito IA, Rothmann C, Malik Z. Nuclear transport of photosensitizers during photosensitization and oxidative stress. *Biol Cell.* 2001; 93: 285-291.
- Weizman E, Rothmann C, Greenbaum L, Shainberg A, Adamek M, Ehrenberg B, Malik Z. Mitochondrial localization and photodamage during photodynamic therapy with tetraphenylporphyrins. *J Photochem Photobiol B: Biol.* 2000; 59: 92-102.
- Coulter CV, Kelso GF, Lin T-K, Smith RAJ, Murphy MP. Mitochondrially targeted antioxidants and thiol reagents. *Free Radical Biol Med.* 2000; 28: 1547-1554.
- Castano AP, Demidova TN, Hamblin MR. Mechanisms in photodynamic therapy: part three - photosensitizer pharmacokinetics, biodistribution, tumor localization and modes of tumor destruction. *Photodiagnosis Photodynamic Ther.* 2005; 2: 91-106.
- Peng Q, Moan J, Nesland JM, Rimmington C. Aluminum phthalocyanines with asymmetrical lower sulfonation and with symmetrical higher sulfonation - a comparison of localizing and photosensitizing mechanism in human tumor LOX xenografts. *Int J Cancer.* 1990; 46: 719-726.
- Rück A, Steiner R. Basic reaction mechanisms of hydrophilic and lipophilic photosensitizers in photodynamic tumour treatment. *Minim Invas Ther.* 1998; 7: 503-509.
- Peng Q, Nesland JM, Moan J, Evenson JF, Konshaug M, Rimmington C. Localization of fluorescent Photofrin-II and aluminum phthalocyanine tetrasulfonate in transplanted human-malignant tumor LOX and normal-tissues of nude-mice using highly light-sensitive video intensification microscopy. *Int J Cancer.* 1990; 45: 972-979.
- Ochsen M. Photophysical and photobiological processes in the photodynamic therapy of tumours. *J Photochem Photobiol B: Biol.* 1997; 39: 1-18.

47. Kessel D. Hematoporphyrin and HPD: photophysics, photochemistry and phototherapy. *Photochem Photobiol.* 1984; 39: 851-859.
48. Bonneau S, Vever-Bizet C. Tetrapyrrole photosensitisers, determinants of subcellular localisation and mechanisms of photodynamic processes in therapeutic approaches. *Expert Opin Ther Pat.* 2008; 18: 1011-1025.
49. Lang K, Mosinger J, Wagnerová DM. Photophysical properties of porphyrinoid sensitizers non-covalently bound to host molecules; models for photodynamic therapy. *Coord Chem Rev.* 2004; 248: 321-350.
50. Bonnett R. Photosensitizers of the porphyrin and phthalocyanine series for photodynamic therapy. *Chem Soc Rev.* 1995; 24: 19-33.
51. Rebeiz CA, Reddy KN, Nandihalli UB, Velu J. Tetrapyrrole-dependent photodynamic herbicides. *Photochem Photobiol.* 1990; 52: 1099-1117.
52. Ben Amor T, Tronchin M, Bortolotto L, Verdiglione R, Jori G. Porphyrins and related compounds as photoactivatable insecticides I. Phototoxic activity of hematoporphyrin toward *Ceratitis capitata* and *Bactrocera oleae*. *Photochem Photobiol.* 1998; 67: 206-211.
53. Keating PB, Hinds MF, Davis SJ. A singlet oxygen sensor for photodynamic cancer therapy. The Proceedings of the International Congress on Applications of Lasers and Laser-Optics. Laser Institute of America, Orlando, Florida. 1999; 253-260.
54. Krasnovsky Jr AA. Primary mechanisms of photoactivation of molecular oxygen. History of development and the modern status of research. *Biochem (Moscow).* 2007; 72: 1065-1080.
55. Plaetzer K, Krammer B, Berlanda J, Berr F, Kiesslich T. Photophysics and photochemistry of photodynamic therapy: fundamental aspects. *Lasers Med Sci.* 2009; 24: 259-268.
56. Kruff BI, Greer A. Photosensitization reactions *in vitro* and *in vivo*. *Photochem Photobiol.* 2011; 87: 1204-1213.
57. Girotti AW. Photosensitized oxidation of membrane lipids: reaction pathways, cytotoxic effects, and cytoprotective mechanisms. *J Photochem Photobiol B: Biol.* 2001; 63: 103-113.
58. van Lier JE. Photosensitization: reaction pathways. In: Valzeno DP, Pottier RH, Mathis P, Douglas RH, ed. *Photobiological techniques, photosensitization: reaction pathways.* NATO ASI Series, Series A: Life Sciences. New York and London: Plenum Press. 1991; 216: 85-98.
59. Foote CS. Definition of Type-I and Type-II photosensitized oxidation. *Photochem Photobiol.* 1991; 54: 659-661.
60. See KL, Forbes IJ, Betts WH. Oxygen dependency of photocytotoxicity with haematoporphyrin derivative. *Photochem Photobiol.* 1984; 39: 631-634.
61. Ma LW, Moan J, Berg K. Evaluation of a new photosensitizer, *meso*-tetra-hydroxyphenyl-chlorin, for use in photodynamic therapy: a comparison of its photobiological properties with those of two other photosensitizers. *Int J Cancer.* 1994; 57: 883-888.
62. Hasan T, Khan AU. Phototoxicity of the tetracyclines: photosensitized emission of singlet delta dioxygen. *Proc Natl Acad Sci USA.* 1986; 83: 4604-4606.
63. von Tappeiner H. *Münch Med Wochenschr. Über die wirkung fluorescirender stoffe auf infusorien nach versuchen von O. Raab.* 1900; 47: 5-7.
64. Hudson R, Carcenac M, Smith K, Madden L, Clarke OJ, Pèlegriin A, Greenman J, Boyle RW. The development and characterisation of porphyrin isothiocyanate monoclonal antibody conjugates for photoimmunotherapy. *Br J Cancer.* 2005; 92: 1442-1449.
65. Malatesti N, Smith K, Savoie H, Greenman J, Boyle RW. Synthesis and *in vitro* investigation of cationic 5,15-diphenylporphyrin-monoclonal antibody conjugates as targeted photodynamic sensitizers. *Int J Oncol.* 2006; 28: 1561-1569.
66. Josefsen LB, Aylott JW, Beeby A, Warburton P, Boyle JP, Peers C, Boyle RW. Porphyrin-nanosensor conjugates. New tools for the measurement of intracellular response to reactive oxygen species. *Photochem Photobiol Sci.* 2010; 9: 801-811.
67. Kopelman R, Koo Y-EL, Philbert M, Moffat BA, Reddy GR, McConville P, Hall DE, Chenevert TL, Bhojani MS, Buck SM, Rehemtulla A, Ross BD. Multifunctional nanoparticle platforms for *in vivo* MRI enhancement and photodynamic therapy of a rat brain cancer. *J Magn Magn Mater.* 2005; 293: 404-410.
68. Lovell JF, Liu TWB, Chen J, Zheng G. Activatable photosensitisers for imaging and therapy. *Chem Rev.* 2010; 110: 2839-2857.
69. Yang K, Gitter B, Rügger R, Wieland GD, Chen M, Liu X, Albrecht V, Fahr A. Antimicrobial peptide-modified liposomes for bacteria targeted delivery of temoporfin in photodynamic antimicrobial chemotherapy. *Photochem Photobiol Sci.* 2011; 10: 1593-1601.
70. Liu TWB, Chen J, Burgess L, Cao W, Shi J, Wilson BC, Zheng G. Multimodal bacteriochlorophyll theranostic agent. *Theranostics.* 2011; 1: 354-362.
71. Brown SB, Brown EA, Walker I. The present and future role of photodynamic therapy in cancer. *Lancet Onco.* 2004; 5: 497-508.
72. Levy JG, Jones CA, Pilson LA. The preclinical and clinical development and potential application of benzoporphyrin derivative. *Int Photodyn.* 1994; 1: 3-5.
73. Aveline BM, Hasan T, Redmond RW. The effects of aggregation, protein binding and cellular incorporation on the photophysical properties of benzoporphyrin derivative monoacid ring A (BPDMA). *J Photochem Photobiol B: Biol.* 1995; 30: 161-169.
74. Stables GI, Ash DV. Photodynamic therapy. *Cancer Treat Rev.* 1995; 21: 311-323.
75. Morgan AR, Garbo GM, Keck RW, Selman SH. New photosensitizers for photodynamic therapy: combined effect of metalloporphyrin derivatives and light on transplantable bladder tumors. *Cancer Res.* 1988; 48: 194-198.
76. Ali H, van Lier JE. Metal complexes as photo- and radio-sensitizers. *Chem Rev.* 1999; 99: 2379-2450.
77. Kübler AC, Haase T, Staff C, Kahle B, Rheinwald M, Mühlhng J. Photodynamic therapy of primary nonmelanomatous skin tumours of the head and neck. *Laser Surg Med.* 1999; 25: 60-68.
78. Ball DJ, Wood SR, Vernon DI, Griffiths J, Dubbelman TMAR, Brown SB. The characterisation of three substituted zinc phthalocyanines of differing charge for use in photodynamic therapy. A comparative study of their aggregation and photosensitising ability in relation to *m*-THPC and polyhaematoporphyrin. *J Photochem Photobiol B: Biol.* 1998; 45: 28-35.
79. Sessler JL, Johnson MR, Lynch V. Synthesis and crystal structure of a novel tripyrrane-containing porphyrinogen-like macrocycle. *J Org Chem.* 1987; 52: 4394-4397.
80. Sessler JL, Hemmi G, Mody TD, Murai T, Burrell A, Young SW. Texaphyrins: synthesis and applications. *Acc Chem Res.* 1994; 27: 43-50.
81. Woodburn KW, Fan Q, Kessel D, Luo Y, Young SW. Photodynamic therapy of B16F10 murine melanoma with lutetium texaphyrin. *J Inv Dermatol.* 1998; 110: 746-751.
82. Woodburn KW, Qing F, Kessel D, Young SW. Photoeradication and imaging of atheromatous plaque with texaphyrins. In: Anderson RR, Bartels KE, Bass LS, Gregory KW, Harris DM, Lui H, Malek RS, Muller GJ, Pankratov MM, Perlmutter AP, Reidenbach HD, Tate LP, Watson GM, Katzir A. *Lasers in surgery: advanced characterization, therapeutics, and systems VII. Proceedings of the photo-optical instrumentation engineers (SPIE).* Washington: SPIE, Bellingham. 1997; 2970: 44-50.
83. Szeimies R-M, Karrer S, Abels C, Steinbach P, Fickweiler S, Messmann H, Bäumler W, Landthaler M. 9-Acetoxy-2,7,12,17-tetrakis(β -methoxyethyl)-porphycene (ATMPn), a novel photosensitizer for photodynamic therapy: uptake kinetics and intracellular localization. *J Photochem Photobiol: B.* 1996; 34: 67-72.
84. Kimel S, Gottfried V, Davidi R, Averbuj C. *In vivo* uptake and photodynamic activity of porphycenes. In: Jori G, Moan J, Star WM, ed. *Photodynamic Therapy of Cancer I. Proceedings of the photo-optical instrumentation engineers (SPIE).* Washington: SPIE, Bellingham. 1994; 2078: 205-211.
85. Aicher A, Müller K, Reich ED, Hautmann RE. Photosensitization of human bladder carcinoma cells *in vitro* by 9-acetoxy-tetra-n-propylporphycene (ATPPn) bound to liposomes from soya phosphatidylcholine. *Optical Engineering.* 1993; 32: 342-346.
86. Karrer S, Abels C, Szeimies R-M, Bäumler W, Dellian M, Hohenleutner U, Goetz AE, Landthaler M. Topical application of a first porphycene dye for photodynamic therapy - penetration studies in human perilesional skin and basal cell carcinoma. *Arch Dermatol Res.* 1997; 289: 132-137.
87. Ochsner M. Light scattering of human skin: a comparison between zinc(II)-phthalocyanine and Photofrin II®. *J Photochem Photobiol B: Biol.* 1996; 32: 3-9.
88. Schieweck K, Capraro H-G, Isele U, van Hoogevest P, Ochsner M, Maurer T, Batt E. CGP 55847, liposome-delivered zinc(II)-phthalocyanine as a phototherapeutic agent for tumors. In: Jori G, Moan J, Star WM ed. *Photodynamic Therapy of Cancer I. Proceedings of the photo-optical instrumentation engineers (SPIE).* Washington: SPIE, Bellingham. 1993; 2078: 107-118.
89. Kaestner L, Cesson M, Kassab K, Christensen T, Edminson PD, Cook MJ, Chambrier I, Jori G. Zinc octa-*n*-alkyl phthalocyanines in photodynamic therapy: photophysical properties, accumulation and apoptosis in cell cultures, studies in erythrocytes and topical application to Balb/c mice skin. *Photochem Photobiol Sci.* 2003; 2: 660-667.
90. Cook MJ. Properties of some alkyl substituted phthalocyanines and related macrocycles. *Chem Rec.* 2002; 2: 225-236.
91. Fabris C, Soncin M, Miotto G, Fantetti L, Chiti G, Dei D, Roncucci G, Jori G. Zn(II)-phthalocyanines as phototherapeutic agents for cutaneous

- diseases. Photosensitization of fibroblasts and keratinocytes. *J Photochem Photobiol B: Biol.* 2006; 83: 48–54.
92. Mantareva V, Kussovski V, Angelov I, Borisova E, Avramov L, Schnurpfeil G, Wöhrle D. Photodynamic activity of water-soluble phthalocyanine zinc(II) complexes against pathogenic microorganisms. *Bioorg Med Chem.* 2007; 15: 4829–4835.
93. Cauchon N, Nader M, Bkaily G, van Lier JE, Hunting D. Photodynamic activity of substituted zinc trisulfophthalocyanines: role of plasma membrane damage. *Photochem Photobiol.* 2006; 82: 1712–1720.
94. Sobolev AS, Stranadko EF. Photodynamic therapy in Russia. Clinical and fundamental aspects. In: Brown S ed. *International Photodynamics. A PDT Forum.* West Sussex, UK: Eurocommunication Publications. 1997; 1: 2–3.
95. Sokolov VV, Chissov VI, Filonenko EV, Yakubovskaya RI, Sukhin GM, Galpern MG, Vorozhtsov GN, Gulina AV, Zhitkova MB, Zharkova NN, Kozlov DN, Smirnov VV. First clinical results with a new drug for PDT. In: Jori G, Moan J, Star WM ed. *Photodynamic Therapy of Cancer II. Proceedings of the photo-optical instrumentation engineers (SPIE).* Washington: SPIE, Bellingham. 1995; 2325: 364–366.
96. Zharkova NN, Kozlov DN, Smirnov VV, Sokolov VV, Chissov VI, Filonenko EV, Sukhin GM, Galpern MG, Vorozhtsov GN. Fluorescence observations of patients in the course of photodynamic therapy of cancer with the photosensitizer PHOTOSENS. In: Jori G, Moan J, Star WM ed. *Photodynamic Therapy of Cancer II. Proceedings of the photo-optical instrumentation engineers (SPIE).* Washington: SPIE, Bellingham. 1995; 2325: 400–403.
97. Oleinick NL, Antunez AR, Clay ME, Rihter BD, Kenney ME. New phthalocyanine photosensitizers for photodynamic therapy. *Photochem Photobiol.* 1993; 57: 242–247.
98. Whitacre CM, Feyes DK, Satoh T, Grossmann J, Mulvihill JW, Mukhtar H, Oleinick NL. Photodynamic therapy with the phthalocyanine photosensitizer PC4 of SW480 human colon cancer xenografts in athymic mice. *Clin Cancer Res.* 2000; 6: 2021–2027.
99. Lo PC, Leung SCH, Chan EYM, Fong W-P, Ko W-H, Ng DNP. Photodynamic effects of a novel series of silicon(IV) phthalocyanines against human colon adenocarcinoma cells. *Photodiagnosis Photodynamic Ther.* 2007; 4: 117–123.
100. Zaidi SIA, Agarwal R, Eichler G, Rihter BD, Kenney ME, Mukhtar H. Photodynamic effects of new silicon phthalocyanines – *in vitro* studies utilising rat hepatic microsomes and human erythrocyte-ghosts as model membrane sources. *Photochem Photobiol.* 1993; 58: 204–210.
101. Colussi VC, Feyes DK, Mulvihill JW, Li Y-S, Kenney ME, Elmets CA, Oleinick NL, Mukhtar H. Phthalocyanine 4 (PC4) photodynamic therapy of human OVCAR-3 tumour xenografts. *Photochem Photobiol.* 1999; 69: 236–241.
102. Whitacre CM, Satoh TH, Xue L-Y, Gordon NH, Oleinick NL. Photodynamic therapy of human breast cancer xenografts lacking caspase-3. *Cancer Letts.* 2002; 179: 43–49.
103. George JE, Ahmad Y, Varghai D, Li X, Berlin J, Jackowe J, Jungermann M, Wolfe MS, Lilge L, Totonchi A, Morris RL, Peterson A, Lust WD, Kenney ME, Hoppel CL, Sun J, Oleinick NL, Dean D. PC4 photodynamic therapy of U87-derived human glioma in the nude rat. *Lasers Surg Med.* 2005; 36: 383–389.
104. Wheeler BL, Nagasubramanian G, Bard AJ, Schechtman LA, Dininny DR, Kenney ME. A silicon phthalocyanine and a silicon naphthalocyanine: synthesis, electrochemistry, and electrogenerated chemiluminescence. *J Am Chem Soc.* 1984; 106: 7404–7410.
105. Margaron P, Langlois R, van Lier JE, Gaspard SJ. Photodynamic properties of naphthosulfobenzoporphyrazines, novel asymmetric, amphiphilic phthalocyanine derivatives. *J Photochem Photobiol B: Biol.* 1992; 14: 187–199.
106. Wöhrle D, Shopova M, Müller S, Milev AD, Mantareva VN, Krastev KK. Liposome delivered Zn(II)-2,3-naphthalocyanines as potential sensitizers for PDT: synthesis, photochemical, pharmacokinetic, and phototherapeutic studies. *J Photochem Photobiol B: Biol.* 1993; 21: 155–165.
107. Shopova M, Wöhrle D, Stoichkova N, Milev A, Mantareva V, Müller S, Kassabov K, Georgiev K. Hydrophobic Zn(II)-naphthalocyanines as photodynamic therapy agents for Lewis-lung carcinoma. *J Photochem Photobiol B: Biol.* 1994; 23: 35–42.
108. Müller S, Mantareva V, Stoichkova N, Kliesch H, Sobbi A, Wöhrle D, Shopova M. Tetraamido-substituted 2,3-naphthalocyanine zinc(II) complexes as phototherapeutic agents: synthesis, comparative photochemical and photobiological studies. *J Photochem Photobiol B: Biol.* 1996; 35: 167–174.
109. Zuk MM, Rihter BD, Kenney ME, Rodgers MAJ, Kreimer-Birnbaum M. Pharmacokinetic and tissue distribution studies of the photosensitizer bis(di-isobutyl octadecylsiloxy)silicon 2,3-naphthalocyanine (isobosinc) in normal and tumor-bearing rats. *Photochem Photobiol.* 1994; 59: 66–72.
110. Cuomo V, Jori G, Rihter BD, Kenney ME, Rodgers MAJ. Liposome-delivered Si(IV)-naphthalocyanine as a photodynamic sensitizer for experimental tumours: pharmacokinetic and phototherapeutic studies. *Br J Cancer.* 1990; 62: 966–970.
111. Mantareva V, Shopova M, Spassova G, Wöhrle D, Müller S, Jori G, Ricchelli F. Si(IV)-methoxyethylene-glycol-naphthalocyanine: synthesis and pharmacokinetic and photosensitizing properties in different tumour models. *J Photochem Photobiol B: Biol.* 1997; 40: 258–262.
112. Brasseur N, Nguyen T-L, Langlois R, Ouellet R, Marengo S, Houde D, van Lier JE. Synthesis and photodynamic activities of silicon 2,3-naphthalocyanine derivatives. *J Med Chem.* 1994; 37: 415–420.
113. Brasseur N, Ouellet R, Lewis K, Potter WR, van Lier JE. Photodynamic activities and skin photosensitivity of the bis(dimethylhexylsiloxy)silicon 2,3-naphthalocyanine in mice. *Photochem Photobiol.* 1995; 62: 1058–1065.
114. Agarwal ML, Clay ME, Harvey EJ, Evans HH, Antunez AR, Oleinick NL. Photodynamic therapy induces rapid cell-death by apoptosis in L5178Y mouse lymphoma-cells. *Cancer Res.* 1991; 51: 5993–5996.
115. Kelso GF, Porteous CM, Coulter CV, Hughes G, Porteous WF, Ledgerwood EC, Smith RAJ, Murphy MP. Selective targeting of a redox-active ubiquinone to mitochondria within cells – antioxidant and antiapoptotic properties. *J Biol Chem.* 2001; 276: 4588–4596.
116. Brunner H, Obermeier H, Szeimies RM. Platin(II)-komplexe mit porphyrinliganden: synthese und synergismen bei der photodynamischen tumortherapie. *Chemische Berichte.* 1995; 128: 173–181.
117. Ding L, Balzarini J, Schols D, Meunier B, De Clercq E. Anti-human immunodeficiency virus effects of cationic metalloporphyrin-ellipticine complexes. *Biochem Pharm.* 1992; 44: 1675–1679.
118. Ding L, Casas C, Etemad-Moghadam G, Meunier B, Cros S. Synthesis of water-soluble, cationic functionalised metalloporphyrins having a cytotoxic activity. *New J Chem.* 1990; 14: 421–431.
119. Dozzo P, Koo M-S, Berger S, Forte TM, Kahl SB. Synthesis, characterization, and plasma lipoprotein association of a nucleus-targeted boronated porphyrin. *J Med Chem.* 2005; 48: 357–359.
120. Boyle RW, Dolphin D. Structure and biodistribution relationships of photodynamic sensitizers. *Photochem Photobiol.* 1996; 64: 469–485.
121. Ehrlich P. Address in pathology on chemotherapeutics: scientific principles, methods, and results. *The Lancet.* 1913; 182: 445–451.
122. Collier RJ, Kaplan DA. Immunotoxins. *Sci Am.* 1984; 251: 56–64.
123. Collard P. *Chemotherapy.* In: *The Development of Microbiology, 1st ed.* Cambridge: Cambridge University Press; 1976: 52–58.
124. Phillips D. Toward targeted photodynamic therapy. *Pure Appl Chem.* 2011; 83: 733–748.
125. Chen X, Hui L, Foster DA, Drain CM. Efficient synthesis and photodynamic activity of porphyrin-saccharide conjugates: targeting and incapacitating cancer cells. *Biochemistry.* 2004; 43: 10918–10929.
126. Bagshawe KD. The 1st Bagshawe lecture - towards generating cytotoxic agents at cancer sites. *Br J Cancer.* 1989; 60: 275–281.
127. Sharma SK. Immune response in ADEPT. *Adv Drug Delivery Rev.* 1996; 22: 369–376.
128. Winter G, Milstein C. Man-made antibodies. *Nature.* 1991; 349: 293–299.
129. Niculescu-Duvaz I, Springer CJ. Antibody-directed enzyme prodrug therapy (ADEPT): a review. *Adv Drug Delivery Rev.* 1997; 26: 151–172.
130. Jungheim LN, Shepherd TA. Design of antitumor prodrugs - substrates for antibody-targeted enzymes. *Chem Rev.* 1994; 94: 1553–1566.
131. Syrigos KN, Epenetos AA. Antibody directed enzyme prodrug therapy (ADEPT): a review of the experimental and clinical considerations. *Anticancer Res.* 1999; 19: 605–613.
132. Wolfe LA, Mullin RJ, Laethem R, Blumenkopf TA, Cory M, Miller JF, Keith BR, Humphreys J, Smith GK. Antibody-directed enzyme prodrug therapy with the T268G mutant of human carboxypeptidase A1: *in vitro* and *in vivo* studies with prodrugs of methotrexate and the thymidylate synthase inhibitors GW1031 and GW1843. *Bioconjugate Chem.* 1999; 10: 38–48.
133. Wentworth P, Datta A, Blakey D, Boyle T, Partridge L, Blackburn GM. Toward antibody-directed "abzyme" prodrug therapy, ADAPT: carbamate prodrug activation by a catalytic antibody and its *in vitro* application to human tumor cell killing. *Proc Natl Acad Sci. USA.* 1996; 93: 799–803.
134. Ma GXB, Batey RA, Taylor SD, Hum G, Jones JB. The synthesis of diencarbamates as ADAPT prodrug models. *Synth Commun.* 1997; 27: 2445–2453.
135. Sharman WM, van Lier JE, Allen CM. Targeted photodynamic therapy via receptor mediated delivery systems. *Adv Drug Delivery Rev.* 2004; 56: 53–76.

136. Chen B, Pogue BW, Hoopes PJ, Hasan T. Vascular and cellular targeting for photodynamic therapy. *Crit Rev Eukar Gene Expression*. 2006; 16: 279-306.
137. Tsuchida T, Zheng G, Pandey RK, Potter WR, Bellnier DA, Henderson BW, Kato H, Dougherty TJ. Correlation between site II-specific human serum albumin (HSA) binding affinity and murine *in vivo* photosensitizing efficacy of some Photofrin® components. *Photochem Photobiol*. 1997; 66: 224-228.
138. Rosenberger V, Margalit R. Thermodynamics of the binding of hematoporphyrin ester, a hematoporphyrin derivative-like photosensitizer, and its components to human serum albumin, human high-density lipoprotein and human low density lipoprotein. *Photochem Photobiol*. 1993; 58: 627-630.
139. Korbelik M. Cellular delivery and retention of photofrin: III. Role of plasma proteins in photosensitizer clearance from cells. *Photochem Photobiol*. 1993; 57: 846-850.
140. Cohen S, Margalit R. Binding of porphyrin to human serum albumin. Structure-activity relationships. *Biochem J*. 1990; 270: 325-330.
141. Durmuş M, Yaman H, Göl C, Ahsen V, Nyokong T. Water-soluble quaternized mercaptopyridine-substituted zinc-phthalocyanines: synthesis, photophysical, photochemical and bovine serum albumin binding properties. *Dyes Pigments*. 2011; 91: 153-163.
142. Konan YN, Gurny R, Allémann E. State of the art in the delivery of photosensitizers for photodynamic therapy. *J Photochem Photobiol B: Biol*. 2002; 66: 89-106.
143. Martins J, Almeida L, Laranjinha J. Simultaneous production of superoxide radical and singlet oxygen by sulphonated chloroaluminum phthalocyanine incorporated in human low-density lipoproteins: implications for photodynamic therapy. *Photochem Photobiol*. 2004; 80: 267-273.
144. Jori G, Reddi E. The role of lipoproteins in the delivery of tumour-targeting photosensitizers. *Int J Biochem*. 1993; 25: 1369-1375.
145. Bonneau S, Morlière P, Brault D. Dynamics of interactions of photosensitizers with lipoproteins and membrane-models: correlation with cellular incorporation and subcellular distribution. *Biochem Pharmacol*. 2004; 68: 1443-1452.
146. Buriankova L, Buzova D, Chorvat Jr D, Sureau F, Brault D, Miskovský P, Jancura D. Kinetics of hypericin association with low-density lipoproteins. *Photochem Photobiol*. 2011; 87: 56-63.
147. Taquet J-P, Frochot C, Manneville V, Barberi-Heyob M. Phthalocyanines covalently bound to biomolecules for a targeted photodynamic therapy. *Curr Med Chem*. 2007; 14: 1673-1687.
148. Lutsenko SV, Feldman NB, Finakova GV, Posypanova GA, Severin SE, Skryabin KG, Kirpichnikov MP, Lukyanets EA, Vorozhtsov GN. Targeting phthalocyanines to tumor cells using epidermal growth factor conjugates. *Tumour Biol*. 1999; 20: 218-224.
149. Hirohara S, Nishida M, Sharyo K, Obata M, Ando T, Tanihara M. Synthesis, photophysical properties and photocytotoxicity of mono-, di-, tri- and tetra-glucosylated fluorophenylporphyrins. *Bioorg Med Chem*. 2010; 18: 1526-1535.
150. Vedachalam S, Choi B-H, Pasunooti KK, Ching KM, Lee K, Yoon HS, Liu X-W. Glycosylated porphyrin derivatives and their photodynamic activity in cancer cells. *Med Chem Commun*. 2011; 2: 371-377.
151. Tomé JPC, Neves MGPMs, Tomé AC, Cavaleiro JAS, Mendonça AF, Pegado IN, Duarte R, Valdeira ML. Synthesis of glycoporphyrin derivatives and their antiviral activity against herpes simplex virus types 1 and 2. *Bioorgan Med Chem*. 2005; 13: 3878-3888.
152. Banfi S, Caruso E, Buccafurni L, Murano R, Monti E, Gariboldi M, Papa E, Gramatica P. Comparison between 5,10,15,20-tetraaryl- and 5,15-diarylporphyrins as photosensitizers: synthesis, photodynamic activity and quantitative structure-activity relationship modeling. *J Med Chem*. 2006; 49: 3293-3304.
153. Ferrand Y, Bourré L, Simonneaux G, Thibaut S, Odobel F, Lajat Y, Patrice T. Hydrophorphyris as tumour photosensitizers: synthesis and photophysical studies of 2,3-dihydro-5,15-di(3,5-dihydroxyphenyl) porphyrin. *Bioorg Med Chem Lett*. 2003; 13: 833-835.
154. Álvarez-Micó X, Calvete MJF, Hanack M, Ziegler T. A new glycosidation method through nitrite displacement on substituted nitrobenzene. *Carbohydr Res*. 2007; 342: 440-447.
155. Lee PPS, Lo P-C, Chan EYM, Fong W-P, Ko W-H, Ng DKP. Synthesis and *in vitro* photodynamic activity of novel galactose-containing phthalocyanines. *Tetrahedron Lett*. 2005; 46: 1551-1554.
156. Ribeiro AO, Tomé JPC, Neves MGPMs, Tomé AC, Cavaleiro JAS, Yamamoto Y, Torres T. [1,2,3,4-tetrakis(α/β -D-galactopyranos-6-yl)-phthalocyaninato] zinc(II): a water-soluble phthalocyanine. *Tetrahedron Lett*. 2006; 47: 9177-9180.
157. Iqbal Z, Lyubimtssev A, Hanack M, Ziegler T. Anomerically glycosylated zinc (II) naphthalocyanines. *Tetrahedron Lett*. 2009; 50: 5681-5685.
158. Jankun J. Protein-based nanotechnology: antibody conjugated with photosensitizer in targeted anticancer photoimmunotherapy. *Int J Oncol*. 2011; 39: 949-953.
159. Staneloudi C, Smith KA, Hudson R, Malatesti N, Savoie H, Boyle RW, Greenman J. Development and characterisation of novel photosensitizer: scFv conjugates for use in photodynamic therapy of cancer. *Immunology*. 2007; 120: 512-517.
160. Palumbo A, Hauler F, Dziunycz P, Schwager K, Soltermann A, Pretto F, Alonso C, Hofbauer GF, Boyle RW, Neri D. A chemically modified antibody mediates complete eradication of tumours by selective disruption of tumour blood vessels. *Br J Cancer*. 2011; 104: 1106-1115.
161. Smith K, Malatesti N, Cauchon N, Hunting D, Lecomte R, van Lier JE, Greenman J, Boyle RW. Mono- and tri-cationic porphyrin-monoconjugated antibody conjugates: photodynamic activity and mechanism of action. *Immunology*. 2011; 132: 256-265.
162. Martin M, Kaul S, Drechsler U, Geyer M, Kurek R, Hanack M, Seeger S, Wallwiener D, Wolfrum JM. *In vitro* phototoxicity of a new phthalocyanine-immunoconjugate for use in photodynamic therapy. In: Brown SB, Ehrenberg B, Moan J, Katzir A, ed. *Photochemotherapy: photodynamic therapy and other modalities II*. Proceedings of the society of photo-optical instrumentation engineers (SPIE). Washington: SPIE, Bellingham. 1996; 2924: 153-159.
163. Bullous AJ, Alonso CMA, Boyle RW. Photosensitizer-antibody conjugates for photodynamic therapy. *Photochem Photobiol Sci*. 2011; 10: 721-750.
164. Mitsunaga M, Ogawa M, Kosaka N, Rosenblum LT, Choyke PL, Kobayashi H. Cancer cell-selective *in vivo* near infrared photoimmunotherapy targeting specific membrane molecules. *Nat Med*. 2011; 17: 1685-1691.
165. Sutton JM, Clarke OJ, Fernandez N, Boyle RW. Porphyrin, chlorin and bacteriochlorin isothiocyanates: useful reagents for the synthesis of photoactive bioconjugates. *Bioconjugate Chem*. 2002; 13: 249-263.
166. Carcenac M, Dorvillius M, Garambois V, Glaussel F, Larroque C, Langlois R, Hynes NE, van Lier JE, Pelegrin A. Internalisation enhances photo-induced cytotoxicity of monoclonal antibody-phthalocyanine conjugates. *Br J Cancer*. 2001; 85: 1787-1793.
167. Partridge WM, Buciac J, Yang J, Wu D. Enhanced endocytosis in cultured human breast carcinoma cells and *in vivo* biodistribution in rats of a humanized monoclonal antibody after cationization of the protein. *J Pharmacol Exp Ther*. 1998; 286: 548-554.
168. Duan WB, Smith KA, Savoie H, Greenman J, Boyle RW. Near IR emitting isothiocyanato-substituted fluorophores: their synthesis and bioconjugation to monoclonal antibodies. *Org Biomol Chem*. 2005; 3: 2384-2386.
169. Morgan J, Lottman H, Abbou C, Chopin DK. Comparison of direct and liposomal antibody conjugates of sulfonated aluminum phthalocyanines for selective photoimmunotherapy of human bladder-carcinoma. *Photochem Photobiol*. 1994; 60: 486-496.
170. Carcenac M, Larroque C, Langlois R, van Lier JE, Artus J-C, Pelegrin A. Preparation, phototoxicity and biodistribution studies of anti-carcinoembryonic antigen monoclonal antibody-phthalocyanine conjugates. *Photochem Photobiol*. 1999; 70: 930-936.
171. Vroenenraets MB, Visser GWM, Stigter M, Oppelaar H, Snow GB, van Dongen GAMS. Targeting of aluminum (III) phthalocyanine tetrasulfonate by use of internalizing monoclonal antibodies: improved efficacy in photodynamic therapy. *Cancer Res*. 2001; 61: 1970-1975.
172. Hongrapipat J, Kopeckova P, Liu J, Prakongpan S, Kopecek J. Combination chemotherapy and photodynamic therapy with Fab' fragment targeted HPMA copolymer conjugates in human ovarian carcinoma cells. *Mol Pharmaceutics*. 2008; 5: 696-709.
173. Birchler M, Viti F, Zardi L, Spiess B, Neri D. Selective targeting and photocoagulation of ocular angiogenesis mediated by a phage-derived human antibody fragment. *Nature Biotech*. 1999; 17: 984-988.
174. Zhang Z, Cao W, Jin H, Lovell JF, Yang M, Ding L, Chen J, Corbin J, Luo Q, Zheng G. Biomimetic nanocarrier for direct cytosolic drug delivery. *Angew Chem Int Edit*. 2009; 48: 9171-9175.
175. Collins-Gold L, Feichtinger N, Wörnheim T. **Are lipid emulsions the drug delivery solution?** *Mod Drug Discovery*. 2000; 3: 44-51.
176. El-Laihy HM, El-Shaboury KMF. The development of Cutina lipogels and gel microemulsion for topical administration of Fluconazole. *AAPS Pharm Sci Tech*. 2003; 3: 1-9.
177. Kurupparachchi M, Savoie H, Lowry A, Alonso C, Boyle RW. Polyacrylamide nanoparticles as a delivery system in photodynamic therapy. *Mol Pharmaceutics*. 2011; 8: 920-931.
178. Cheng Y, Meyers JD, Broome A-M, Kenney ME, Basilion JP, Burda C. Deep penetration of a pdt drug into tumours by noncovalent drug-gold nanoparticle conjugates. *J Am Chem Soc*. 2011; 133: 2583-2591.

179. Camerin M, Magaraggia M, Soncin M, Jori G, Moreno M, Chambrier J, Cook MJ, Russell DA. The *in vivo* efficacy of phthalocyanine-nanoparticle conjugates for the photodynamic therapy of amelanotic melanoma. *Eur J Cancer*. 2010; 46: 1910-1918.
180. Wang S, Fan W, Kim G, Hah HJ, Lee Y-EK, Kopelman R, Ethirajan M, Gupta A, Goswami LN, Pera P, Morgan J, Pandey RK. Novel methods to incorporate photosensitizers into nanocarriers for cancer treatment by photodynamic therapy. *Laser Surg Med*. 2011; 43: 686-695.
181. Tang W, Xu H, Park EJ, Philbert MA, Kopelman R. Encapsulation of methylene blue in polyacrylamide nanoparticle platforms protects its photodynamic effectiveness. *Biochem Biophys Res Commun*. 2008; 369: 579-583.
182. Alvarez MG, Vittar NBR, Principe F, Bergesse J, Romanini MC, Romanini S, Bertuzzi M, Durantini EN, Rivarola V. Pharmacokinetic and phototherapeutic studies of monocationic methoxyphenylporphyrin derivative. *Photodiagnosis Photodynamic Ther*. 2004; 1: 335-344.
183. Allison R, Moghissi K, Downie G, Dixon K. Photodynamic therapy (PDT) for lung cancer. *Photodiagnosis and Photodynamic Ther*. 2011; 8: 231-239.
184. DaCosta RS, Lilje LD, Kost J, Cirroco M, Hassaram S, Marcon NE, Wilson BC. Confocal fluorescence microscopy, microspectrofluorimetry, and modelling studies of laser-induced fluorescence endoscopy (LIFE) of human colon tissue. In: Jacques SL, ed. Eighth international symposium on laser-tissue interaction. SPIE. *Proceedings of the photo-optical instrumentation engineers (SPIE)*. Washington: SPIE, Bellingham. 1997; 2975: 98-107.
185. Moghissi K, Stringer MR, Dixon K. Fluorescence photodiagnosis in clinical practice. *Photodiagnosis Photodynamic Ther*. 2008; 5: 235-237.
186. Moghissi K, Dixon K, Stringer MR. Current indications and future perspective of fluorescence bronchoscopy: a review study. *Photodiagnosis Photodynamic Ther*. 2008; 5: 238-246.
187. Stringer MR, Moghissi K, Dixon K. Autofluorescence bronchoscopy in volunteer asymptomatic smokers. *Photodiagnosis Photodynamic Ther*. 2008; 5: 148-152.
188. Moghissi K. Role of bronchoscopic photodynamic therapy in lung cancer management. *Curr Opin Pulm Med*. 2004; 10: 256-260.
189. Lee P, van den Berg RM, Lam S, Gazdar AF, Grunberg K, McWilliams A, LeRiche J, Postmus PE, Sutudja TG. Color fluorescence ratio for detection of bronchial dysplasia and carcinoma *in situ*. *Clin Cancer Res* 2009; 15: 4700-4705.
190. McWilliams A, Mayo J, MacDonald S, LeRiche JC, Palcic B, Szabo E, Lam S. Lung Cancer Screening. *Am J Resp Crit Care Med*. 2003; 168: 1167-1173.
191. Zheng HS, MacAulay C, Lam S, Palcic B. Light induced fluorescence endoscopy (LIFE) imaging system for early cancer detection. In: Luo Q, Chance B, Wang L, Jacques SL, ed. International conference on biomedical optics. *Proceedings of the photo-optical instrumentation engineers (SPIE)*. Washington: SPIE, Bellingham. 1999; 3863: 275-282.
192. Lam S, MacAulay C, Hung J, LeRiche J, Profio AE, Palcic B. Detection of dysplasia and carcinoma *in situ* with a lung imaging fluorescence endoscope device. *J Thoracic Cardiovasc Sur*. 1993; 105: 1035-1040.
193. Lam S, MacAulay CE, LeRiche JC, Ou JY, Krosi G, Zeng H, Korbelik M, Palcic B. Fluorescence imaging of premalignant and malignant tissues with and without photosensitizers. In: Dougherty TJ ed. Optical methods for tumor treatment and detection: mechanisms and techniques in photodynamic therapy II. *Proceedings of the photo-optical instrumentation engineers*. Washington: SPIE, Bellingham. 1993; 1881: 160-167.
194. Celli JP, Spring BQ, Rizvi I, Evans CL, Samkoe KS, Verma S, Pogue BW, Hasan T. Imaging and photodynamic therapy: mechanisms, monitoring and optimization. *Chem Rev*. 2010; 110: 2795-2838.
195. Mitsunga M, Nakajima T, Sano K, Choyke PL, Kobayashi H. Near-infrared theranostic photoimmunotherapy (PIT): repeated exposure of light enhances the effect of immunconjugate. *Bioconjugate Chem*. 2012; 23: 604-609.
196. McCann TE, Kosaka N, Turkbey B, Mitsunaga M, Choyke PL, Kobayashi H. Molecular imaging of tumor invasion and metastases: the role of MRI. *NMR Biomed*. 2011; 24: 561-568.
197. Cheng S-H, Lee C-H, Chen M-C, Souris JS, Tseng F-G, Yang C-S, Mou C-Y, Chen C-T, Lo L-W. Tri-functionalization of mesoporous silica nanoparticles for comprehensive cancer theranostics-the trio of imaging, targeting and therapy. *J Mater Chem*. 2010; 20: 6149-6157.
198. Pandey SK, Gryshuk AL, Sajjad M, Zheng X, Chen Y, Abouzeid MM, Morgan J, Charamisinau I, Nabi HA, Oseroff A, Pandey RK. Multimodality agents for tumor imaging (PET, fluorescence) and photodynamic therapy. A possible "see and treat" approach. *J Med Chem*. 2005; 48: 6286-6295.
199. Shi J, Liu TWB, Chen J, Green D, Jaffray D, Wilson BC, Wang F, Zheng G. Transforming a targeted porphyrin theranostic agent into a PET imaging probe for cancer. *Theranostics*. 2011; 1: 363-370.
200. Ackroyd R, Kely C, Brown N, Reed M. The history of photodetection and photodynamic therapy. *Photochem Photobiol*. 2001; 74: 656-669.
201. Ikeda S. The flexible bronchofiberscope. *Keio J Med*. 1968; 17: 1-16.
202. Smyth CM, Stead RJ. Survey of flexible fibreoptic bronchoscopy in the United Kingdom. *Eur Respir J*. 2002; 19: 458-463.
203. Palcic B, Lam S, Hung J, MacAulay C. Detection and localization of early lung cancer by imaging techniques. *Chest*. 1991; 99: 742-743.
204. Hung J, Lam S, LeRiche JC, Palcic B. Autofluorescence of normal and malignant bronchial tissue. *Laser Surg Med*. 1991; 11: 99-105.
205. Lam S, Palcic B, McLean D, Hung J, Korbelik M, Profio AE. Detection of early lung cancer using low dose Photofrin II. *Chest*. 1990; 97: 333-337.
206. Hirsch FR, Franklin WA, Gazdar AF, Bunn PA. Early detection of lung cancer: clinical perspectives of recent advances in biology and radiology. *Clin Cancer Res*. 2001; 7: 5-22.
207. Lam S, Kennedy T, Unger M, Miller YE, Gelmont D, Rusch V, Gipe B, Howard D, LeRiche JC, Coldman A, Gazdar AF. Localization of bronchial intraepithelial neoplastic lesions by fluorescence bronchoscopy. *Chest*. 1998; 113: 696-702.
208. Policard A. Etude sur les aspects offerts par des tumeurs expérimentales examinées à la lumière de Wood. *C R Soc Biol*. 1924; 91: 1423-1424.
209. Auler H, Banzer G. Untersuchungen über die rolle der porphyrine bei geschwulstkranken menschen und tieren. *J Cancer Res Clin Oncol*. 1942; 53: 65-68.
210. Figge FJ, Wieland GS, Manganiello LJ. Cancer detection and therapy. Affinity of neoplastic, embryonic, and traumatized tissues for porphyrins and metallo-porphyrins. *Proc Soc Exp Biol Med*. 1948; 68: 640-641.
211. Rassmussen-Taxdal DS, Ward GE, Figge FHJ. Fluorescence of human lymphatic and cancer tissues following high doses of intravenous hematoporphyrin. *Cancer*. 1955; 8: 78-81.
212. Lipson RL, Baldes EJ, Olsen AM. Hematoporphyrin derivative: a new aid for endoscopic detection of malignant disease. *J Thoracic Cardiovasc Surg*. 1961; 42: 623-629.
213. Lipson RL, Baldes EJ, Olsen AM. The use of a derivative of hematoporphyrin for tumor detection. *J Natl Cancer Inst*. 1961; 26: 1-11.
214. Sutro CJ, Burman MS. Examination of pathological tissue by filtered ultraviolet radiation. *Arch Pathol*. 1933; 16: 346-349.
215. Gregorie Jr HB, Horger EO, Ward JL, Green JF, Richards T, Robertson Jr HC, Stevenson TB. Hematoporphyrin-derivative fluorescence in malignant neoplasms. *Ann Surg*. 1968; 167: 820-828.
216. Gomer CJ, Dougherty TJ. Determination of [³H]- and [¹⁴C]-hematoporphyrin derivative distribution in malignant and normal tissue. *Cancer Res*. 1979; 39: 146-151.
217. Jori G, Pizzi GB, Reddi E, Tomio L, Salvato B, Zorat P, Calzavara F. Time dependence of hematoporphyrin distribution in selected tissues of normal rats and in ascites hepatoma. *Tumori*. 1979; 65: 425-434.
218. Kessel D. Components of hematoporphyrin derivatives and their tumor localizing capacity. *Cancer Res*. 1982; 42: 1703-1706.
219. Unsöld E, Eil C, Jocham D, Sroka R, Stocker S. Quantitative and comparative study of hematoporphyrin-derived photosensitizers on a murine mouse model. *Lasers Med Sci*. 1990; 5: 309-316.
220. Balchum OJ, Doiron ER, Profio AE, Huth GC. Fluorescence bronchoscopy for localizing bronchial cancer. *Recent Results Cancer Res*. 1982; 82: 97-120.
221. Hayata Y, Kato H, Konaka C, Ono J, Matsushima Y, Yoneyama K, Nishimiya K. Fiberoptic bronchoscopic laser photoradiation for tumor localization in lung cancer. *Chest*. 1982; 82: 10-14.
222. Cortese DA, Kinsey JH, Woolner LB, Sanderson DR, Fontana RS. Hematoporphyrin derivative in the detection and localization of radiologically occult lung cancer. *Am Rev Respir Dis*. 1982; 126: 1087-1088.
223. Pierard P, Vermylen P, Bosschaerts T, Roufosse C, Berghmans T, Sculier J-P, Ninane V. Synchronous roentgenographically occult lung carcinoma in patients with resectable primary lung cancer. *Chest*. 2000; 117: 779-785.
224. Loewen G, Natarajan N, Tan D, Nava E, Klippenstein D, Mahoney M, Cummings M, Reid M. Autofluorescence bronchoscopy for lung cancer surveillance based on risk assessment. *Thorax*. 2007; 62: 335-340.
225. Weigel TL, Yousem S, Dacic S, Kosco PJ, Siegfried J, Luketich JD. Fluorescence bronchoscopic surveillance after curative surgical resection for non-small cell lung cancer. *Ann Surg Oncol*. 2000; 7: 176-180.
226. Weigel TL, Kosco PJ, Dacic S, Rusch VW, Ginsberg RJ, Luketich JD. Postoperative fluorescence bronchoscopic surveillance in non-small cell lung cancer patients. *Ann Thorac Surg*. 2001; 71: 967-970.

227. Kato H, Harada M, Ichinose S, Usuda J, Tsuchida T, Okunaka T. Photodynamic therapy (PDT) of lung cancer: experience of the Tokyo Medical University. *Photodiagnosis Photodynamic Ther.* 2004; 1: 49-55.
228. Moghissi K, Kate D, Thorpe JAC, Stringer M, Oxtoby C. Photodynamic therapy (PDT) in early central lung cancer: a treatment option for patients ineligible for surgical resection. *Thorax.* 2007; 62: 391-395.
229. Borle F, Radu A, Monnier P, van den Bergh H, Wagnières G. Evaluation of the photosensitizer Tookad® for photodynamic therapy on the Syrian Golden hamster cheek pouch model: light dose, drug dose and drug-light interval effects. *Photochem Photobiol.* 2003; 78: 377-383.
230. Bourre L, Thibaut S, Briffaud A, Rousset N, Eleouet S, Lajat Y, Patrice T. Indirect detection of photosensitizer *ex vivo*. *J Photochem Photobiol B: Biol.* 2002; 67: 23-31.
231. Kennedy JC, Pottier RH. New trends in photobiology: endogenous protoporphyrin IX, a clinically useful photosensitizer for photodynamic therapy. *J Photochem Photobiol B: Biol.* 1992; 14: 275-292.
232. Kennedy JC, Pottier RH, Pross DC. Photodynamic therapy with endogenous protoporphyrin IX: basic principles and present clinical experience. *J Photochem Photobiol B: Biol.* 1990; 6: 143-148.
233. Krieg RC, Messmann H, Rauch J, Seeger S, Knuechel R. Metabolic characterization of tumor cell-specific protoporphyrin IX accumulation after exposure to 5-aminolevulinic acid in human colonic cells. *Photochem Photobiol.* 2002; 76: 518-525.
234. Witjes JA, Douglass J. The role of hexaminolevulinate fluorescence cystoscopy in bladder cancer. *Nat Clin Pract Urol.* 2007; 4: 542-549.
235. Kirkali Z, Chan T, Manoharan M, Algaba F, Busch C, Cheng L, Kiemenev L, Kriegmair M, Montironi R, Murphy WM, Sesterhenn IA, Tachibana M, Weider J. Bladder cancer: epidemiology, staging and grading, and diagnosis. *Urol.* 2005; 66: 4-34.
236. Sylvester RJ, van der Meijden APM, Oosterlinck W, Witjes JA, Bouffouix C, Denis L, Newling DWW, Kurth K. Predicting recurrence and progression in individual patients with stage Ta T1 bladder cancer using EORTC risk tables: a combined analysis of 2596 patients from seven EORTC trials. *Eur Urol.* 2006; 49: 466-477.
237. Botteman MF, Pashos CL, Redaelli A, Laskin B, Hauser R. The health economics of bladder cancer: a comprehensive review of the published literature. *Pharmacoeconomics.* 2003; 21: 1315-1330.
238. Kriegmair M, Ehsan A, Baumgartner R, Lumper W, Knüchel R, Hofstädter F, Steinbach P, Hofstetter A. Fluorescence photodetection of neoplastic urothelial lesions following intravesical instillation of 5-aminolevulinic acid. *Urology.* 1994; 44: 836-841.
239. Kriegmair M, Baumgartner R, Knüchel R, Stepp H, Hofstädter F, Hofstetter A. Detection of early bladder cancer by 5-aminolevulinic acid induced porphyrin fluorescence. *J Urol.* 1996; 155: 105-110.
240. Koenig F, McGovern FJ, Larne R, Enquist H, Schomacker KT, Deutsch TF. Diagnosis of bladder carcinoma using protoporphyrin IX fluorescence induced by 5-aminolevulinic acid. *BJU Int.* 1999; 83: 129-135.
241. Zaak D, Kriegmair M, Stepp H, Stepp H, Baumgartner R, Oberneder R, Schneede P, Corvin S, Frimberger D, Knüchel R, Hofstetter A. Endoscopic detection of transitional cell carcinoma with 5-aminolevulinic acid: results of 1012 fluorescence endoscopies. *Urology.* 2001; 57: 690-694.
242. Riedl CR, Daniltchenko D, Koenig F, Simak R, Loening SA, Pflueger H. Fluorescence endoscopy with 5-aminolevulinic acid reduces early recurrence rate in superficial bladder cancer. *J Urol.* 2001; 165: 1121-1123.
243. Kriegmair M, Zaak D, Rothenberger K-H, Rassweiler J, Jocham D, Eisenberger F, Tauber R, Stenzl R, Hofstetter H. Transurethral resection for bladder cancer using 5-aminolevulinic acid induced fluorescence endoscopy versus white light endoscopy. *J Urol.* 2002; 168: 475-478.
244. Lange N, Jichlinski P, Zellweger M, Forrer M, Marti A, Guillou L, Kucera P, Wagnières G, van den Bergh H. Photodetection of early human bladder cancer based on the fluorescence of 5-aminolevulinic acid hexylester induced protoporphyrin IX: a pilot study. *Br J Cancer.* 1999; 80: 185-193.
245. Stummer W, Pichlmeier U, Meinel T, Wiestler OD, Zanella F, Reulen HJ. Fluorescence-guided surgery with 5-aminolevulinic acid for resection of malignant glioma: a randomised controlled multicentre phase III trial. *Lancet Oncol.* 2006; 7: 392-401.
246. Zimmermann A, Ritsch-Marte M, Kostron H. mTHPC-mediated photodynamic diagnosis of malignant brain tumors. *Photochem Photobiol.* 2001; 74: 611-616.
247. Kostron H, Rossler K. Surgical intervention in patients with malignant glioma. *Wien Med Wochenschr.* 2006; 156: 338-341.
248. Stepp H, Beck T, Pongratz T, Meinel T, Kreth F-W, Tonn JC, Stummer WJ. ALA and malignant glioma: fluorescence-guided resection and photodynamic treatment. *J Environ Pathol Toxicol Oncol.* 2007; 26: 157-164.
249. Yang VX, Muller PJ, Herman P, Wilson BC. A multispectral fluorescence imaging system: design and initial clinical tests in intra-operative Photofrin-photodynamic therapy of brain tumors. *Lasers Surg Med.* 2003; 32: 224-232.
250. Olivo M, Wilson BC. Mapping ALA-induced PPIX fluorescence in normal brain and brain tumour using confocal fluorescence microscopy. *Int J Oncol.* 2004; 25: 37-45.
251. Bogaards A, Varma A, Zhang K, Zach D, Bisland SK, Moriyama EH, Lilge L, Muller PJ, Wilson BC. Fluorescence image-guided brain tumour resection with adjuvant metronomic photodynamic therapy: pre-clinical model and technology development. *Photochem Photobiol Sci.* 2005; 4: 438-442.
252. Bogaards A, Varma A, Collens SP, Lin AH, Giles A, Yang VXD, Bilbao JM, Lilge LD, Muller PJ, Wilson BC. Increased brain tumor resection using fluorescence image guidance in a preclinical model. *Lasers Surg Med.* 2004; 35: 181-190.
253. Gibbs-Strauss SL, O'Hara JA, Hoopes PJ, Hasan T, Pogue BW. Non-invasive measurement of aminolevulinic acid-induced protoporphyrin IX fluorescence allowing detection of murine glioma *in vivo*. *J Biomed Opt.* 2009; 14: 014007.
254. Reddy GR, Bhojani MS, McConville P, Moody J, Moffat BA, Hall DE, Kim G, Koo Y-EL, Woolliscroft MJ, Sugai JV, Johnson TD, Philbert MA, Kopelman R, Rehemtulla A, Ross BD. Vascular targeted nanoparticles for imaging and treatment of brain tumors. *Clin Cancer Res.* 2006; 12: 6677-6686.
255. Chan JK, Monk BJ, Cuccia D, Pham H, Kimel S, Gu M, Hammer-Wilson MJ, Liaw L-HL, Osann K, DiSaia PJ. Laparoscopic photodynamic diagnosis of ovarian cancer using 5-aminolevulinic acid in a rat model. *Gynecol Oncol.* 2002; 87: 64-70.
256. Lüdicke F, Gabrecht T, Lange N, Wagnières G, van den Bergh H, Berclaz L, Major AL. Photodynamic diagnosis of ovarian cancer using hexaminolevulinate: a preclinical study. *Br J Cancer.* 2003; 88: 1780-1784.
257. Cho KR, Shih L-M. Ovarian Cancer. *Annu Rev Pathol.* 2009; 4: 287-313.
258. Davila GW, Estape R. Gynecologic laparoscopy. *Surg Oncol Clin N Am.* 2001; 10: 557-569.
259. Tammela J, Lele S. New modalities in detection of recurrent ovarian cancer. *Curr Opin Obstet Gynecol.* 2004; 16: 5-9.
260. Löning M, Diddens H, Küpker W, Diedrich K, Hüttmann G. Laparoscopic fluorescence detection of ovarian carcinoma metastases using 5-aminolevulinic acid-induced protoporphyrin IX. *Cancer.* 2004; 100: 1650-1656.
261. Zhong W, Celli JP, Rizvi I, Mai Z, Spring BQ, Yun SH, Hasan T. *In vivo* high-resolution fluorescence microendoscopy for ovarian cancer detection and treatment monitoring. *Br J Cancer.* 2009; 101: 2015-2022.
262. Andersson-Engels S, Elner A, Johansson J, Karlsson S-E, Salford LG, Strömblad LG, Svanberg K, Svanberg S. Clinical recording of laser-induced fluorescence spectra for evaluation of tumour demarcation feasibility in selected clinical specialities. *Lasers Med Sci.* 1991; 6: 415-424.
263. Andersson-Engels S, Berg R, Svanberg K, Svanberg S. Multi-colour fluorescence imaging in connection with photodynamic therapy of δ -amino levulinic acid (ALA) sensitised skin malignancies. *Bioimaging.* 1995; 3: 134-143.
264. Hewett J, Nadeau V, Ferguson J, Moseley H, Ibbotson S, Allen JW, Sibbett W, Padgett M. The application of a compact multispectral imaging system with integrated excitation source to *in vivo* monitoring of fluorescence during topical photodynamic therapy of superficial skin cancers. *Photochem Photobiol.* 2001; 73: 278-282.
265. Martin A, Tope WD, Grevelink JM, Starr JC, Fewkes JL, Flotte TJ, Deutsch TF, Anderson RR. Lack of selectivity of protoporphyrin IX fluorescence for basal cell carcinoma after topical application of 5-aminolevulinic acid: implications for photodynamic treatment. *Arch Dermatol Res.* 1995; 287: 665-674.
266. Fritsch C, Homey B, Stahl W, Lehmann P, Ruzicka T, Sies H. Preferential relative porphyrin enrichment in solar keratoses upon topical application of 5-aminolevulinic acid methylester. *Photochem Photobiol.* 1998; 68: 218-221.
267. Juzeniene A, Juzenas P, Ma L-W, Iani V, Moan J. Topical application of 5-aminolevulinic acid, methyl 5-aminolevulinate and hexyl 5-aminolevulinate on normal human skin. *Br J Dermatol.* 2006; 155: 791-799.
268. Kuijpers DI, Thissen MR, Thissen CA, Neumann MH. Similar effectiveness of methyl aminolevulinic acid and 5-aminolevulinic acid in topical photodynamic therapy for nodular basal cell carcinoma. *J Drugs Dermatol.* 2006; 5: 642-645.

269. Wiegell SR, Wulf HC. Photodynamic therapy of acne *vulgaris* using 5-aminolevulinic acid versus methyl aminolevulinate. *J Am Acad Dermatol.* 2006; 54: 647-651.
270. Leunig A, Rick K, Stepp H, Gutmann R, Alwin G, Baumgartner R, Feyh J. Fluorescence imaging and spectroscopy of 5-aminolevulinic acid induced protoporphyrin IX for the detection of neoplastic lesions in the oral cavity. *Am J Surg.* 1996; 172: 674-677.
271. Redondo P, Marquina M, Pretel M, Aguado L, Iglesias ME. Methyl-ALA-induced fluorescence in photodynamic diagnosis of basal cell carcinoma prior to Mohs micrographic surgery. *Arch Dermatol.* 2008; 144: 115-117.
272. Jemal A, Siegel R, Ward E, Hao Y, Xu J, Thun MJ. Cancer Statistics 2009. *CA: Cancer J Clin.* 2009; 59: 225-249.
273. Leunig A, Betz CS, Mehlmann M, Stepp H, Arbogast S, Grevers G, Baumgartner R. Detection of squamous cell carcinoma of the oral cavity by imaging 5-aminolevulinic acid-induced protoporphyrin IX fluorescence. *Laryngoscope.* 2000; 110: 78-83.
274. Betz CS, Stepp H, Janda P, Arbogast S, Grevers G, Baumgartner R, Leunig A. A comparative study of normal inspection, autofluorescence and 5-ALA-induced PPIX fluorescence for oral cancer diagnosis. *Int J Cancer.* 2002; 97: 245-252.
275. Ebihara A, Krasieva TB, Liaw L-HL, Fago S, Messadi D, Osann K, Wilder-Smith P. Detection and diagnosis of oral cancer by light-induced fluorescence. *Lasers Surg Med.* 2003; 32: 17-24.
276. Duska LR, Wimberly J, Deutsch TF, Ortel B, Haas J, Houck K, Hasan T. Detection of female lower genital tract dysplasia using orally administered 5-aminolevulinic acid induced protoporphyrin IX: a preliminary study. *Gynecol Oncol.* 2002; 85: 125-128.
277. Stefflova K, Chen J, Zheng G. Using molecular beacons for cancer imaging and treatment. *Front Biosci.* 2007; 12: 4709-4721.
278. Weissleder R, Tung C-H, Mahmood U, Bogdanov A, Jr. *In vivo* imaging of tumors with protease-activated near-infrared fluorescent probes. *Nat Biotechnol.* 1999; 17: 375-378.
279. Choi Y, Weissleder R, Tung C-H. Selective antitumor effect of novel protease-mediated photodynamic agent. *Cancer Res.* 2006; 66: 7225-7229.
280. Lovell JF, Chen J, Jarvi MT, Cao W-G, Allen AD, Liu Y, Tidwell TT, Wilson BC, Zheng G. FRET quenching of photosensitizer singlet oxygen generation. *J Phys Chem B.* 2009; 113: 3203-3211.
281. Zheng G, Chen J, Stefflova K, Jarvi M, Li H, Wilson BC. Photodynamic molecular beacon as an activatable photosensitizer based on protease-controlled singlet oxygen quenching and activation. *Proc Natl Acad Sci USA.* 2007; 104: 8989-8994.
282. Zheng X, Sallum UW, Verma S, Athar H, Evans CL, Hasan T. Exploiting a bacterial drug-resistance mechanism: a light-activated construct for the destruction of MRSA. *Angew Chem Int Ed.* 2009; 48: 2148-2151.
283. Cubeddu R, Canti G, Taroni P, Valentini G. Tumour visualization in a murine model by time-delayed fluorescence of sulfonated aluminium phthalocyanine. *Lasers Med Sci.* 1997; 12: 200-208.
284. Cubeddu R, Pifferi A, Taroni P, Torricelli A, Valentini G, Comelli D, D'Andrea C, Angelini V, Canti G. Fluorescence imaging during photodynamic therapy of experimental tumors in mice sensitized with disulfonated aluminum phthalocyanine. *Photochem Photobiol.* 2000; 72: 690-695.
285. Bérard V, Rousseau JA, Cadorette J, Hubert L, Bentourkia MH, van Lier JE, Lecomte R. Dynamic imaging of transient metabolic processes by small-animal PET for the evaluation of photosensitizers in photodynamic therapy of cancer. *J Nucl Med.* 2006; 47: 1119-1126.
286. Lapointe D, Brasseur N, Cadorette J, La Madeleine C, Rodrigue S, van Lier JE, Lecomte R. High-resolution PET imaging for *in vivo* monitoring of tumor response after photodynamic therapy in mice. *J Nucl Med.* 1999; 40: 876-882.
287. Kruijt B, de Bruijn HS, van der Ploeg-van den Heuvel A, Sterenborg HJCM, Robinson DJ. Laser speckle imaging of dynamic changes in flow during photodynamic therapy. *Lasers Med Sci.* 2006; 21: 208-212.
288. Chen Z, Milner TE, Wang X, Srinivas S, Nelson JS. Optical Doppler tomography: imaging *in vivo* blood flow dynamics following pharmacological intervention and photodynamic therapy. *Photochem Photobiol.* 1998; 67: 56-60.
289. Mariampillai A, Standish BA, Moriyama EH, Khurana M, Munce NR, Leung MKK, Jiang J, Cable A, Wilson BC, Vitkin AA, Yang VXD. Speckle variance detection of microvasculature using swept-source optical coherence tomography. *Opt Lett.* 2008; 33: 1530-1532.
290. Standish BA, Jin X, Smolen J, Mariampillai A, Munce NR, Wilson BC, Vitkin AI, Yang VXD. Interstitial Doppler optical coherence tomography monitors microvascular changes during photodynamic therapy in a Dunning prostate model under varying treatment conditions. *J Biomed Opt.* 2007; 12: 034022.
291. Standish BA, Yang VXD, Munce NR, Song L-MWK, Gardiner G, Lin A, Mao YI, Vitkin A, Marcon NE, Wilson BC. Doppler optical coherence tomography monitoring of microvascular tissue response during photodynamic therapy in an animal model of Barrett's esophagus. *Gastrointest Endosc.* 2007; 66: 326-333.
292. Yu G, Durduran T, Zhou C, Wang H-W, Putt ME, Saunders HM, Sehgal CM, Glatstein E, Yodh AG, Busch TM. Non-invasive monitoring of murine tumor blood flow during and after photodynamic therapy provides early assessment of therapeutic efficacy. *Clin Cancer Res.* 2005; 11: 3543-3552.
293. Mason C, Markusen JF, Town MA, Dunnill P, Wang RK. Doppler optical coherence tomography for measuring flow in engineered tissue. *Biosens Bioelectron.* 2004; 20: 414-423.
294. Major A, Kimel S, Mee S, Milner TE, Smithies DJ, Srinivas SM, Chen Z, Nelson JS. Microvascular photodynamic effects determined *in vivo* using optical Doppler tomography. *IEEE J Sel Top Quantum Electron.* 1999; 5: 1168-1175.
295. Khurana M, Moriyama EH, Mariampillai A, Wilson BC. Intravital high-resolution optical imaging of individual vessel response to photodynamic treatment. *J Biomed Opt.* 2008; 13: 040502.
296. Haider MA, Davidson SRH, Kale AV, Weersink RA, Evans AJ, Toi A, Gertner MR, Bogaards A, Wilson BC, Chin JL, Elhilali M, Trachtenberg J. Prostate gland: MR imaging appearance after vascular targeted photodynamic therapy with palladium-bacteriopheophorbide. *Radiology.* 2007; 244: 196-204.
297. Huang Z, Haider MA, Kraft S, Chen Q, Blanc D, Wilson BC, Hetzel FW. Magnetic resonance imaging correlated with the histopathological effect of Pd-bacteriopheophorbide (Tookad) photodynamic therapy on the normal canine prostate gland. *Lasers Surg Med.* 2006; 38: 672-681.
298. Winsborrow BG, Grondey H, Savoie H, Fyfe CA, Dolphin D. Magnetic resonance imaging evaluation of photodynamic therapy-induced hemorrhagic necrosis in the murine M1 tumor model. *Photochem Photobiol.* 1997; 66: 847-852.
299. Zilberstein J, Schreiber S, Bloemers MCWM, Bendel P, Neeman M, Schechtman E, Kohen F, Scherz A, Salomon Y. Antivascular treatment of solid melanoma tumors with bacteriochlorophyll-serine-based photodynamic therapy. *Photochem Photobiol.* 2001; 73: 257-266.
300. Samkoe KS, Chen A, Rizvi I, O'Hara JA, Hoopes PJ, Hasan T, Pogue BW. Magnetic resonance image-guided photodynamic therapy of xenograft pancreas tumors with Verteporfin. In Kessel D, ed. *Optical methods for tumor treatment and detection: mechanisms and techniques in photodynamic therapy XVIII. Proceedings of the photo-optical instrumentation engineers (SPIE).* Washington: SPIE, Bellingham. 2009; 7164: 71640D.
301. Moore JV, Waller ML, Zhao S, Dodd NJF, Acton PD, Jeavons AP, Hastings DL. Feasibility of imaging photodynamic injury to tumours by high-resolution positron emission tomography. *Eur J Nucl Med Mol Imaging.* 1998; 25: 1248-1254.
302. Barbazetto I, Burdan A, Bressler SB, Haynes L, Kapetanios AD, Lukas J, Olsen K, Potter M, Reaves A, Rosenfeld P, Schachat AP, Strong HA, Wenkster A, Burdan M, Reaves D. Photodynamic therapy of subfoveal choroidal neovascularization with Verteporfin fluorescein angiographic guidelines for evaluation and treatment-TAP and VIP Report No. 2. Treatment of Age-Related Macular Degeneration with photodynamic therapy (TAP) and Verteporfin in photodynamic therapy (VIP) study groups. *Arch Ophthalmol.* 2003; 121: 1253-1268.
303. Helmchen F, Denk W. Deep tissue two-photon microscopy. *Nat Methods.* 2005; 2: 932-940.
304. Kyriazis GA, Balin H, Lipson RL. Hematoporphyrin-derivative-fluorescence test colposcopy and colpophotography in the diagnosis of atypical metaplasia, dysplasia, and carcinoma *in situ* of the cervix uteri. *Am J Obstet Gynecol.* 1973; 117: 375-380.
305. Fisher WG, Partridge Jr WP, Dees C, Wachter EA. Simultaneous two-photon activation of Type-I photodynamic therapy agents. *Photochem Photobiol.* 1997; 66: 141-155.
306. Bhawalkar JD, Kumar ND, Zhao CF, Prasad PN. Two-photon photodynamic therapy. *J Clin Laser Med Surg.* 1997; 15: 201-204.
307. Oar MA, Dichtel WR, Serin JM, Frechet MJM, Rogers JE, Slagle JE, Fleitz PA, Tan L-S, Ohulchanskyy TY, Prasad PN. Light-harvesting chromophores with metalated porphyrin cores for tuned photosensitization of singlet oxygen *via* two-photon excited FRET. *Chem Mater.* 2006; 18: 3682-3692.
308. Kim S, Ohulchanskyy TY, Pudarav HE, Pandey RK, Prasad PN. Organically modified silica nanoparticles co-encapsulating photosensitizing drug and aggregation-enhanced two-photon absorbing fluorescent dye aggregates for two-photon photodynamic therapy. *J Am Chem Soc.* 2007; 129: 2669-2675.

309. Reed MW, Mullins AP, Anderson GL, Miller FN, Wieman TJ. The effect of photodynamic therapy on tumor oxygenation. *Surg.* 1989; 106: 94-99.
310. Tromberg BJ, Orenstein A, Kimel S, Barker SJ, Hyatt J, Nelson JS, Berns MW. *In vivo* tumor oxygen tension measurements for the evaluation of the efficiency of photodynamic therapy. *Photochem Photobiol.* 1990; 52: 375-385.
311. Hofmann B, Bogdanov Jr A, Marecos E, Ebert W, Semmler W, Weissleder R. Mechanism of gadophrin-2 accumulation in tumor necrosis. *J Magn Reson Imaging.* 1999; 9: 336-341.
312. Li G, Slansky A, Dobhal MP, Goswami LN, Graham A, Chen Y, Kanter P, Alberico RA, Sperryak J, Morgan J, Mazurchuk R, Oseroff A, Grossman Z, Pandey RK. Chlorophyll-*a* analogues conjugated with aminobenzyl-DTPA as potential bifunctional agents for magnetic resonance imaging and photodynamic therapy. *Bioconjugate Chem.* 2005; 16: 32-42.
313. Bases R, Brodie SS, Rubenfeld S. Attempts at tumor localization using Cu 64-labelled copper porphyrins. *Cancer.* 1958; 11: 259-63.
314. Wrenn Jr FR, Good ML, Handler P. The use of positron-emitting radioisotopes for the localization of brain tumors. *Science.* 1951; 113: 525-7.
315. Firnao G, Maass D, Wilson BC, Jeeves WP. ⁶⁴Cu labelling of hematoporphyrin derivative for non-invasive *in-vivo* measurements of tumour uptake. *Prog Clin Biol Res.* 1984; 170: 629-36.
316. Burns BC, Firnao G, Jeeves WP, Brown KL, Burns-McCormick DM. Chromatographic analysis and tissue distribution of radiocopper-labelled haematoporphyrin derivatives. *Laser Med Sci.* 1988; 3: 71-80.
317. Zhang X, Cai W, Cao F, Schreiber E, Wu Y, Wu JC, Xing L, Chen X. ¹⁸F-Labeled bombesin analogs for targeting GRP receptor-expressing prostate cancer. *J Nucl Med.* 2006; 47: 492-501.
318. Bennett JJ, Tjuvajev J, Johnson P, Doubrovina M, Akhurst T, Malholtra S, Hackman T, Balatoni J, Finn R, Larson SM, Federoff H, Blasberg R, Fong Y. Positron emission tomography imaging for herpes virus infection: implications for oncolytic viral treatments of cancer. *Nat Med.* 2001; 7: 859-863.
319. Dong D, Dubeau L, Bading J, Nguyen K, Luna M, Yu H, Gazit-Bornstein G, Gordon EM, Gomer C, Hall FL, Gambhir SS, Lee AS. Spontaneous and controllable activation of suicide gene expression driven by the stress-inducible *Grp78* promoter resulting in eradication of sizable human tumors. *Hum Gene Ther.* 2004; 15: 553-561.
320. Westermann P, Glanzmann T, Anderjelic S, Braichotte DR, Forrer M, Wagnier GA, Monnier P, van den Bergh H, Mach J-P, Folli S. Long circulating half-life and high tumor selectivity of the photosensitizer meta-tetrahydroxyphenylchlorin conjugated to polyethylene glycol in nude mice grafted with a human colon carcinoma. *Int J Cancer.* 1998; 76: 842-850.
321. Sugiyama M, Sakahara H, Sato K, Harada N, Fukumoto D, Kakiuchi T, Hirano T, Kohno E, Tsukada H. Evaluation of 3'-deoxy-3'-¹⁸F-fluorothymidine for monitoring tumor response to radiotherapy and photodynamic therapy in mice. *J Nucl Med.* 2004; 45: 1754-1758.
322. Phelps ME. Positron emission tomography provides molecular imaging of biological processes. *Proc Natl Acad Sci USA.* 2000; 97: 9226-9233.
323. Ma B, Li G, Kanter P, Lamonica D, Grossman Z, Pandey RK. Bifunctional HPPH-N₂S₂-^{99m}Tc conjugates as tumor imaging agents: synthesis and biodistribution studies. *J Porphyrins Phthalocyanines.* 2003; 7: 500-507.
324. Chen Y, Zheng X, Dobhal MP, Gryshuk A, Morgan J, Dougherty TJ, Oseroff A, Pandey RK. Methyl pyropheophorbide-*a* analogues: potential fluorescent probes for the peripheral-type benzodiazepine receptor. Effect of central metal in photosensitizing efficacy. *J Med Chem.* 2005; 48: 3692-3695.
325. Fahmy TM, Fong PM, Goyal A, Saltzman WM. Targeted for drug delivery. *Nanotoday.* 2005; 18-26.
326. Flynn T, Wei C. The pathway to commercialization for nanomedicine. *Nanomed: Nanotechnol Biol Med.* 2005; 1: 47-51.
327. Roy I, Ohulchanskyy TY, Bharali DJ, Pudavar HE, Mistretta RA, Kaur N, Prasad PN. Optical tracking of organically modified silica nanoparticles as DNA carriers: a nonviral, nanomedicine approach for gene delivery. *Proc Natl Acad Sci USA.* 2005; 102: 279-284.
328. Wang G-P, Song E-Q, Xie H-Y, Zhang Z-L, Tian Z-Q, Zuo C, Pang D-W, Wu D-C, Shi Y-B. Biofunctionalization of fluorescent-magnetic-bifunctional nanospheres and their applications. *Chem Commun.* 2005; 34: 4276-4278.
329. Levy L, Sahoo Y, Kim K-S, Bergey EJ, Prasad PN. Nanochemistry: synthesis and characterization of multifunctional nanoclinics for biological applications. *Chem Mater.* 2002; 14: 3715-3721.
330. Freitas Jr RA. What is nanomedicine? *Nanomed: Nanotechnol Biol Med.* 2005; 1: 2-9.
331. Smith S, Nagel DJ. Nanotechnology-enabled sensors: possibilities, realities, and applications. Operating on the scale of atoms and molecules, emerging nanotechnologies promise dramatic changes in sensor designs and capabilities. *Sensors Mag.* 2003; 20.
332. Huh Y-M, Jun Y-W, Song H-I, Kim S, Choi J-S, Lee J-H, Yoon S, Kim K-S, Shin J-S, Suh J-S, Cheon J. *In vivo* magnetic resonance detection of cancer by using multifunctional magnetic nanocrystals. *J Am Chem Soc.* 2005; 127: 12387-12391.
333. Moffat BA, Reddy GR, McConville P, Hall DE, Chenevert TL, Kopelman R, Philbert M, Weissleder R, Rehemtulla A, Ross BD. A novel polyacrylamide magnetic nanoparticle contrast agent for **molecular imaging** using MRI. *Mol Imaging.* 2003; 2: 324-332.
334. Aylott JW. Optical nanosensors - an enabling technology for intracellular measurements. *Analyst.* 2003; 128: 309-312.
335. Tartaj P, del Puerto Morales M, Veintemillas-Verdaguer S, González-Carreño T, Serna CJ. The preparation of magnetic nanoparticles for applications in biomedicine. *J Phys D: Appl Phys.* 2003; 36: R182-R197.
336. Zahr AS, de Villiers M, Pishko MV. Encapsulation of drug nanoparticles in self-assembled macromolecular nanoshells. *Langmuir.* 2005; 21: 403-410.
337. Arduini M, Marcuz S, Montolli M, Rampazzo E, Mancin F, Gross S, Armelao L, Teci P, Tonellato U. Turning fluorescent dyes into Cu(II) nanosensors. *Langmuir.* 2005; 21: 9314-9321.
338. Cullum BM, Vo-Dinh T. The development of optical nanosensors for biological measurements. *TIBTECH.* 2000; 18: 388-393.
339. Burns A, Ow H, Weisner U. Fluorescent core-shell silica nanoparticles: towards "lab on a particle" architectures for nanobiotechnology. *Chem Soc Rev.* 2006; 35: 1028-1042.
340. Pegaz B, Debefve E, Borle F, Ballini JP, van den Bergh H, Kouakou-Konan YN. Encapsulation of porphyrins and chlorins in biodegradable nanoparticles: the effect of dye lipophilicity on the extravasation and the photothrombotic activity. A comparative study. *J Photochem Photobiol B: Biol.* 2005; 80: 19-27.
341. Zhu H, McShane MJ. Loading of hydrophobic materials into polymer particles: implications for fluorescent nanosensors and drug delivery. *J Am Chem Soc.* 2005; 127: 13448-13449.
342. Roy I, Ohulchanskyy TY, Pudavar HE, Bergey EJ, Oseroff AR, Morgan J, Dougherty TJ, Prasad PN. Ceramic-based nanoparticles entrapping water-insoluble photosensitizing anticancer drugs: a novel drug-carrier system for photodynamic therapy. *J Am Chem Soc.* 2003; 125: 7860-7865.
343. Maxwell DJ, Taylor JR, Nie S. Self-assembled nanoparticle probes for recognition and detection of biomolecules. *J Am Chem Soc.* 2002; 124: 9606-9612.
344. Zhang H, Sun Y, Ye K, Zhang P, Wang Y. Oxygen sensing materials based on mesoporous silica MCM-41 and Pt(II)-porphyrin complexes. *J Mater Chem.* 2005; 15: 3181-3186.
345. O'Donovan C, Hynes J, Yashunski D, Papkovsky D. Phosphorescent oxygen-sensitive materials for biological applications. *J Mater Chem.* 2005; 15: 2946-2951.
346. Bharali DJ, Klejbor I, Stachowiak EK, Dutta P, Roy I, Kaur N, Bergey EJ, Prasad PN, Stachowiak MK. Organically modified silica nanoparticles: a nonviral vector for *in vivo* gene delivery and expression in the brain. *Proc Natl Acad Sci USA.* 2005; 102: 11539-11544.
347. Couvreur P, Barratt G, Fattal E, Legrand P, Vauthier C. Nanocapsule technology: a review. *Crit Rev Ther Drug.* 2002; 19: 99-134.
348. Hirsch LR, Stafford RJ, Bankson JA, Sershen SR, Rivera B, Price RE, Hazle JD, Halas NJ, West JL. Nanoshell-mediated near-infrared thermal therapy of tumors under magnetic resonance guidance. *Proc Nat Acad Sci USA.* 2003; 100: 13549-13554.
349. Zhao X, Hilliard LR, Mechery SJ, Wang Y, Bagwe RP, Jin S, Tan W. A rapid bioassay for single bacterial cell quantitation using bioconjugated nanoparticles. *Proc Natl Acad Sci USA.* 2004; 101: 15027-15032.
350. Konan YN, Cerny R, Favet J, Berton M, Gurny R, Allémann E. Preparation and characterization of sterile sub-200nm meso-tetra(4-hydroxyphenyl)porphyrin-loaded nanoparticles for photodynamic therapy. *Eur J Pharm Biopharm.* 2003; 55: 115-124.
351. Bae Y, Jang W-D, Nishiyama N, Fukushima S, Kataoka K. Multifunctional polymeric micelles with folate-mediated cancer cell targeting and pH-triggered drug releasing properties for active intracellular drug delivery. *Mol Biosyst.* 2005; 1: 242-250.
352. Bae Y, Nishiyama N, Fukushima S, Koyama H, Yasuhiro M, Kataoka K. Preparation and biological characterization of polymeric micelle drug carriers with intracellular pH-triggered drug release property: tumor permeability, controlled subcellular drug distribution, and enhanced *in vivo* antitumor efficacy. *Bioconjugate Chem.* 2005; 16: 122-130.

353. Gu H, Xu K, Yang Z, Chang CK, Xu B. Synthesis and cellular uptake of porphyrin decorated iron oxide nanoparticles - a potential candidate for bimodal anticancer therapy. *Chem Commun.* 2005; 4270-4272.
354. Kikuchi K, Komatsu K, Nagano T. Zinc sensing for cellular application. *Curr Opin Chem Biol.* 2004; 8: 182-191.
355. Howard AG, Khadry NH. Nanoscavenger based dispersion preconcentration; sub-micron particulate extractants for analyte collection and enrichment. *Analyst.* 2005; 130: 1432-1438.
356. Balaji T, Sasidharan M, Matsunaga H. Optical sensor for the visual detection of mercury using mesoporous silica anchoring porphyrin moiety. *Analyst.* 2005; 130: 1162-1167.
357. Papkovsky DB, O'Riordan C. Emerging applications of phosphorescent metalloporphyrins. *J Fluorescence.* 2005; 15: 569-584.
358. Shin JH, Schoenfish MH. Improving the biocompatibility of *in vivo* sensors *via* nitric oxide release. *Analyst.* 2006; 13: 609-615.
359. Li C-Y, Zhang X-B, Han Z-X, Åkermark B, Sun L, Shen G-L, Yu R-Q. A wide pH range optical sensing system based on a sol-gel encapsulated amino-functionalised corrole. *Analyst.* 2006; 131: 388-393.
360. Nakanishi T, Fukushima S, Okamoto K, Suzuki M, Matsumura Y, Yokoyama M, Okano T, Sakurai Y, Kataoka K. Development of the polymer micelle carrier system for doxorubicin. *J Control Release.* 2001; 74: 295-302.
361. Vargas A, Pegaz B, Debeffe E, Kouakou Y-K, Lange N, Ballini JP, van den Bergh H, Gurny R, Delie F. Improved photodynamic activity of porphyrin loaded into nanoparticles: an *in vivo* evaluation using chick embryos. *Int J Pharm.* 2004; 286: 131-145.
362. Zguris JC, Itle LJ, Koh W-G, Pishko MV. A novel single-step fabrication technique to create heterogeneous poly(ethylene glycol) hydrogel microstructures containing multiple phenotypes of mammalian cells. *Langmuir.* 2005; 21: 4168-4174.
363. Thote AJ, Gupta RB. Formation of nanoparticles of a hydrophilic drug using supercritical carbon dioxide and microencapsulation for sustained release. *Nanomed: Nanotechnol Biol Med.* 2005; 1: 85-90.
364. Kullberg M, Mann K, Owens JL. Improved drug delivery to cancer cells: a method using magnetoliposomes that target epidermal growth factor receptors. *Med Hypotheses.* 2005; 64: 468-470.
365. Hughes GA. Nanostructure-mediated drug delivery. *Nanomed.* 2005; 1: 22-30.
366. Kam NWS, O'Connell M, Wisdom JA, Dai H. Carbon nanotubes as multifunctional biological transporters and near-infrared agents for selective cancer cell destruction. *Proc Natl Acad Sci USA.* 2005; 102: 11600-11605.
367. Paunov VN, MacKenzie G, Stoyanov SD. Nanostructure-mediated drug delivery. *J Mater Chem.* 2007; 17: 609-612.
368. Almdal K, Sun H, Poulsen AK, Arleth L, Jakobsen I, Gu H, Scharff-Poulsen A-M. Fluorescent gel particles in the nanometer range for detection of metabolites in living cells. *Polym Adv Technol.* 2006; 17: 790-793.
369. Crespo-Biel O, Ravoo BJ, Huskens J, Reinhoudt DN. Writing with molecules on molecular printboards. *Dalton Trans.* 2006; 2737-2741.
370. Hazarika P, Jickells SM, Wolff K, Russell DA. Multiplexed detection of metabolites of narcotic drugs from a single latent fingerprint. *Anal Chem.* 2010; 82: 9150-9154.
371. Yu MK, Park J, Jon S. Targeting strategies for multifunctional nanoparticles in cancer imaging and therapy. *Theranostics.* 2012; 2: 3-44.
372. Glickson JD, Lund-Katz S, Zhou R, Choi H, Chen IW, Li H, Corbin I, Popov AV, Cao WG, Song LP, Qi CZ, Marotta D, Nelson DS, Chen J, Chance B, Zheng G. Lipoprotein nanoplatform for targeted delivery of diagnostic and therapeutic agents. In: Liss P, Hansell P, Bruley DF, Harrison DK, ed. *Advances in Experimental Medicine and Biology*, 1st edn. UK: Springer; 2009: 227-239.
373. Huh AJ, Kwon YJ. "Nan antibiotics": a new paradigm for treating infectious diseases using nanomaterials in the antibiotic resistant era. *J Control Release.* 2011; 156: 128-145.
374. Sortino S. Photoactivated nanomaterials for biomedical release applications. *J Mater Chem.* 2012; 22: 301-318.
375. Corbin IR, Li H, Chen J, Lund-Katz S, Zhou R, Glickson JD, Zheng G. Low-density lipoprotein nanoparticles as magnetic resonance imaging contrast agents. *Neoplasia.* 2006; 8: 488-498.
376. Song L, Li H, Sunar U, Chen J, Corbin I, Yodh AG, Zheng G. Naphthalocyanine-reconstituted LDL nanoparticles for *in vivo* cancer imaging and treatment. *Int J Nanomedicine.* 2007; 2: 767-774.
377. Si D, Epstein T, Koo Lee Y-E, Kopelman R. Nanoparticle PEBBLE sensors for quantitative nanomolar imaging of intracellular free calcium ions. *Anal Chem.* 2012; 84: 978-986.
378. Jin H, Lovell JF, Chen J, Lin Q, Ding L, Ng KK, Pandey RK, Manoharan M, Zhang Z, Zheng G. Mechanistic insights into LDL nanoparticle-mediated siRNA delivery. *Bioconjugate Chem.* 2012; 23: 33-41.
379. Ng KK, Lovell JF, Zheng G. Lipoprotein-inspired nanoparticles for cancer theranostics. *Accounts Chem Res.* 2011; 44: 1105-1113.
380. Dresco PA, Zaitsev VS, Gambino RJ, Chu B. Preparation and properties of magnetite and polymer magnetite nanoparticles. *Langmuir.* 1999; 15: 1945-1951.
381. Stark DD, Weissleder R, Elizondo G, Hahn PF, Saini S, Todd LE, Wittenberg J, Ferrucci JT. Superparamagnetic iron oxide: clinical application as a contrast agent for MR imaging of the liver. *Radiology.* 1988; 168: 297-301.
382. Duncan R. Nanomedicine gets clinical. *Nanotoday.* 2005; 8: 16-17.
383. Gomm JJ, Browne PJ, Coope RC, Liu Q-Y, Buluwela L, Coombes RC. Isolation of pure populations of epithelial and myoepithelial cells from the normal human mammary gland using immunomagnetic separation with dynabeads. *Anal Biochem.* 1995; 226: 91-99.
384. Cho SJ, Jarrett BR, Louie AY, Kauzlarich SM. Gold-coated iron nanoparticles: a novel magnetic resonance agent for T₁ and T₂ weighted imaging. *Nanotechnology.* 2006; 17: 640-644.
385. Euliss LE, DuPont JA, Gratton S, DeSimone J. Imparting size, shape, and composition control of materials for nanomedicine. *Chem Soc Rev.* 2006; 35: 1095-1104.
386. O'Reilly RK, Hawker CJ, Wooley KL. Cross-linked block copolymer micelles: functional nanostructures of great potential and versatility. *Chem Soc Rev.* 2006; 35: 1068-1083.
387. Vo-Dinh T, Cullum BM, Stokes DL. Nanosensors and biochips: frontiers in biomolecular diagnostics. *Sens Actuators B.* 2001; 74: 2-11.
388. Freitas I. Lipid accumulation: The common feature to photosensitizer-retaining normal and malignant tissues. *J Photochem Photobiol B: Biol.* 1990; 7: 359-361.
389. Tan W, Shi Z-Y, Kopelman R. Miniaturized fiber-optic chemical sensors with fluorescent dye-doped polymers. *Sens Actuators B.* 1995; 28: 157-163.
390. Voss R, Thomas A, Antonietti M, Ozin GA. Synthesis and characterization of highly amine functionalized mesoporous organosilicas by an "all-in-one" approach. *J Mater Chem.* 2005; 15: 4010-4014.
391. Birkert O, Haake H-M, Schütz A, Mack J, Brecht A, Jung G, Gauglitz G. A streptavidin surface on planar glass substrates for the detection of biomolecular interaction. *Anal Biochem.* 2000; 282: 200-208.
392. Yim EK, Leong KW. Significance of synthetic nanostructures in dictating cellular response. *Nanomed.* 2005; 1: 10-21.
393. Metzger SW, Natesan M, Yanavich C, Schneider J, Lee GU. Development and characterization of surface chemistries for microfabricated biosensors. *J Vac Sci Technol A.* 1999; 17: 2623-2628.
394. Jang J, Oh JH, Li XL. A novel synthesis of nanocapsules using identical polymer core/shell nanospheres. *J Mater Chem.* 2004; 14: 2872-2880.
395. Barratt G. Colloidal drug carriers: achievements and perspectives. *Cell Mol Life Sci.* 2003; 60: 21-37.
396. Daubresse C, Grandfils C, Jérôme R, Teyssié P. Enzyme immobilization in nanoparticles produced by inverse microemulsion polymerization. *J Colloid Interface Sci.* 1994; 168: 222-229.
397. Gref R, Couvreur P, Barratt G, Mysiakine E. Surface-engineered nanoparticles for multiple ligand coupling. *Biomaterials.* 2003; 24: 4529-4537.
398. Kim GJ, Nie S. Targeted cancer nanotherapy. *Nanotoday.* 2005; 28-33.
399. Candau F, Selb J. Hydrophobically-modified polyacrylamides prepared by micellar polymerization. *Adv Colloid Interface Sci.* 1999; 79: 149-172.
400. Wieder ME, Hone DC, Cook MJ, Handsley MM, Gavriloic J, Russell DA. Intracellular photodynamic therapy with photosensitizer-nanoparticle conjugates: cancer therapy using a 'Trojan horse'. *Photochem Photobiol Sci.* 2006; 5: 727-734.
401. Funkhouser J. Reintroducing pharma: the theranostic revolution. *Curr Drug Discovery.* 2002; 17-19.
402. Kelkar SS, Reineke TM. Theranostics: combining imaging and therapy. *Bioconjugate Chem.* 2011; 22: 1879-1903.
403. Pan D, Caruthers SD, Hu G, Senpan A, Scott MJ, Gaffney PJ, Wickline SA, Lanza GM. Ligand-directed nanobialys as theranostic agent for drug delivery and manganese-based magnetic resonance imaging of vascular targets. *J Am Chem Soc.* 2008; 130: 9186-9187.
404. McCarthy JR, Jaffer FA, Weissleder R. A macrophage-targeted theranostic nanoparticle for biomedical applications. *Small.* 2006; 2: 983-987.
405. Jaffer FA, Nahrendorf M, Sosnovik D, Kelly KA, Aikawa E, Weissleder R. Cellular imaging of inflammation in atherosclerosis using magneto-fluorescent nanomaterials. *Mol Imaging.* 2006; 5: 85-92.
406. Pande AN, Kohler RH, Aikawa E, Weissleder R, Jaffer FA. Detection of macrophage activity in atherosclerosis *in vivo* using multichannel,

- high-resolution laser scanning fluorescence microscopy. *J Biomed Opt.* 2006; 11: 21009-21016.
407. Cheng S-H, Lee C-H, Yang C-S, Tseng F-G, Mou C-Y, Lo L-W. Mesoporous silica nanoparticles functionalized with an oxygen-sensing probe for cell photodynamic therapy: potential cancer theranostics. *J Mater Chem.* 2009; 19: 1252-1257.
408. Zhang P, Steelant W, Kumar M, Scholfield M. Versatile photosensitizers for photodynamic therapy at infrared excitation. *J Am Chem Soc.* 2007; 129: 4526-4527.
409. de la Zerda A, Kim J-W, Galanzha EI, Gambhir SS, Zharov VP. Advanced contrast nanoagents for photoacoustic molecular imaging, cytometry, blood test and photothermal theranostics. *Contrast Media Mol Imaging.* 2011; 6: 346-369.
410. Resch-Genger U, Grabolle M, Cavaliere-Jaricot S, Nitschke R, Nann T. Quantum dots *versus* organic dyes as fluorescent labels. *Nat Methods.* 2008; 5: 763-775.
411. Lovell JF, Jin CS, Huynh E, Jin H, Kim C, Rubinstein JL, Chan WCW, Cao W, Wang LV, Zheng G. Porphysome nanovesicles generated by porphyrin bilayers for use as multimodal biophotonic contrast agents. *Nature Mat.* 2011; 10: 324-332.
412. Kuo PH. Gadolinium-containing MRI contrast agents: important variations on a theme for NSF. *J Am Coll Radiol.* 2008; 5: 29-35.
413. Caravan P, Ellison JJ, McMurry TJ, Laufer RB. Gadolinium(III) chelates as MRI contrast agents: structure, dynamics, and applications. *Chem Rev.* 1999; 99: 2293-2352.
414. Naghavi M, Libby P, Falk E, Casscells SW, Litovsky S, Rumberger J, Badimon JJ, Stefanadis C, Moreno P, Pasterkamp G, Fayad Z, Stone PH, Waxman S, Raggi P, Madjid M, Zarrabi A, Burke A, Yuan C, Fitzgerald PJ, Siscovick DS, de Korte CL, Aikawa M, Juhani Airaksinen KE, Assmann G, Becker CR, Chesebro JH, Farb A, Galis ZS, Jackson C, Jang I-K, Koenig W, Lodder RA, March K, Demirovic J, Navab M, Priori SG, Reekter MD, Bahr R, Grundy SM, Mehran R, Colombo A, Boerwinkle E, Ballantyne C, Insull Jr W, Schwartz RS, Vogel R, Serruys PW, Hansson GK, Faxon DP, Kaul S, Drexler H, Greenland P, Muller JE, Virmani R, Ridker PM, Zipes DP, Shah PK, Willerson JT. From vulnerable plaque to vulnerable patient a call for new definitions and risk assessment strategies: part I. *Circulation.* 2003; 108: 1664-1672.
415. Jaffer FA, Libby P, Weissleder R. Molecular and cellular imaging of atherosclerosis: emerging applications. *J Am Coll Cardiol.* 2006; 47: 1328-1338.
416. Jaffer FA, Weissleder R. Molecular imaging in the clinical arena. *J Am Med Assoc.* 2005; 293: 855-862.
417. Li AC, Glass CK. The macrophage foam cell as a target for therapeutic intervention. *Nature Medicine.* 2002; 8: 1235-1242.
418. Libby P. Inflammation in atherosclerosis. *Nature.* 2002; 420: 868-874.
419. Rockson SG, Lorenz DP, Cheong WF. Photoangioplasty: an emerging clinical cardiovascular role for photodynamic therapy. *Circulation.* 2000; 102: 591-596.
420. Hsiang Y, Stonefield M, Bower RD, Fragoso M, Tsang V, Crespo MT, Lundkvist A. Assessing Photofrin[®] uptake in atherosclerosis with a fluorescent probe: comparison with photography and tissue measurements. *Lasers Surg Med.* 1993; 13: 271-278.
421. Hsiang YN, Crespo MT, Richter AM, Jain AK, Fragoso M, Levy JG. *In vitro* and *in vivo* uptake of benzoporphyrin derivative into human and miniswine atherosclerotic plaque. *Photochem Photobiol.* 1993; 57: 670-674.
422. Litvack F, Grundfest WS, Forrester JS, Fishbein MC, Swan HJC, Corday E, Rider DM, McDermid IS, Pacala TJ, Laudenslager JB. Effects of hematoporphyrin derivative and photodynamic therapy on atherosclerotic rabbits. *Am J Cardiol.* 1985; 56: 667-671.
423. Neave V, Giannotta S, Hyman S, Schneider J. Hematoporphyrin uptake in atherosclerotic plaques: therapeutic potentials. *Neurosurg.* 1988; 23: 307-312.
424. Pagnan A, Scannapieco G, Pualetto P, Perin A, Jori G. Haematoporphyrin and atherosclerosis in the broad-breasted white turkey: distribution and quantitation in thoracic and abdominal aorta. *Int J Tissue React.* 1989; 11: 93-99.
425. Pollock ME, Eugene J, Hammer-Wilson M, Berns MW. Photosensitization of experimental atheromas by porphyrins. *J Am Coll Cardiol.* 1987; 9: 639-646.
426. Tang G, Hyman S, Schneider Jr JH, Giannotta SL. Application of photodynamic therapy to the treatment of atherosclerotic plaques. *Neurosurg.* 1993; 32: 438-443.
427. Kereiakes DJ, Szyniszewski AM, Wahr D, Herrmann HC, Simon DI, Rogers C, Kramer P, Shear W, Yeung AC, Shunk KA, Chou TM, Popma J, Fitzgerald P, Carroll TE, Forer D, Adelman DC. Phase I drug and light dose-escalation trial of motexafin lutetium and far-red light activation (phototherapy) in subjects with coronary artery disease undergoing percutaneous coronary intervention and stent deployment: procedural and long-term results. *Circulation.* 2003; 108: 1310-1315.
428. Rockson SG, Kramer P, Razavi M, Szuba A, Filardo S, Fitzgerald P, Cooke JP, Yousuf S, DeVault AR, Renschler MF, Adelman DC. Photoangioplasty for human peripheral atherosclerosis. Results of a phase I trial of photodynamic therapy with motexafin lutetium (Antrin). *Circulation.* 2000; 102: 2322-2324.
429. Konan YN, Berton M, Gurny R, Allémann E. Enhanced photodynamic activity of meso-tetra(4-hydroxyphenyl)porphyrin by incorporation into sub-200 nm nanoparticles. *Eur J Pharm Sci.* 2003; 18: 241-249.
430. McCarthy JR, Perez JM, Brückner C, Weissleder R. Polymeric nanoparticle preparation that eradicates tumors. *Nano Lett.* 2005; 5: 2552-2556.
431. Yan F, Kopelman R. The embedding of meta-tetra(hydroxyphenyl)-chlorin into silica nanoparticle platforms for photodynamic therapy and their singlet oxygen production and pH-dependent optical properties. *Photochem Photobiol.* 2003; 78: 587-591.
432. Weissleder R, Kelly K, Sun EY, Shtatland T, Josephson L. Cell-specific targeting of nanoparticles by multivalent attachment of small molecules. *Nat Biotechnol.* 2005; 23: 1418-1423.
433. Ohulchanskyy TY, Roy I, Goswami LN, Chen Y, Bergey EJ, Pandey RK, Oseroff AR, Prasad PN. Organically modified silica nanoparticles with covalently incorporated photosensitizer for photodynamic therapy of cancer. *Nano Lett.* 2007; 7: 2835-2842.
434. Guo Y, Kumar M, Zhang P. Nanoparticle-based photosensitizers under CW infrared excitation. *Chem Mater.* 2007; 19: 6071-6072.
435. Mehnert C, Ying J. Palladium-grafted mesoporous MCM-41 material as heterogeneous catalyst for Heck reactions. *Chem Commun.* 1997; 2215-2216.
436. Erathodiyil N, Ooi S, Seayad AM, Han Y, Lee SS, Ying JY. Palladium nanoclusters supported on propylurea-modified siliceous mesocellular foam for coupling and hydrogenation reactions. *Chem Eur J.* 2008; 14: 3118-3125.
437. Vallet-Regi M, Balas F, Arcos D. Mesoporous materials for drug delivery. *Angew Chem Int Ed.* 2007; 46: 7548-7558.
438. Trewyn BG, Giri S, Slowing II, Lin VS-Y. Mesoporous silica nanoparticle based controlled release, drug delivery, and biosensor systems. *Chem Commun.* 2007; 3236-3245.
439. Lu J, Liong M, Zink JJ, Tamanoi F. Mesoporous silica nanoparticles as a delivery system for hydrophobic anticancer drugs. *Small.* 2007; 3: 1341-1346.
440. Wen L-X, Li Z-Z, Zou H-K, Liu A-Q, Chen J-F. Controlled release of avermectin from porous hollow silica nanoparticles. *Pest Manag Sci.* 2005; 61: 583-590.
441. Zhu Y-F, Shi J-L, Li Y-S, Chen H-R, Shen W-H, Dong X-P. Storage and release of ibuprofen drug molecules in hollow mesoporous silica spheres with modified pore surface. *Micropor Mesopor Mat.* 2005; 85: 75-81.
442. Li ZZ, Xu SA, Wen LX, Liu F, Liu AQ, Wang Q, Sun HY, Yu W, Chen JF. Controlled release of avermectin from porous hollow silica nanoparticles: influence of shell thickness on loading efficiency, UV-shielding property and release. *J Control Release.* 2006; 111: 81-88.
443. Wu SH, Lin Y-S, Hung Y, Chou Y-H, Hsu Y-H, Chang C, Mou C-Y. Multifunctional mesoporous silica nanoparticles for intracellular labeling and animal magnetic resonance imaging studies. *ChemBiochem.* 2008; 9: 53-57.
444. Chung T-H, Wu S-H, Yao M, Lu C-W, Lin Y-S, Hung Y, Mou C-Y, Chen Y-C, Huang DM. The effect of surface charge on the uptake and biological function of mesoporous silica nanoparticles in 3T3-L1 cells and human mesenchymal stem cells. *Biomaterials.* 2007; 28: 2959-2966.
445. Lu C-W, Hung Y, Hsiao J-K, Yao M, Chung T-H, Lin Y-S, Wu S-H, Hsu S-C, Liu H-M, Mou C-Y, Yang C-S, Huang D-M, Chen Y-S. Bifunctional magnetic silica nanoparticles for highly efficient human stem cell labeling. *Nano Lett.* 2007; 7: 149-154.
446. Vinogradov SA, Wilson DF. Phosphorescence lifetime analysis with a quadratic programming algorithm for determining quencher distributions in heterogeneous systems. *Biophys J.* 1994; 67: 2048-2059.
447. Lo L-W, Koch CJ, Wilson DF. Calibration of oxygen-dependent quenching of the phosphorescence of Pd-meso-tetra(4-carboxyphenyl)porphyrin: a phosphor with general application for measuring oxygen concentration in biological systems. *Anal Biochem.* 1996; 236: 153-160.
448. Jin I, Yuji M, Yoshinori N, Makoto K, Mikio M. Anti-tumor effect of PDT using Photofrin in a mouse angiosarcoma model. *Arch Dermatol Res.* 2008; 300: 161-166.

449. Pan D, Caruthers SH, Chen J, Winter PM, SenPan A, Schmieder AH, Wickline SA, Lanza GM. Nanomedicine strategy for molecular targets with MRI and optical imaging. *Future Med Chem.* 2010; 2: 471-490.
450. Zharov VP, Galanzha EI, Shashkov EV, Kim J-W, Khlebtsov NG, Tuchin VV. Photoacoustic flow cytometry: principle and application for real-time detection of circulating single nanoparticles, pathogens, and contrast dyes *in vivo*. *J Biomed Opt.* 2007; 12: 051503.
451. Galanzha EI, Shashkov EV, Tuchin VV, Zharov VP. *In vivo* multispectral, multiparameter, photoacoustic lymph flow cytometry with natural cell focusing, label-free detection and multicolor nanoparticle probes. *Cytom A.* 2008; 73A: 884-894.
452. de la Zerde A, Zavaleta C, Keren S, Vaithilingam S, Bodapati S, Liu Z, Levi J, Smith BR, Ma T-J, Oralkan O, Cheng Z, Chen X, Dai H, Khuri-Yakub BT, Gambhir SS. Carbon nanotubes as photoacoustic molecular imaging agents in living mice. *Nat Nanotechnol.* 2008; 3: 557-562.
453. de la Zerde A, Liu Z, Bodapati S, Teed R, Vaithilingam S, Khuri-Yakub BT, Chen X, Dai H, Gambhir SS. Ultrahigh sensitivity carbon nanotube agents for photoacoustic molecular imaging in living mice. *Nano Lett.* 2010; 10: 2168-2172.
454. Galanzha EI, Shashkov EV, Kelly T, Kim J-W, Yang L, Zharov VP. *In vivo* magnetic enrichment and multiplex photoacoustic detection of circulating tumour cells. *Nat Nanotechnol.* 2009; 4: 855-860.
455. Kim J-W, Galanzha EI, Shashkov EV, Moon H-M, Zharov VP. Golden carbon nanotubes as multimodal photoacoustic and photothermal high-contrast molecular agents. *Nat Nanotechnol* 2009; 4: 688-694.
456. Xiang L, Yuan Y, Xing D, Ou Z, Yang S, Zhou F. Photoacoustic molecular imaging with antibody-functionalized single-walled carbon nanotubes for early diagnosis of tumor. *J Biomed Opt.* 2009; 14: 021008.
457. Galanzha EI, Shashkov EV, Kokoska MS, Myhill JA, Zharov VP. *In vivo* noninvasive detection of metastatic cells in vasculature and sentinel lymph nodes by photoacoustic cytometry. *Laser Surg Med.* 2008; 52(0): 81-81.
458. Galanzha EI, Kim J-W, Zharov VP. Nanotechnology-based molecular photoacoustic and photothermal flow cytometry platform for *in-vivo* detection and killing of circulating cancer stem cells. *J Biophoton.* 2009; 2: 725-735.
459. Nedosekin DA, Shashkov EV, Galanzha EI, Hennings L, Zharov VP. Photothermal multispectral image cytometry for quantitative histology of nanoparticles and micrometastasis in intact, stained and selectively burned tissues. *Cytom A.* 2010; 77: 1049-1058.
460. Zharov VP, Galitovskaya V, Viegas M. Photothermal detection of local thermal effects during selective nanophotothermolysis. *Appl Phys Lett.* 2003; 83: 4897-4899.
461. Zharov VP, Galitovskaya EN, Jonson C, Kelly T. Synergistic enhancement of selective nanophotothermolysis with gold nanoclusters: potential for cancer therapy. *Laser Surg Med.* 2005; 37: 219-226.
462. Zharov VP, Letfullin RR, Galitovskaya EN. Microbubbles-overlapping mode for laser killing of cancer cells with absorbing nanoparticle clusters. *J Phys D Appl Phys.* 2005; 38: 2571-2581.
463. Zharov VP, Kim J-W, Everts M, Curiel DT. Self-assembling nanoclusters in living systems: application for integrated photothermal nanodiagnostics and nanotherapy. *Nanomedicine : Nanotechnology, Biology and Medicine.* 2005; 1: 326-345.
464. Zharov VP, Mercer KE, Galitovskaya EN, Smeltzer MS. Photothermal nanotherapeutics and nanodiagnostics for selective killing of bacteria targeted with gold nanoparticles. *Biophys J.* 2006; 90: 619-627.
465. Kim J-W, Shashkov EV, Galanzha EI, Kotagiri N, Zharov VP. Photothermal antimicrobial nanotherapy and nanodiagnostics with self-assembling carbon nanotube clusters. *Lasers Surg Med.* 2007; 39: 622-634.
466. Khlebtsov B, Zharov VP, Melnikov A, Tuchin V, Khlebtsov N. Optical amplification of photothermal therapy with gold nanoparticles and nanoclusters. *Nanotechnol.* 2006; 17: 5167-5179.
467. Letfullin RR, Joenathan C, George TF, Zharov VP. Laser-induced explosion of gold nanoparticles: potential role for nanophotothermolysis of cancer. *Nanomedicine.* 2006; 1: 473-480.
468. Galanzha EI, Tuchin VV, Zharov VP. Advances in small animal mesentery models for *in vivo* flow cytometry, dynamic microscopy, and drug screening. *Wld J Gastroenterol.* 2007; 13: 192-218.
469. Galanzha EI, Shashkov EV, Spring P, Suen JY, Zharov VP. *In vivo*, non-invasive, label-free detection and eradication of circulating metastatic melanoma cells by two-color photoacoustic flow cytometry and a diode laser. *Cancer Res.* 2009; 69: 7926-7934.
470. Zharov VP. Ultrasharp nonlinear photothermal and photoacoustic resonances and holes beyond the spectral limit. *Nat Photonics.* 2011; 5: 110-116.
471. Nikolaev P, Bronikowski MJ, Bradley RK, Rohmund F, Colbert DT, Smith KA, Smalley RE. Gas-phase catalytic growth of single-walled carbon nanotubes from carbon monoxide. *Chem Phys Lett.* 1999; 313: 91-97.
472. Meyyappan M, Delzeit L, Cassell A, Hash D. Carbon nanotube growth by PECVD: a review. *Plasma Sources Sci Technol.* 2003; 12: 205-216.
473. Gamaly EG, Ebbesen TW. Mechanism of carbon nanotube formation in the arc discharge. *Phys Rev B Condens Matter.* 1995; 52: 2083-2089.
474. Yudasaka M, Komatsu T, Ichihashi T, Iijima S. Single-wall carbon nanotube formation by laser ablation using double-targets of carbon and metal. *Chem Phys Lett.* 1997; 278: 102-106.
475. Galanzha EI, Kokoska MS, Shashkov EV, Kim J-W, Tuchin VV, Zharov VP. *In vivo* fiber-based multicolor photoacoustic detection and photothermal purging of metastasis in sentinel lymph nodes targeted by nanoparticles. *J Biophotonics.* 2009; 2: 528-539.
476. Pramanik M, Song KH, Swierczewska M, Green D, Sitharaman B, Wang LV. *In vivo* carbon nanotube-enhanced non-invasive photoacoustic mapping of the sentinel lymph node. *Phys Med Biol.* 2009; 54: 3291-3301.
477. Pramanik M, Swierczewska M, Green D, Sitharaman B, Wang LV. Single-walled carbon nanotubes as a multimodal-thermoacoustic and photoacoustic-contrast agent. *J Biomed Opt.* 2009; 14: 034018.
478. Bell AG. On the production and reproduction of sound by light. *Am J Sci.* 1880; 20: 305-324.
479. O'Connell MJ, Bachilo SM, Huffman CB, Moore VC, Strano MS, Haroz EH, Rialon KL, Boul PJ, Noon WH, Kittrell C, Ma JP, Hauge RH, Weisman RB, Smalley RE. Band gap fluorescence from individual single-walled carbon nanotubes. *Science.* 2002; 297: 593-596.
480. Rao AM, Richter E, Bandow S, Chase B, Eklund PC, Williams KA, Fang S, Subbaswamy KR, Menon M, Thess A, Smalley RE, Dresselhaus G, Dresselhaus MS. Diameter-selective Raman scattering from vibrational modes in carbon nanotubes. *Science.* 1997; 275: 187-191.
481. Keren S, Zavaleta C, Cheng Z, de la Zerde A, Gheysens O, Gambhir SS. Noninvasive molecular imaging of small living subjects using Raman spectroscopy. *Proc Natl Acad Sci USA.* 2008; 105: 5844-5849.
482. Liu Z, Davis C, Cai W, He L, Chen X, Dai H. Circulation and long-term fate of functionalized, biocompatible single-walled carbon nanotubes in mice probed by Raman spectroscopy. *Proc Natl Acad Sci USA.* 2008; 105: 1410-1415.
483. Zavaleta C, de la Zerde A, Liu Z, Keren S, Cheng Z, Schipper M, Chen X, Dai H, Gambhir SS. Noninvasive Raman spectroscopy in living mice for evaluation of tumor targeting with carbon nanotubes. *Nano Lett.* 2008; 8: 2800-2805.
484. Biris AS, Galanzha EI, Li Z, Mahmood M, Xu Y, Zharov VP. *In vivo* Raman flow cytometry for real-time detection of carbon nanotube kinetics in lymph, blood, and tissues. *J Biomed Opt.* 2009; 14: 021006.
485. Niyogi S, Hamon MA, Hu H, Zhao B, Bhowmik P, Sen R, Itkis ME, Haddon RC. Chemistry of single-walled carbon nanotubes. *Acc Chem Res.* 2002; 35: 1105-1113.
486. Rosca ID, Watari F, Uo M, Akasaka T. Oxidation of multiwalled carbon nanotubes by nitric acid. *Carbon.* 2005; 43: 3124-3131.
487. Liu Z, Sun X, Nakayama-Ratchford N, Dai H. Supramolecular chemistry on water-soluble carbon nanotubes for drug loading and delivery. *ACS Nano.* 2007; 1: 50-56.
488. Zhao B, Hu H, Yu A, Perea D, Haddon RC. Synthesis and characterization of water soluble single-walled carbon nanotube graft copolymers. *J Am Chem Soc.* 2005; 127: 8197-8203.
489. Guldi DM, Taieb H, Rahman GMA, Tagmatarchis N, Prato M. Novel photoactive single-walled carbon nanotube-porphyrin polymer wraps: efficient and long-lived intracomplex charge separation. *Adv Mater.* 2005; 17: 871-875.
490. Chen RJ, Zhang Y, Wang D, Dai H. Noncovalent sidewall functionalization of single-walled carbon nanotubes for protein immobilization. *J Am Chem Soc.* 2001; 123: 3838-3839.
491. Wu P, Chen X, Hu N, Tam UC, Blixt O, Zettl A, Bertozzi CR. Biocompatible carbon nanotubes generated by functionalization with glycodendrimers. *Angew Chem Int Edn.* 2008; 47: 5022-5025.
492. Kim J-W, Kotagiri N, Kim J-H, Deaton R. *In situ* fluorescence microscopy visualization and characterization of nanometer-scale carbon nanotubes labeled with 1-pyrenebutanoic acid, succinimidyl ester. *Appl Phys Lett.* 2006; 88: 213110.
493. Liu Z, Cai W, He L, Nakayama N, Chen K, Sun X, Chen X, Dai H. *In vivo* biodistribution and highly efficient tumour targeting of carbon nanotubes in mice. *Nat Nanotechnol.* 2007; 2: 47-52.
494. Ghosh P, Han G, De M, Kim CK, Rotello VM. Gold nanoparticles in delivery applications. *Adv Drug Deliv Rev.* 2008; 60: 1307-1315.
495. Lewinski N, Colvin V, Drezek R. Cytotoxicity of nanoparticles. *Small.* 2008; 4: 26-49.

496. Nel A, Xia T, Mädler L, Li N. Toxic potential of materials at the nanolevel. *Science*. 2006; 311: 622-627.
497. Peer D, Karp JM, Seungpyo H, Farokhzad OC, Margalit R, Langer R. Nanocarriers as an emerging platform for cancer therapy. *Nature Nanotechnol*. 2007; 2: 751-760.
498. Suzuki Y, Tanabe K, Shioi Y. Determination of chemical oxidation products of chlorophyll and porphyrin by high-performance liquid chromatography. *J Chromatogr A*. 1999; 839: 85-91.
499. Kirby C, Clarke J, Gregoriadis G. Effect of the cholesterol content of small unilamellar liposomes on their stability *in vivo* and *in vitro*. *Biochem J*. 1980; 186: 591-598.
500. Barrett JF. MRSA: status and prospects for therapy? An evaluation of key papers on the topic of MRSA and antibiotic resistance. *Expert Opin Ther Targets*. 2004; 8: 515-519.
501. Vince RV, Madden LA, Alonso CMA, Savoie H, Boyle RW, Todman M, Paget T, Greenman J. Identification of methicillin-resistant *Staphylococcus aureus*-specific peptides for targeted photoantimicrobial chemotherapy. *Photochem Photobiol Sci*. 2011; 10: 515-522.
502. Tavares A, Carvalho CMB, Faustino MA, Neves MGPMS, Tomé JPC, Tomé AC, Cavaleiro JAS, Cunha A, Gomes NCM, Alves E, Almeida A. Antimicrobial photodynamic therapy: study of bacterial recovery viability and potential development of resistance after treatment. *Mar Drugs*. 2010; 8: 91-105.
503. Alves E, Costa L, Carvalho CMB, Tomé JPC, Faustino MA, Neves MGPMS, Tomé AC, Cavaleiro JAS, Cunha A, Almeida A. Charge effect on the photoinactivation of Gram-negative and Gram-positive bacteria by cationic *meso*-substituted porphyrins. *BMC Microbiol*. 2009; 9: 70-83.
504. Yu KG, Li DH, Zhou CH, Diao JL. Study on the synthesis and antimicrobial activity of novel cationic porphyrins. *Chinese Chem Lett*. 2009; 20: 411-414.
505. Maisch T. A new strategy to destroy antibiotic resistant microorganisms: antimicrobial photodynamic treatment. *Mini-Rev Med Chem*. 2009; 9: 974-983.
506. Giuliani F, Martinelli M, Cocchi A, Arbia D, Fantetti L, Roncucci G. *In vitro* resistance selection studies of RLP068/CL, a new Zn(II) phthalocyanine suitable for antimicrobial photodynamic therapy. *Antimicrob Agents Ch*. 2010; 54: 637-642.
507. Mantareva V, Kussovski V, Angelov I, Wöhrle D, Dimitrov R, Popova E, Dimitrov S. Non-aggregated Ga(III)-phthalocyanines in the photodynamic inactivation of planktonic and biofilm cultures of pathogenic microorganisms. *Photochem Photobiol Sci*. 2011; 10: 91-102.
508. Mantareva V, Angelov I, Kussovski V, Wöhrle D, Dimitrov S. Metallophthalocyanines as photodynamic sensitizers for treatment of pathogenic bacteria. Uptake and photoinactivation properties. *Acad Bulg Sci*. 2010; 1: 77-84.
509. Huang L, Huang Y-Y, Mroz P, Tegos GP, Zhiyentayev T, Sharma SK, Lu Z, Balasubramanian T, Krayner M, Ruzić C, Yang E, Kee HL, Kirmaier C, Diers JR, Bocian DF, Holten D, Lindsey JS, Hamblin MR. Stable synthetic cationic bacteriochlorins as selective antimicrobial photosensitizers. *Antimicrob Agents Ch*. 2010; 54: 3834-3841.
510. Ragàs X, Sánchez-García D, Ruiz-González R, Dai T, Agut M, Hamblin MR, Nonell S. Cationic porphycenes as potential photosensitizers for antimicrobial photodynamic therapy. *J Med Chem*. 2010; 53: 7796-7803.
511. Bourré L, Giuntini F, Eggleston IM, Mosse CA, MacRobert AJ, Wilson M. Effective photoinactivation of Gram-positive and Gram-negative bacterial strains using an HIV-1 TAT peptide-porphyrin conjugate. *Photochem Photobiol Sci*. 2010; 9: 1613-1620.
512. Vahabi S, Fekrazad R, Ayremiou S, Taheri S, Lizarelli RFZ, Kalhori KAM. Antimicrobial photodynamic therapy with two photosensitizers on two oral streptococci: an *in vitro* study. *Laser Phys*. 2011; 21: 2132-2137.
513. Nonaka T, Nanashima, Nonaka M, Uehara M, Isomoto H, Nonaka Y, Nagayasu T. Advantages of Laserphyrin compared with Photofrin in photodynamic therapy for bile duct carcinoma. *J Hepato-Biliary-Pancreatic Sci*. 2011; 18: 592-600.
514. Lam M, Jou PC, Latiff AA, Yoojin L, Malbasa CL, Mukherjee PK, Oleinick NL, Ghannoum MA, Cooper KD, Baron ED. Photodynamic therapy with Pc4 induces apoptosis of *Candida albicans*. *Photochem Photobiol*. 2011; 87: 904-909.
515. Giuntini F, Alonso CMA, Boyle RW. Synthetic approaches for the conjugation of porphyrins and related macrocycles to peptides and proteins. *Photochem Photobiol*. 2011; 10: 759-791.
516. Bombelli C, Bordini F, Ferro S, Giansanti L, Jori G, Mancini G, Mazza C, Monti D, Ricchelli F, Sennato S, Venanzi M. New cationic liposomes as vehicles of *m*-tetrahydroxyphenylchlorin in photodynamic therapy of infectious diseases. *Mol Pharmaceutics*. 2008; 5: 672-679.
517. Tanaka M, Kinoshita M, Yoshihara Y, Shinomiya N, Seki S, Nemoto K, Hirayama T, Dai T, Huang L, Hamblin MR, Morimoto Y. Optimal photosensitizers for photodynamic therapy of infections should kill bacteria but spare neutrophils. *Photochem Photobiol*. 2012; 88: 227-232.
518. Schwartz J, Wiehe A, Gräfe S, Gitter B, Epple M. Calcium phosphate nanoparticles as efficient carriers for photodynamic therapy against cells and bacteria. *Biomater*. 2009; 30: 3324-3331.